JOURNAL OF LIQUID CHROMATOGRAPHY & RELATED TECHNOLOGIES

HPLC
TLC
Capillary Electrophoresis
Supercritical Fluid Techniques
Membrane Technology
Field-Flow Fractionation
Preparative & Analytical Separations

formerly Journal of Liquid Chromatography

Subscribe Today!

Use the cards below to subscribe to the *Journal of Liquid Chromatography & Related Technologies* or to recommend the journal to your library for acquisition.

Order Form

Journal of Liquid Chromatography & Related Technologies

Please enter my subscription to Vol. 19, 20 Numbers, 1996 at the ☐ institutional rate of $1595.00; ☐ individual rate of $797.50 *Individual subscriptions must be prepaid in American currency by personal check or credit card. Please add $3.50 per issue (number) for shipping outside the U.S. For airmail to Europe, add $5.50 per issue; to Asia, add $6.50 per issue. Canadian customers please add 7% GST.*

_____ Please send me a proforma invoice.
_____ Check enclosed made payable to Marcel Dekker, Inc.
_____ Charge my: ☐ MasterCard ☐ Visa ☐ American Express

Card No._____ Exp. Date_____

Signature_____

Name_____

Address_____

City/State/Zip_____

Does your library subscribe to the **Journal of Liquid Chromatography & Related Technologies**? Just complete this card and submit it to your librarian or department head.

Attention: Librarian/Department Head: I have examined the *Journal of Liquid Chromatography & Related Technologies* and would like to recommend the journal for acquisition.

Signature_____ Date_____

Name_____ Department_____

Journal of Liquid Chromatography & Related Technologies
Volume 19, 20 Numbers, 1996: $1595.00
ISSN: 1082–6076   CODEN: JLCTFC

Sample copy and proforma invoice available upon request.

Please contact the Promotion Department at: **Marcel Dekker, Inc.**
270 Madison Avenue
New York, NY 10016
(212) 696-9000 phone
(212) 685-4540 fax

Subscribe Today!

Use the cards below to subscribe to the *Journal of Liquid Chromatography & Related Technologies* **or to recommend the journal to your library for acquisition.**

Journal of Liquid Chromatography & Related Technologies

Editor: **JACK CAZES**
Cherry Hill, New Jersey

The *Journal of Liquid Chromatography & Related Technologies* now publishes an outstanding selection of critical, peer-reviewed papers dealing with analytical, preparative and process-scale liquid chromatography of all types and related technologies such as TLC; capillary electrophoresis; supercritical fluid extraction and chromatography; membrane separation technology; field-flow techniques; and others. As new separation technologies are introduced, they will also be included in the journal. On a regular basis, special topical issues are devoted to specific technologies and applications. Book reviews, software reviews, and schedules of meetings, symposiums and expositions are also included.

Formerly the *Journal of Liquid Chromatography*

JOURNAL OF LIQUID CHROMATOGRAPHY

& RELATED TECHNOLOGIES

SURFACE AND STRUCTURAL PROPERTIES OF SILICA GELS USED IN HIGH PERFORMANCE LIQUID CHROMATOGRAPHY

Y. Bereznitski, M. Jaroniec,* M. Kruk

Separation and Surface Science Center
Department of Chemistry
Kent State University
Kent, Ohio 44242

ABSTRACT

Complete nitrogen adsorption-desorption isotherms were measured over the entire pressure range including the region of very low pressures for a series of silica gels used in high performance liquid chromatography. In addition to standard characterization of the silicas studied, which included the evaluation of the specific surface area and the total pore volume, the experimental adsorption isotherms were used to calculate the adsorption energy distributions and the pore volume distributions by employing an advanced numerical algorithm based on the regularization method. For most silica samples studied, the resulting energy distributions are similar indicating that their surface properties are analogous. For some silicas, which are able to chemisorb greater amounts of water as shown by supplementary thermogravimetric studies, the adsorption energy distributions are different. Analysis, of the resulting pore volume distributions for most silicas studied, shows a relatively narrow range of mesopores and no substantial evidence for the presence of micropores.

1523

INTRODUCTION

Porous silicas are widely applied in many areas of modern science and technology, especially in sorption-based separations, chromatography and catalysis.[1,2]   They are extensively used in gas (GC) and liquid (LC) chromatography due to their high mechanical, chemical and thermal stability. Silica gels can be easily modified by bonding different types of ligands to their surface.[3,4]   Their high surface reactivity provides a unique opportunity for preparing various stationary phases of desired chemical properties which enable even very involved and refined separations.

Chromatographic performance of silica packings and silica-based stationary phases depends significantly on the surface and structural properties of the silica particles.   The surface properties in turn are determined by the surface roughness as well as by surface silanols, siloxane groups and various bonded impurities (mostly metal oxides).   The structural properties are determined by the presence of pores of different shape and size and by their connectivity.   In order to control the synthesis of chemically bonded phases, the starting silica needs to be well characterized.[4]

An appropriate characterization of silicas is crucial in selecting porous supports suitable to prepare chemically bonded phases for gas and liquid chromatographic separations.   In the current work, a series of porous silicas used in high performance liquid chromatography is characterized in terms of the adsorption energy distribution evaluated from the low-pressure nitrogen adsorption isotherm data.   In addition, their porous structures are determined on the basis of the complete nitrogen adsorption isotherms.

METHODS

Sorption Measurements

Eight commercial chromatographic silicas were selected to carry out extensive sorption studies.   Prior to performing sorption measurements silica gels were degassed at 473 K for 2 hours under the vacuum of approximately 10^{-4} Torr by using the degas port of the sorption analyzer. High purity (99.99 %) nitrogen   was used to carry out   sorption   measurements.   Complete adsorption-desorption isotherms were measured by ASAP 2010 volumetric sorption   instrument from Micromeritics (Norcross,GA). This instrument
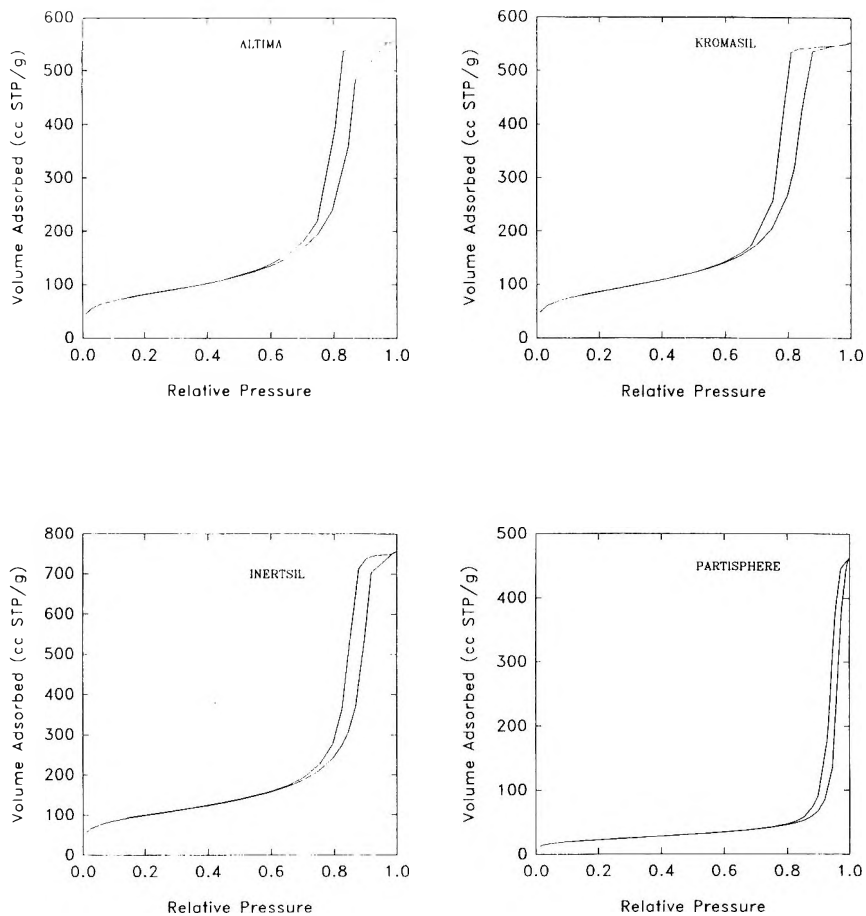
Figure 1. Nitrogen adsorption-desorption isotherms on Altima, Inertsil, Kromasil and Partisphere at 77.35 K.

allows to perform high-resolution adsorption measurements over a wide range of relative pressures from 10^{-6} to 1. The adsorption-desorption isotherms are shown in Figures 1 and 2.
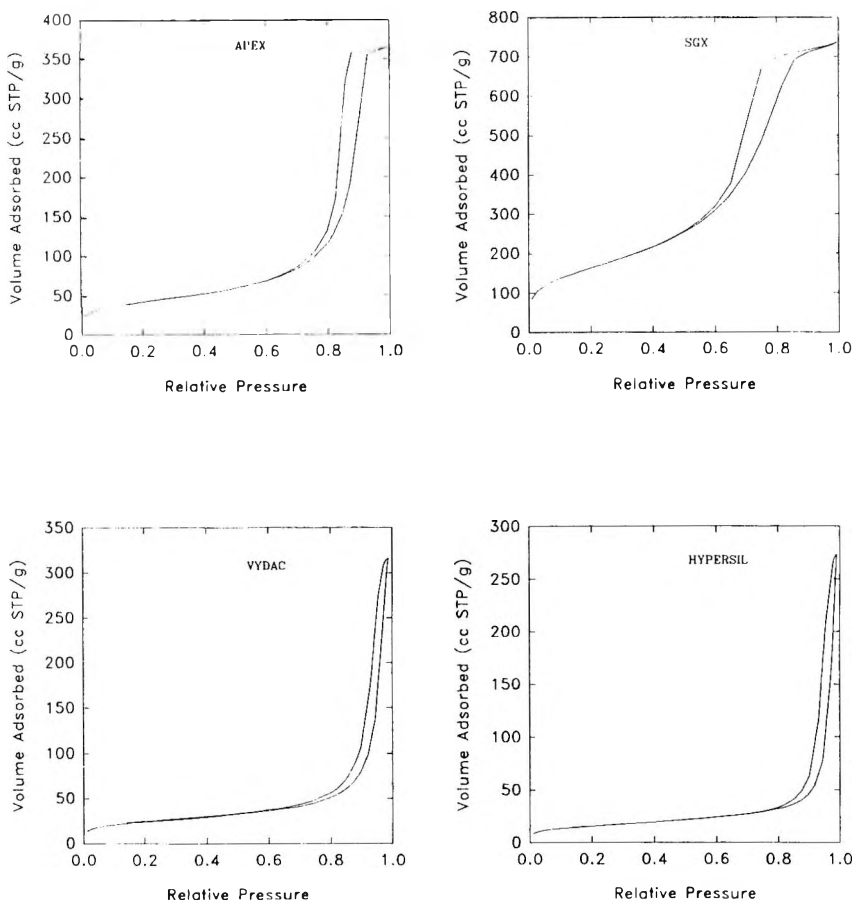
Figure 2. Nitrogen adsorption-desorption isotherms on Apex, SGX, Vydac and Hypersil at 77.35K.

Standard Characterization

The low temperature nitrogen adsorption-desorption isotherms were used to evaluate such standard quantities as the BET specific surface area, the external surface area, the total pore volume and the micropore volume.[5,6] The methods of calculation of these quantities from adsorption data are well described in basic adsorption books.[6] The total specific surface area was evaluated according to the well-known BET equation from nitrogen adsorption data at the relative pressure range from 0.05 to 0.25. The total pore volume was

estimated by converting the volume adsorbed at the relative pressure of 0.975 to the volume of liquid adsorbate. The external (mesopore) surface area and the micropore volume were evaluated from the t-plot method, which is based on the comparison of the adsorption isotherm for the sample studied with the standard isotherm measured on a reference nonporous material.[6] In the latter method, the standard isotherm on the reference solid is expressed in terms of the thickness of the adsorbed layer t. The intercept and slope of the linear segment of the t-plot was used to evaluate the micropore volume and the external surface area, respectively.

Calculation of the Pore Volume Distribution

Nitrogen adsorption isotherms at 77.5 K were used to obtain information about structural heterogeneity of the silicas studied. The pore volume distribution $J(x)$ is related to the volume adsorbed V through the following integral equation:[5,7]

$$V(p) = V_t \int_{\Omega} \theta_x(p, x) J(x) dx \qquad (1)$$

where V_t denotes the maximum volume adsorbed, p is the equilibrium pressure, $J(x)dx$ denotes the fraction of pores between widths x and $x+dx$, $\theta_x(p, x)$ stands for the local adsorption isotherm in the pores of the width x, and Ω denotes the integration region with respect to x. The pore volume distribution $J(x)$ was calculated by employing the regularization method[8] to invert the integral Eq. 1 for *a priori* assumed local adsorption model. Since there is no analytical equation to describe the complete volume filling of uniform pores, the local adsorption isotherm in Eq. 1 was calculated via the density functional theory.[9-11] Olivier *et al.*[12] combined the density functional theory approach[11] with the regularization procedure[8] in order to elaborate an advanced numerical method (DFT software) for calculating the pore volume distribution from the entire adsorption isotherm. In the current work, this method was used to calculate the incremental pore volume distribution function, from which the cumulative pore volume distribution can be obtained by performing appropriate summations of incremental pore volumes. Differentiation of the latter distribution leads to the differential pore volume distribution $J(x)$.

Calculation of the Adsorption Energy Distribution

The energy distribution $F(U)$ was calculated from low pressure nitrogen adsorption data by inverting the following integral equation,[7] which is analogous to Eq. 1:

$$\Theta(p) = \Theta_1 \int_\Lambda (p, U) F(U) dU \tag{2}$$

where $\Theta(p)$ is the relative adsorption in the submonolayer range, which is the ratio of the adsorbed amount to the BET monolayer capacity; U is the adsorption energy, $\Theta_1(p, U)$ is the local adsorption isotherm as a function of the adsorption energy, Δ is the integration region and $F(U)dU$ denotes the fraction of the surface with adsorption energies between U and $U+dU$. To invert the integral Eq. 2 with respect to the energy distribution function $F(U)$ one needs to assume a local adsorption model. In the current work, the well-known Fowler-Guggenheim (FG) equation, which describes the localized monolayer adsorption with lateral interactions, was used:

$$\theta_1(p, U) = \frac{Kp \exp(zw\Theta / kT)}{1 + Kp \exp(zw\Theta / kT)} \tag{3}$$

with:

$$K = K_0(T) \exp(U / kT) \tag{4}$$

where Θ is the relative adsorption defined above, z stands for the number of the nearest neighbors of a molecule in the monolayer and w is the interaction energy between nearest neighbors. K is the Langmuir constant for adsorption on monoenergetic sites and the pre-exponential factor $K_0(T)$ is expressed in terms of the partition functions for an isolated molecule in the gas and surface phases.[7] The above factor was estimated according to the Adamson method.[13] The FG Eq. 3 describes the local adsorption with lateral interactions (where w is the interaction energy and z is the number of nearest neighbors) on the surfaces of random distribution of adsorption sites, which appears to be realistic for silica surfaces.[14] The energy distributions for the silicas studied were calculated by employing the regularization method (INTEG program)[8] to invert Eq. 2 with respect to F(U). The interaction paremeters $z = 4$ and $w / k = 95K$ were assumed.

RESULTS AND DISCUSSION

Complete adsorption-desorption isotherms, measured at 77.35 K for all silicas studied, are shown in Figures 1 and 2. These isotherms can be considered as type IV according to the common classification of the gas/solid adsorption isotherms.[6] The shape of the adsorption isotherms for all samples reflects monolayer adsorption followed by the multilayer formation and

subsequently by the capillary condensation, which is the source of the hysteresis loop in the higher pressure region. Except the SGX silica, the hysteresis loops for the other silicas show type H1 with some resemblance to type H2 according to the IUPAC classification.[6,15,16] The model H1 hysteresis loop has the adsorption and desorption branches almost vertical and nearly parallel over a considerable range of pressures.[6] This type of hysteresis loop is characteristic for agglomerates or compacts of spheroidal particles of similar size arranged in a fairly uniform way.

Hysteresis loops for Partisphere, Hypersil and Vydac resemble type H1 and are located in the range of relative pressures between 0.8 and 1.0, which indicates that their porous structure contains mostly large mesopores and small macropores. Note that according to the IUPAC recommendations,[15,16] the pores are clasified into micropores (widths below 2 nm), mesopores (widths between 2-50 nm) and macropores (widths above 50 nm).

For the remaining silicas the hysteresis loop starts at the relative pressure range between 0.6 and 0.7, and tends to be similar to the loop type H2, which is often observed for silica gels of relatively narrow mesopore distribution with maximum about 10 nm. For the SGX silica the hysteresis loop exhibits type H2 and differs significantly from the hysteresis loops for other samples studied.

A standard numerical analysis of nitrogen adsorption isotherms was carried out in order to provide a quantitative estimation of the BET specific surface area S_{BET}, the total pore volume V_t and the average pore diameter w. The latter was calculated on the basis of the incremental pore volume distributions obtained by using the DFT software.[12] They are summarized in Table 1 and occur to be significantly different from those reported in the manufacturer catalogs, which provide average values for a given brand of the silica.

While the BET specific surface areas are in a reasonable agreement with the available catalog data, the average pore widths show greater discrepancies. It is known that the surface and structural properties of two batches of the same brand of silica can differ significantly. The latter properties also depend on the pretreatment methods and analysis conditions. Moreover, there may be some disagreement between results obtained on the basis of different methods.

In spite of the above comments, Table 1 provides valuable information about surface and structural differences among the silicas studied in the current work because all adsorption measurements were carried out under the same conditions.
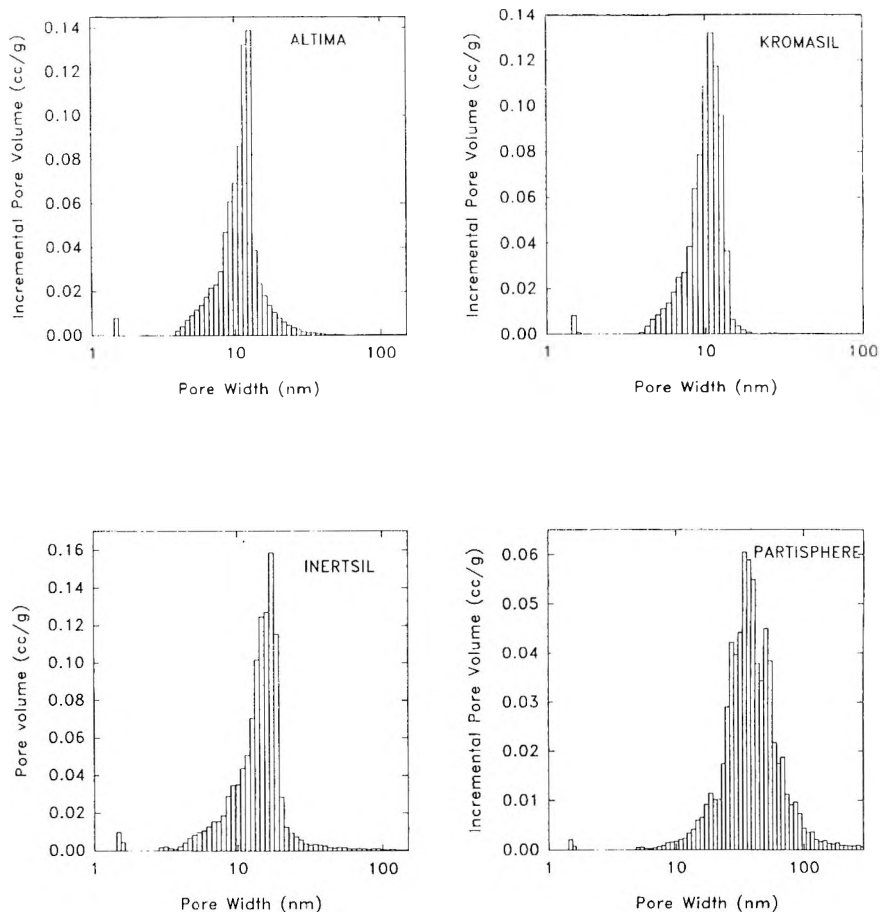
Figure 3.   Incremental pore volume distributions for Altima, Inertsil, Kromasil and Partisphere calculated from the entire nitrogen adsorption isotherms.

   As can be seen in Table 1 the silicas under study showed different surface and structural characteristics.   Their BET specific surface areas vary from 60 to 600 m^2/g.   The specific surface areas of Hypersil, Partisphere and Vydac are about 60-80 m^2/g, whereas Kromasil, Inertsil and Altima exhibit the surface area about 300 m^2/g.   The surface area of the SGX silica is about 600 m^2/g. The t-plot analysis showed no substantial evidence for the presence of fine pores (widths below 2 nm) in the silicas studied except SGX, which possesses a small fraction of micropores.   The total pore volumes of the silicas studied   are
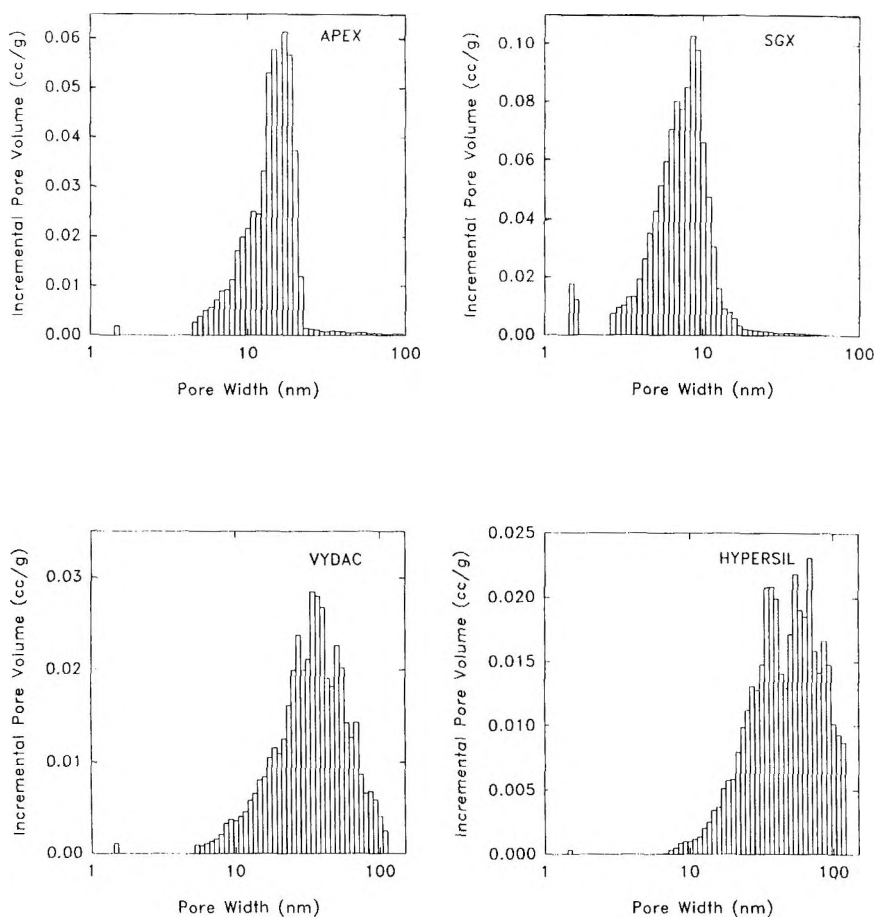
Figure 4. Incremental pore volume distributions for Apex, SGX, Vydac and Hypersil calculated from the entire nitrogen adsorption isotherms.

in the range between 0.24 and 1.16 cc/g. For silicas of the specific surface area about 300 m^2/g or greater the total pore volumes are about 0.8-1.1 cc/g and the average pore widths are about 10 nm.

For remaining silicas, the total pore volumes are much lower and the average pore widths much higher. The average pore widths were calculated on the basis of the incremental pore volume distributions shown in Figures 3 and 4 and obtained by using the DFT software.[12]

BEREZNITSKI ET AL.
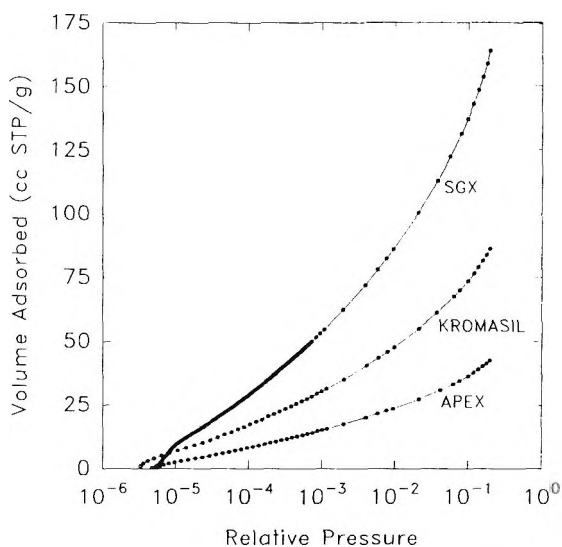
Figure 5. Low pressure nitrogen adsorption isotherms for Apex, Kromasil and SGX silica.

Table 1

Surface and Structural Parameters of the Chromatographic Silicas Studied

Silica	Source	$S_{BET}(m^2/g)$	$V_t(cc/g)$	w(nm)
Hypersil	Altech	56	0.24	52
Partisphere	Whatman	81	0.52	45
Vydac	Supelco	86	0.36	38
Apex	Jones Chrom.	153	0.57	15
Altima	Altech	294	0.86	12
Kromasil	Eka Nobel	311	0.85	11
Intersil	MetaChem Tech	357	1.16	16
SGX	Tesske	596	1.13	8

One can notice relatively narrow incremental pore volume distributions for Altima, Inertsil and Kromasil. Relatively broad pore volume distributions were obtained for Hypersil, Partisphere and Vydac. The pore volume distributions for Apex and SGX silicas are slightly broader than those for Altima, Inertsil and

Kromasil. Moreover, the pore volume distribution for the SGX silica shows a relatively high fraction of small pores and therefore its specific surface area is the highest among the samples studied.

The adsorption energy distributions for all silica samples were calculated on the basis of data from the submonolayer range of nitrogen adsorption isotherms. An illustration of this range of adsorption data is shown in Figure 5, in which the volume adsorbed is plotted as a function of the logarithm of the relative pressure in order to demonstrate the differences between adsorption isotherms at the low pressure range. Only experimental points below the relative pressure corresponding to the BET monolayer capacity were used to calculate the adsorption energy distributions according to Eq. 2.

The Fowler-Guggenheim model for a random distribution of adsorption sites was used to represent the local adsorption and gave much better results than the model for the patchwise distribution of adsorption sites. The numerically stable energy distributions were obtained by assuming four nearest neighbors. The interaction parameter for nitrogen was equal to 95 K and the regularization parameter was equal to 0.1. The resulting adsorption energy distribution functions provide only approximate information about the energetic heterogeneity of the samples studied due to the simplicity of the FG model employed.

All energy distributions consist of at least two overlapping peaks with maxima located about 6 and 13 kJ/mol, respectively (see Figures 6 and 7). The appearance of two peaks in the energy distribution function suggests the presence of two main types of adsorption sites on the silica surface and agrees with previous studies.[7] For most silicas studied the upper adsorption energy is about 16-17 kJ/mol. Note that the energy distribution for the SGX silica does not exhibit two overlapping peaks of clearly pronounced maxima.

The small fraction of high energy sites can be noticed on the energy distributions for Partisphere, Vydac and Hypersil. For these silicas the energy distributions cover the range up to 20 kJ/mol.

The supplementary studies of the samples were performed by thermogravimetry[17] and showed that the three silicas mentioned above contain much more chemisorbed water than the remaining samples. Therefore, in order to estimate the impact of the surface water and silanols on the energetic heterogeneity of silicas further thermoanalytical and spectroscopic studies are desirable. These studies can provide valuable information about high-energy sites on the silica surface.
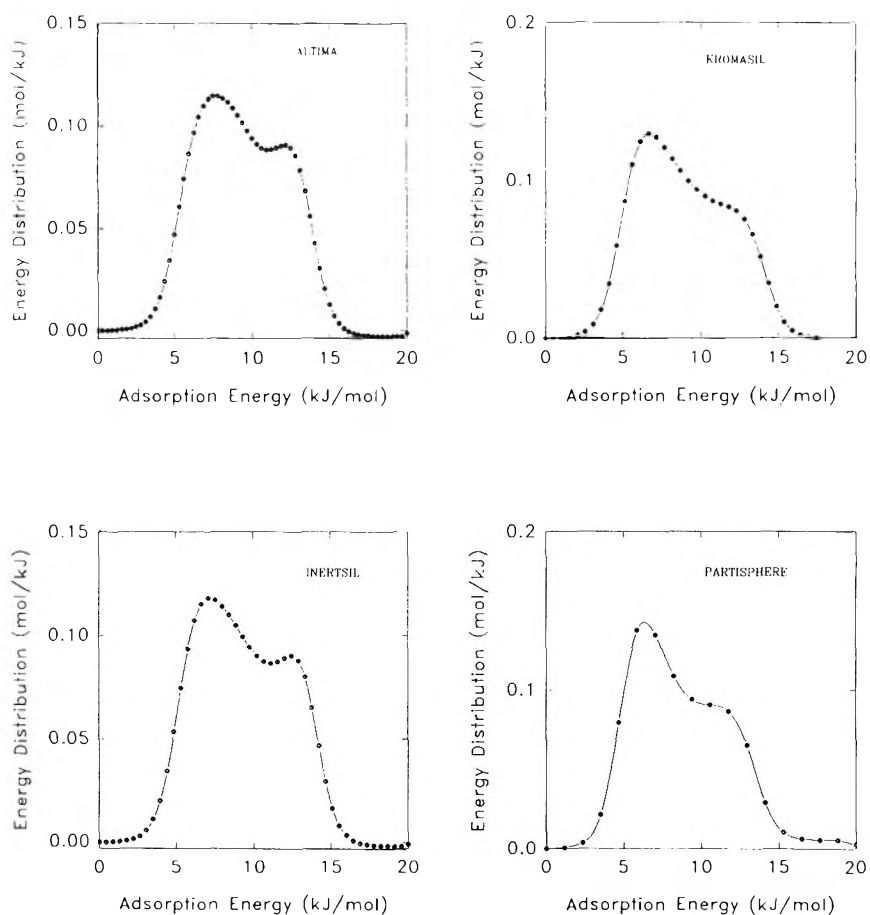
Figure 6. Adsorption energy distributions for Altima,Inertsil, Kromasil and Partisphere calculated from the low-pressure nitrogen adsorption data.

CONCLUSIONS

It is known that three major factors are responsible for the energetic heterogeneity of silicas: (i) different types of silanol groups present on the surface, (ii) impurities (usually metal oxides), and (iii) microporosity. For the silicas studied, except the SGX sample, the microporosity does not seem to play a significant role, so the remaining two factors account for their heterogeneity.
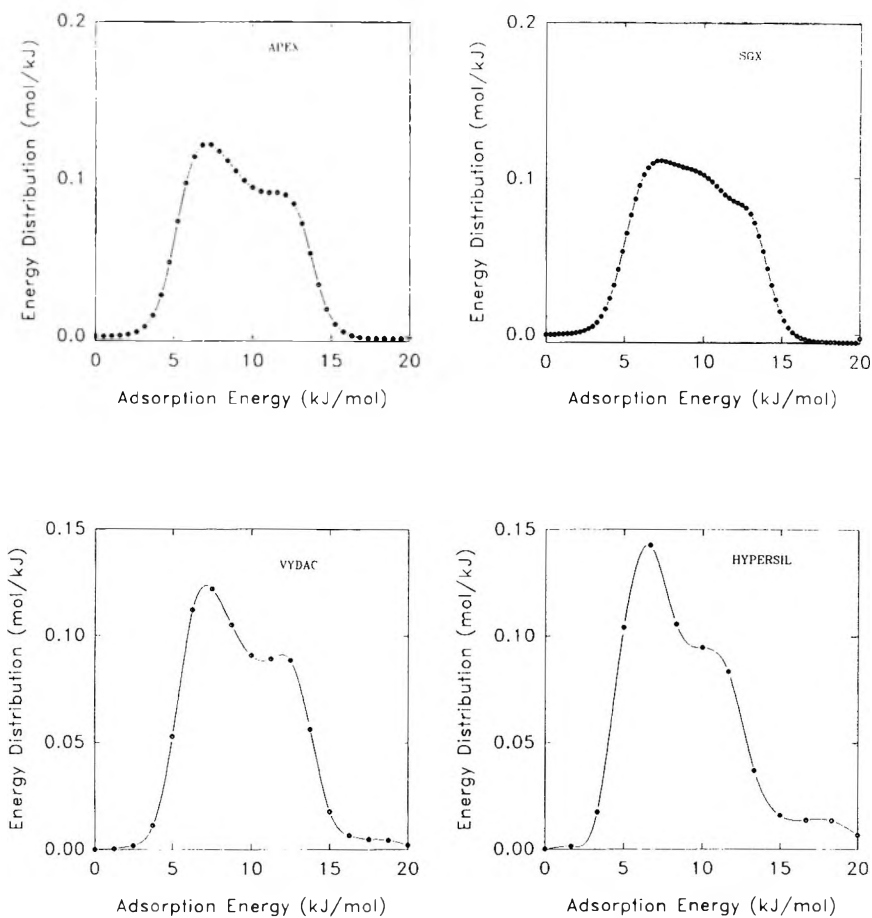
Figure 7. Adsorption energy distributions for Apex, SGX, Vydac and Hypersil calculated from the low-pressure nitrogen adsorption data.

Although the impurity level can be controlled, the silica surface possesses different types of silanol groups arranged in various topological patterns, which are an intrinsic feature of this surface and the primary source of its heterogeneity. It is shown, that adsorption methods allow for characterization of the energetic heterogeneity and provide information about porous structure of the samples, which are useful for optimization of the preparation conditions of chemically bonded stationary phases.

REFERENCES

1. **Characterization and Modification of the Silica Surface**, E. F. Vansant, P. Van der Voort, K. C. Vrancken, eds., Elsevier, Amsterdam, 1995.

2. **The Colloid Chemistry of Silica**, H. E. Bergna, ed., Amer. Chem. Soc., Washington, D.C., 1994.

3. **Packings and Stationary Phases in Chromatographic Techniques**, K. K. Unger , ed., Marcel Dekker, New York, 1990.

4. R. P. W. Scott, **Silica Gel and Bonded Phases**, John Wiley & Sons, Inc., Chichester, 1993.

5. M. Jaroniec, in **Access in Nanoporous Materials**, T. J. Pinnavaia, M. F. Thorpe, eds., Plenum Publ. Co., New York, 1995, pp. 255-272.

6. S. J. Gregg, K. S. W. Sing, **Adsorption, Surface Area and Porosity**, Academic Press, London, 1982, 2nd Edition.

7. M. Jaroniec, R. Madey, **Physical Adsorption on Heterogeneous Solids**, Elsevier, Amsterdam, 1988.

8. M. v. Szombathely, P. Brauer, M. Jaroniec, J. Comput. Chem., **13**, 17-32 (1992).

9. C. Lastoskie, K. E. Gubbins, N. Quirke, J. Phys. Chem., **97**, 4786-4796 (1993).

10. C. Lastoskie, K. E. Gubbins, N. Quirke, Langmuir, **9**, 2693-2702 (1993).

11. J. P. Olivier, J. Porous Mater., **2**, 9-17 (1995).

12. J. P. Olivier, W. B. Conklin and M. v. Szombathely, Stud. Surf. Sci. Catal., **87**, 81-89 (1994).

13. W. A. Adamson, **Physical Chemistry of Surfaces**, John Wiley & Sons, Inc., New York, 1990.

14. M. Jaroniec, in **Adsorption and Chemisorption on Inorganic Oxides**, A. Dabrowski, V. A. Tertykh, eds., Elsevier, Amsterdam, 1995.

15. K. S. W. Sing, D. H. Everett, R. A. W. Haul, L. Moscou, R. A. Pierotti, J. Rouquerol, T. Siemieniewska, Pure Appl. Chem., **57**, 603-619 (1985).

16. J. Rouquerol, D. Avnir, C. W. Fairbridge, D. H. Everett, J. H. Haynes, N. Pernicone, J. D. F. Ramsay, K. S. W. Sing, K. K. Unger, Pure Appl. Chem., **66**, 1739-1758 (1994).

17. V. Bhagwat, Thesis, Kent State University, 1994.

PERFORMANCE AND ECONOMICS IN MICROPREPARATIVE CAPILLARY ELECTROPHORESIS OF OLIGOSACCHARIDES

András Guttman,[*][1] Edit Sperling,[2] István Mazsaroff[3]

[1]Beckman Instruments, Inc., Fullerton, CA 92714
[2]Gensia Laboratories, Inc., Irvine, CA 92714
[3]Genetics Institute, Inc., Andover, MA 01810

ABSTRACT

The advantages of micropreparative capillary gel electrophoresis include very high resolution, high speed and good recovery, with full automation. Nanomolar quantities of biopolymers, such as complex carbohydrates, can be collected for use in subsequent microsequencing or mass spectrometry. As in other preparative separation processes, the goal in preparative capillary gel electrophoresis is to maximize the production of a product with a given purity in the shortest time, i.e., to achieve the highest throughput. Another important factor is the economics of the operation. The cost of production in preparative capillary electrophoresis is a function of the cost of the automated system, the loading capacity of the capillary column and the system cycle time. Here we suggest a simple economic model for analyzing the economics of preparative capillary electrophoresis.

INTRODUCTION

Capillary electrophoresis is predominantly an analytical tool[1] but also can be used for micropreparative purposes.[2-15] The feasibility of micropreparation was demonstrated in the early work of Hjerten et al.[2] They used open tubular capillaries, employing sweep liquid at the outlet end of the capillary, to move the sample components into a conventional HPLC detector and, subsequently, into a fraction collector. By taking advantage of the electroosmotic flow, the liquid containing the sample components could be easily moved from the capillary into the fraction collector.[3] Others used porous glass junction with no flow interruption during fraction collection.[9] Zare and co-workers employed an on-column frit which enabled them to collect fractions without interrupting the flow and the electrophoretic process.[4] Karger and coworkers[10] suggested the use of sheath flow assisted design that is able to collect fractions with uninterrupted applied electric field. The preparative capability is enhanced by employing wider bore capillaries, e.g., 0.2 mm i.d. or larger. Using gel-filled capillaries, with no electroosmotic bulk flow, the end of the capillary is dipped into a small collection vial containing 1-5 μL of water or buffer and acts as collection device.[7-12] Field programming can also be very useful for precise preparation of a single peak from the closely migrating other components in a complex mixture.[12,13] Just recently, Rush and coworkers[14] reported on multiple sequential fraction collection of peptides and glycopeptides by CE under applied voltage. Biologically active species, peptides, proteins or DNA fragments, could be easily collected with high recoveries for microsequencing as well as other microcharacterization methods, using capillary electrophoresis in either open or gel-filled capillaries.[8,12,13,15] Some of the commercially available capillary electrophoresis units, however, are equipped with automated fraction collectors and, thus, feature micropreparative capability.[16]

In analytical work, the objective is to obtain information on the composition of the sample and to separate a large number of components in a short period of time. In preparative work, however, the goal is often the purification of only one or several components; therefore, the separation of the other components in the sample may be unimportant.[17,18] Consequently, in preparative applications, the electrophoretic parameters must be optimized differently than in analytical work.

One of the most important factors in preparative capillary electrophoresis, besides the technical parameters and variables, is the economics of the system. It is important to note that, in preparative capillary electrophoresis, the amount of the collected material is small (nano- or micromolar range), but its value may be high enough to consider microfraction collection. Therefore, cost should also be taken into account in the optimization of the parameters of preparative capillary electrophoresis. Capillary electrophoresis processing costs are

functions of the expense of the automated system, the loading capacity of the capillary column and the system cycle time. In this paper, we suggest an economic model for evaluating the efficiency of preparative capillary electrophoresis, based on loading capacity, product purity, yield, throughput and operating costs.

MATERIALS AND METHODS

Apparatus

In all these studies, the P/ACE™ system 5500 capillary electrophoresis apparatus (Beckman Instruments, Inc., Fullerton, CA, U.S.A.) was used in reversed (cathode on the injection side) polarity mode. The separations were monitored on-column by laser induced fluorescent (LIF) detection, employing a 4 mW Argon-ion laser with excitation wavelength of 488 nm/emission 520 nm. The temperature of the cartridge holding the gel filled capillary column was thermostated at $20^{\circ}C \pm 0.1^{\circ}C$ by the liquid cooling system of the P/ACE instrument. The electropherograms were acquired and stored on an IBM 486/66 MHz computer and were evaluated with the System Gold™ software package (Beckman Instruments, Inc., Fullerton, CA, U.S.A.).

Procedures

In the capillary gel electrophoresis experiments, the eCAP N-linked Oligosaccharide Profiling Kit (Beckman Instruments, Inc., Fullerton, CA) was used in conjunction of a PVA-I coated capillary column with a 20 cm effective length (27 cm total length, i.d. 50 μm /o.d. 375 μm). The samples were injected by pressure (0.5 psi, 5 sec) in the case of analytical or electrokinetically (10 kV for 10 sec) in the case of preparative load and reinjection of the collected fraction into the capillary. The fraction collection was accomplished by field programming, so the applied electric field strength was deceased from 1000 V/cm to 100 V/cm during collection in order to obtain higher precision.[8]

Chemicals

The maltooligosaccharide test mixture was labeled by 1-aminopyrene-3,6,8-trisulfonate (APTS) (both form Beckman Instruments, Inc., Fullerton, CA) via reductive amination as described elsewhere.[19] Fractions were collected into sample micro-vials containing 4 μL water.

The samples were stored at $-20^{\circ}C$ or freshly used. All the buffer solutions were filtered through a 0.20 μm pore size nylon filter and carefully vacuum degassed (100 mbar) before use.

THEORY

Maximum resolution in capillary gel electrophoresis for a given mixture requires optimization of the operational parameters such as effective column length, applied field strength, temperature, as well as composition of the buffer and the gel.[12,20,21] Resolution of any two components by capillary electrophoresis in a mixture is given by:[16]

$$R_s = 0.18 \, \Delta\mu_e (E \, l \, / D \, \bar{\mu}_e)^{1/2} \tag{1}$$

where $\Delta\bar{\mu}_e$ is the electrophoretic mobility difference between the two substances and μ_e is the arithmetic mean mobility for those species, E is the applied electric field, l is the effective length of the capillary and D is the diffusion coefficient of the solute in the gel-buffer system. Equation 1 demonstrates that, in capillary electrophoresis, higher potential gradients should lead to higher resolution. However, higher applied voltage increases Joule heating which, in turn, increases solute diffusion.

A concomitant increase in band spreading results in decreased separation efficiency. With longer effective column lengths, using the same applied electric field, the separation power can be increased in the price of longer migration time. Lower diffusion coefficients, due to lower temperature or higher media viscosity (higher polymer concentration and/or molecular weight), could also result in increased resolution. These separation variables must be optimized together with the preparative variables, such as sample load, yield, recovery, throughput and economics.

Similarly to preparative HPLC,[17,22] economical efficiency (E_f) in preparative capillary gel electrophoresis can be defined as the ratio of profit (P_r) and electrophoretic cycle time (t_c):

$$E_f = P_r/t_c \tag{2}$$

The difference between produced value and production cost gives profit. With production cost, feed value and product value related to unit mass of feed, economical efficiency can be expressed as a function of throughput, T_p:

$$E_f = T_p(v_p - c_E) - v_o m_o / t_c \tag{3}$$

where $T_p = m_p / t_c$ and m_p is the mass of product. v_p and c_E are the specific value of the product and the specific cost of the electrophoretic procedure; v_o and m_o are the specific value and mass of the feed with respect to the product. Although Equation 3 indicates that throughput may be increased by increasing m_p, this should not be at the expense of product purity, since lower purity reduces v_p and requires recycling of the overlapped fractions. Throughput can also be increased by decreasing the cycle time (t_c) of the process that strongly depends on the migration time of the solute, the recycle/re-equilibration time and the injection (feed) time. As long as the desired resolution between product and impurities is achieved, recycle/ re-equilibration time can be decreased in order to reduce cycle time. For example, the feed time can be decreased by increasing the injection voltage during electrokinetic injection.

Equation 4 shows the throughput as a function of feed (m_o):

$$T_p = \frac{m_0}{t_c}\Big[1 - (1 - p_0)r - p_0(1 - y_0)\Big] \tag{4}$$

Key parameters in this equation are the cleanup ratio, r (mass of removed impurities/total mass of impurities in the feed) and yield, y_o, of the desired product. Using these terms, the mass of impurities removed and the loss of the desired component can be written as: $m_o(1 - p_0)r$ and $m_o p_0(1 - y_o)$, respectively. In these expressions $p_0 = m_m / m_o$ is the purity of the initial feed and m_m is the mass of desired product in the feed.

RESULTS AND DISCUSSION

As a model, we have examined the capillary gel electrophoretic separation of APTS-labelled malto-oligosaccharide mixture in which the components differ only by one glucose unit between each other. Figure 1 shows the electropherograms of the malto-oligosaccharide test mixture in analytical (A) and preparative (B) injections as well as the reinjection of the collected glucose nonadekamer, (19-mer) (C) and octadekamer, (18-mer) (D). It is apparent that, in the analytical separation mode, all the components are well separated (Figure 1, trace A), but in the preparative mode (see overloading in Figure 1, trace B), they mostly overlap with each other. They even form doublets, suggesting that the local solute concentration is, probably, less than two orders of magnitude
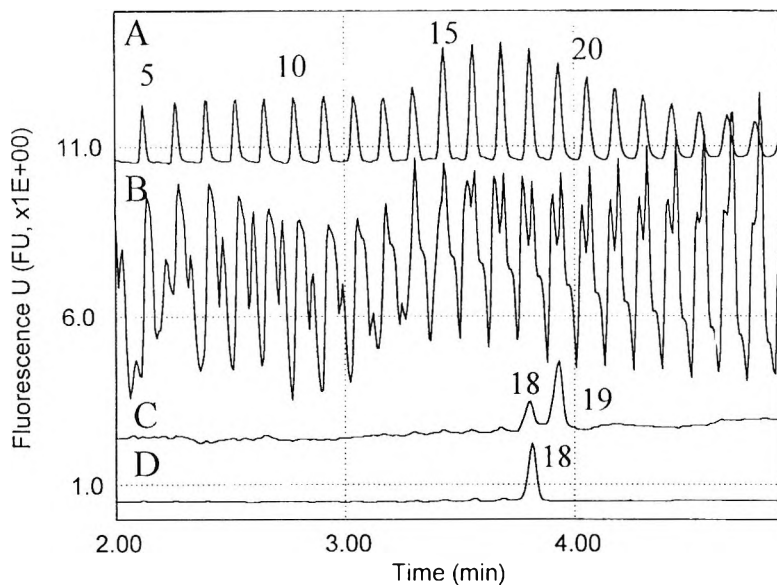
Figure 1. Capillary electrophoresis traces of the APTS-labelled malto-oligosaccharide test mixture in analytical (A) and preparative (B) separation modes and the re-injection of the collected nonadekamer, (19-mer) (C) and octadekamer, (18-mer) (D). Capillary: 270 x 0.05 mm (effective length, 200 mm); buffer, 25 mM acetate, pH 4.75; 0.4% polymeric additive; applied field, E = 1000 V/cm. The applied electric field during the fraction collection was 100 V/cm. Temperature: 20°C; LIF detection: excitation: 488 nm, emission: 520 nm. Injections: (A) 5 sec pressure, (B, C, and D): 10kV, 10 sec.

different from the background electrolyte concentration.[23] Figure 1, trace C shows the reinjection of the collected 19-mer. Figure 2 shows that the collection of the glucose nonadekamer (19-mer) began at point t_{19} - w_A and ended at point t_{19} + w_B (w_A and w_B are distances on the graph). Here, a fraction, but not all of the very closely migrating (m_{r18}) of the total mass of the 18-mer, is eliminated as the 19-mer is collected. The removed mass of 18-mer (m_{r18}) can be calculated:[17]

$$m_{r18} = \frac{m_{18}}{A_{18}} \int_{t=0}^{t_{19}-wA} c_{18} dt \qquad (5)$$

where A_{18} is the total peak area of the 18-mer (concentration x time units) and c_{18} is the concentration at time t. Although, it is not the case here, the fraction of any closely migrating succeeding peak (e.g. 20-mer) could be calculated
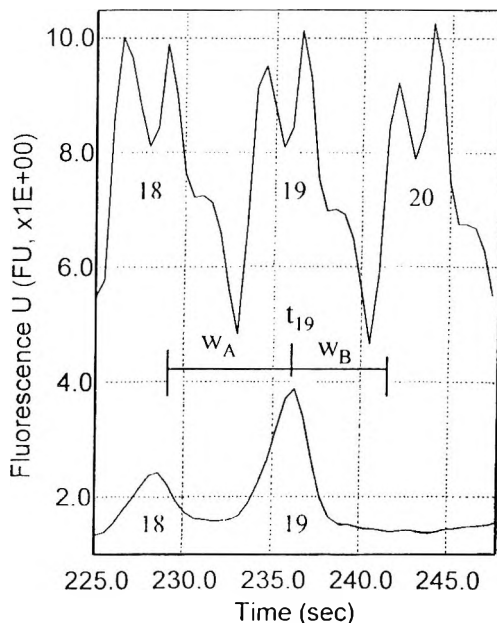
Figure 2. Preparative (upper trace) capillary electrophoretic separation of the APTS-labelled malto-oligosaccharide test mixture and the re-injection of the collected glucose nonadecamer (lower trace). The migration time of the 19-mer is t_{19}; w_A is the start and w_B is the end time of the fraction collection, respectively. Conditions are the same as in Figure 1.

likewise. Thus, the cleanup ratio for the 19-mer, which is contaminated only by the components immediately preceding and following, can be expressed as:

$$r_{19} = \frac{m_{r18} + m_{r20}}{m_{18} + m_{20}} \qquad (6)$$

Figure 1, trace C and Figure 2, lower trace, show the analytical electropherogram of the fraction collected between points w_A and w_B. As expected from Fig.2 and Equations 5 and 6, the main peak is the 19-mer and the small preceding peak is the 18-mer.

As Equation 1 shows, in capillary gel electrophoresis, resolution can be increased by increasing the applied voltage and the effective column length,[16] or by decreasing the diffusion coefficient of the solute by using higher concentration and/or molecular weight polymer in the separation buffer. Also,

decreasing the time window of the fraction collection $(w_A + w_B)$ will also increase the degree of purification at the expense of yield. Figure 1, trace D shows the very precise collection of the octadekamer (18-mer) with a decreased time window $[(w_A + w_B)_{18} < (w_A + w_B)_{19}]$.

Electric field programming has been proven very useful in capillary electrophoresis fraction collection.[12,19] Then, a higher field, which is employed prior to and after the collection of the desired peak, can also be used to improve collection. The field can be decreased to a low value (usually 1/10 of the separation field strength) during collection without introducing significant band broadening.[12] Using this approach, high resolution can be accomplished and maintained during fraction collection in a simplified way due to the wider time window.

For the calculation of the throughput (Eq. 4), one needs to know the overall cleanup ratio of the purification process. Based on the example above, and considering that m_j is the mass of the j-th impurity, the overall cleanup ratio, the sum of all cleanup ratios, can be expressed as:

$$r = \sum_{i=1(\neq k)}^{n} r_i = \frac{\displaystyle\sum_{i=1}^{k=1} \frac{m_i}{A_i} \int_{t_0}^{t_k - w_A} c_i \, dt + \sum_{i=k+1}^{n} \frac{m_i}{A_i} \int_{t_k + w_B}^{t_T} c_i \, dt}{\displaystyle\sum_{j=1(\neq k)}^{n} m_j} \qquad (7)$$

where n is the number of components, k is the required component and t_T the total separation time.

Sometimes, the required amount of material cannot be collected in a single separation step, or the purity of the collected fraction is not satisfactory. In both cases, further purification/collection steps are required and the overall economical efficiency of the process will depend on the efficiency of all the steps. When the same separation is repeated over and over, the overall economical efficiency of preparative capillary electrophoresis, E_f, is the same as that of a single cycle and the overall economical efficiency is independent of the value of the intermediate products. When production of the desired component requires several different separation steps, Bellmann's principle of optimality can be applied to optimize the total efficiency of the overall purification process.[24]

The minimum cost of purification in multiple electrophoretic steps can also be expressed in terms of yield and cleanup ratio:

$$\sum_{k=1}^{n} \frac{\sum_{i=1}^{n} T_{pi}c_i}{r_k} + \sum_{k=1}^{m} \frac{\sum_{i=1}^{n} T_{pi}c_i}{y_k} = 0 \tag{8}$$

where n is the number of electrophoretic procedures. This equation shows that either the cleanup ratio (r) or the yield (y) can be adjusted (at the expense of the other) to achieve the optimum.

Throughput, specific cost and profit should be optimized as a function of all independent variables in order to achieve maximum economical efficiency. All variables discussed above will affect the viability of the purification process.

CONCLUSIONS

In this paper, an economic treatment is presented for the evaluation of preparative capillary electrophoretic procedures. Compared to conventional slab gel electrophoresis, micropreparative capillary electrophoresis offers the advantages of higher speed (minutes), recovery and resolution, combined with automation. If non-denaturing gel systems are used, even biologically active species can be collected without losing their activities. Rapid preparative separations with wider bore capillary columns are possible using an efficient cooling system. Multiple injections can also increase production. Using a gel-filled capillary column with optimal conditions, pure fractions can be conveniently collected up to the low microgram range. Commercially available instruments, equipped with fraction collectors that are computer controlled, are necessary for routine operation.

ACKNOWLEDGMENT

REFERENCES

1. J. W. Jorgenson, K. D. Lukacs, Science, **222**, 266 (1983).

2. S. Hjerten, M. D. Zhu, J. Chromatogr., **327**, 157 (1985).

3. D. J. Rose, J. W. Jorgenson, J. Chromatogr., **438**, 23 (1988).

4. X. Huang, N. R. Zare, Anal. Chem., **62**, 443 (1990).

5. C. Fujimoto, Y. Muramatsu, M. Suzuki, K. Jinno, J. High Resosolut. Chromatogr., **14**, 178 (1991).

6. N. A. Guzman, M. A. Trebilcock, J. Advis, J. Liq. Chromatogr., **14**, 997 (1991).

7. N. A. Guzman, M. A. Trebilock, J. P. Avis, Anal. Chim. Acta, **249**, 247 (1991).

8. A. Guttman, A. S. Cohen, A. Paulus, B. L. Karger, H. Rodriguez, W. S. Hancock, in **Electrophoresis '88**, C. Shaefer-Nielsen (Editor), VCH Publishers, New York, 1988, p. 151.

9. T. M. Olefirowitz, A. G. Ewing, Anal. Chem., **59**, 1762 (1987).

10. O. Muller, F. Foret, B. L. Karger, Anal. Chem., **67**, 2974 (1995).

11. A. S. Cohen, N. T. Najarian, A. Paulus, A. Guttman, J. A. Smith, B. L. Karger, Proc. Natl. Acad. Sci., U. S. A., **85**, 9660 (1988).

12. A. Guttman, A. S. Cohen, D. N. Heiger, B. L. Karger, Anal. Chem., **62**, 137 (1990).

13. S. Pentoney, N. R. Zare, J. F. Quint, Anal. Chem., **61**, 1642 (1989).

14. H. J. Boss, M. F. Rohde, R. S. Rush, Poster presentation 587-T, 9th Symposium of the Protein Society, Boston, MA July 8-12, 1995.

15. E. Sperling, A. Guttman, I. Kifor, B. L. Karger, in **Proceedings of the First International Conference on Capillary Electrophoresis**, Boston, MA, April, 1989, p.137.

16. B. L. Karger, A. S. Cohen, A. Guttman, J. Chromatogr. **492**, 585 (1989).

17. I. Mazsaroff, F. Regnier, J. Liquid Chrom., **9**, 2563 (1986).

18. R. M.Nicoud, H. Colin, LC/GC **8**, 24 (1990).

19. A. Guttman, F.-T. A. Chen, R. A. Evangelista, N. Cooke, Anal. Biochem., **233**, 234 (1996).

20. A. Guttman, C. Starr, N. Cooke, Electrophoresis, **15**, 1518 (1995).

21. A. Guttman, T. Pritchett, Electrophoresis, **16**, 1906 (1995).

22. F. Frenz, Cs. Horváth, J. Chromatogr., **282**, 249 (1983).

23. R. E. P. Mikkers, F. M. Everaerts, Th. P. E. M. Verheggen, J. Chromatogr., **169**, 1 (1979).

24. R. Bellmann, **Dynamic Programming**, Princeton Univ. Press, Prinecton, NJ, 1957.

QUANTITATIVE DETERMINATION OF AROMATIC AMINO ACIDS AT PROTEIN SURFACE BY SIZE EXCLUSION HPLC COUPLED WITH SECOND ORDER DERIVATIVE SPECTROSCOPY

Qiuyu Zhao,* Catherine Lecoeur, Frederic Sannier
Isabelle Garreau, Jean Marie Piot

Laboratoire de Génie Protéique et cellulaire
Pôle des Sciences et Technologies
Université de La Rochelle
Av. Marillac
17042 - La Rochelle Cédex 1, France

ABSTRACT

Second order derivative spectroscopy in the ultraviolet (UV) region has the potential to detect subtle differences in the environments of the aromatic residues of proteins. We show here that second order derivative UV spectrum of protein can be a tool to determine quantitatively the aromatic amino acid apparent composition "AAAAC" at protein surface. This non destructive method allows us to obtain conformational information for protein structure-function research and for protein identification in chromatographic process.

INTRODUCTION

Size exclusion high-performance liquid chromatography (SE-HPLC) has been for a long time a widely used technique for both purification and analysis of proteins and peptides. Many applications of SE-HPLC in the research of proteins, such as molecular weight estimation,[1,2] analysis of protein folding[3] and on line conformational monitoring of proteins[4] were investigated. This can sometimes yield many useful informations in protein structure research.

Advances in HPLC photodiode array detection technology have made possible not only to carry out the fly-real time spectral scanning during the chromatographic process, but also to obtain derivative spectra simultaneously.[5-7] Derivative spectroscopy has become a very useful analytical tool to identify and determine aromatic amino acids in proteins and peptides.[8-10]

Derivative spectroscopy offers the advantage of sharper spectral features compared to conventional absorbance (i. e. zero order derivative) spectroscopy. For instance, a peak shoulder present in a zero order derivative spectrum can be transformed into a peak minimum when the second order derivative spectrum is obtained. Furthermore, overlapping band can be transformed into resolved bands.[10] Each aromatic amino acid (Phe, Tyr and Trp) shows a unique near-UV spectrum. Since there is no appreciable peptide bond absorbance above 240 nm,[10] analysis of a second order derivative spectrum from 240 nm to 300 nm shows whether single or multiple aromatic amino acids are present. The determination of three aromatic amino acids in proteins in the presence of denaturant by second derivative spectrometry has been already reported[11-13] and the detection of completely exposed aromatic residues in the denatured proteins was achieved.

In a previous study,[14] we defined the term amplitude as the absorption minima at a specific wavelength for each aromatic amino acid in order to quantify it. Consequently, taking into account that absorption of each aromatic amino acid is additive, one can determine a ratio of one aromatic amino acid to another.[14] Furthermore, the amplitude of minima at certain wavelength is proportional to the amount of each aromatic amino acid. This led us to use free aromatic amino acids as standard to determine the quantity of aromatic amino acids at protein surface by SE-HPLC coupled with on line photodiode array detection. These exposed aromatic residues are often important conformational markers for protein structure function research.[15]

The aim of our paper was to get information about proteins conformations and to apply it for further protein identification during chromatographic process by a non-destructive method.

MATERIALS AND METHODS

All common chemicals and solvents were of analytical grade from commercial sources. Tryptophan, tyrosine, phenylalanine, horse myoglobin (From horse skeletal muscle) and carbonic anhydrase (EC 4.2.1.1. from bovine erythrocytes) were purchased from Sigma Chemicals.

Purification of Yellowfin-Tuna Myoglobin

Myoglobin was isolated from the red skeletal muscle of yellowfin-tuna using a method adapted from Suzuki procedure.[16] The red skeletal muscle of yellowfin-tuna was supplied from Paulet Society (Douarnenez, France). The tissue was homogeneized in distilled water (1:1, w:v) in an ice cold waring blendor. The suspension was then centrifuged (3000 g, 15min., 4°C). The solution was saturated to 60% (w/v) by addition of solid ammonium sulfate.

After centrifugation (3000 g, 15min., 4°C), the precipitate was discarded and the supernatant was saturated to 80% (w/v) with solid amonium sulfate. The new precipitate obtained after centrifugation (3000 g, 15min., 4°C) was dissolved in water and then ultrafiltered and diafiltered (PTGC type membrane, Millipore, 10 KD cut-off) against water.

The crude solution was then loaded on a D.E.A.E Sephacel column (3 cm i.d. x 32 cm.) equilibrated with 50 mM Tris - HCl buffer (pH 8.6). Pure myoglobin was firstly eluted with the same buffer at a flow rate of 60 mL/h. Other impurities were subsequently eluted with the same buffer containing 0.2 M NaCl.[17]

Aromatic Amino Acid Solution Preparation

Tryptophan, tyrosine and phenylalanine were dissolved in 10 mM ammonium acetate buffer pH 6.0 at different concentrations (5.00×10^{-2}, 1.25×10^{-2}, 3.13×10^{-3}, 7.81×10^{-4}, 1.95×10^{-4}, 4.80×10^{-5}, 1.20×10^{-5}, 6.00×10^{-6}, 3.00×10^{-6}M) for calibration curve analyses in SE-HPLC system.

Other solutions of phenylalanine and tyrosine (5.00×10^{-3}M, 5.00×10^{-4} M) and tryptophan (5.00×10^{-4}M, 5.00×10^{-5}M) were prepared to investigate the effect of injected volume on the chromatographic resolution.

Preparation of Protein Solutions

For SE-HPLC analysis, tuna myoglobin, horse mylglobin and carbonic anhydrase were dissolved in 10 mM ammonium acetate buffer pH 6.0 to the respective concentrations (8.28 x 10^{-4}M (14.00g/L), 2.19 x 10^{-3}M (37.00g/L) and 4.66 x 10^{-4}M (13.50g/L)).

HPLC System

The liquid chromatographic system consisted of a Waters 600 automated gradient controller-pump module, a Waters Wisp 717 automatic sampling device and a Waters 996 photodiode array detector. Spectral and chromatographic data were stored on a NEC image 466 computer. Millennium software was used to plot, acquire and treat chromatographic data.

Mobile phase for TSK G2000 SWG column (7.6 mm i.d. x 600 mm)

The mobile phase consisted of 10 mM ammonium acetate buffer pH 6.0. The flow rate was 0.75 mL/min. Samples were dissolved in the same buffer, filtered through 0.22 μm filters and injected.

Procedure

In order to investigate response pattern between the second order derivative absorbance of tryptophan, tyrosine and phenylalanine and their amounts in SE-HPLC system, 10 μL and 20 μL of each solution (from 3.00 x 10^{-6} to 5.00 x 10^{-2}M) of aromatic amino acid were loaded on a TSK G2000SWG column.

The other solutions of phenylalanine and tyrosine (5.00 x 10^{-3}M, 5.00 x 10^{-4}M) and tryptophan (5.00 x 10^{-4}M, 5.00 x 10^{-5}M) were loaded on the same column under the same conditions with injected volume from 5 μl to 160 μl to investigate the effect of injected volume on the chromatographic resolution.

5 μL to 40 μL of tuna myoglobin, horse myoglobin and carbonic anhydrase solutions were chromatographed at room temperature on the TSK G2000 SWG column respectively, under conditions described above.
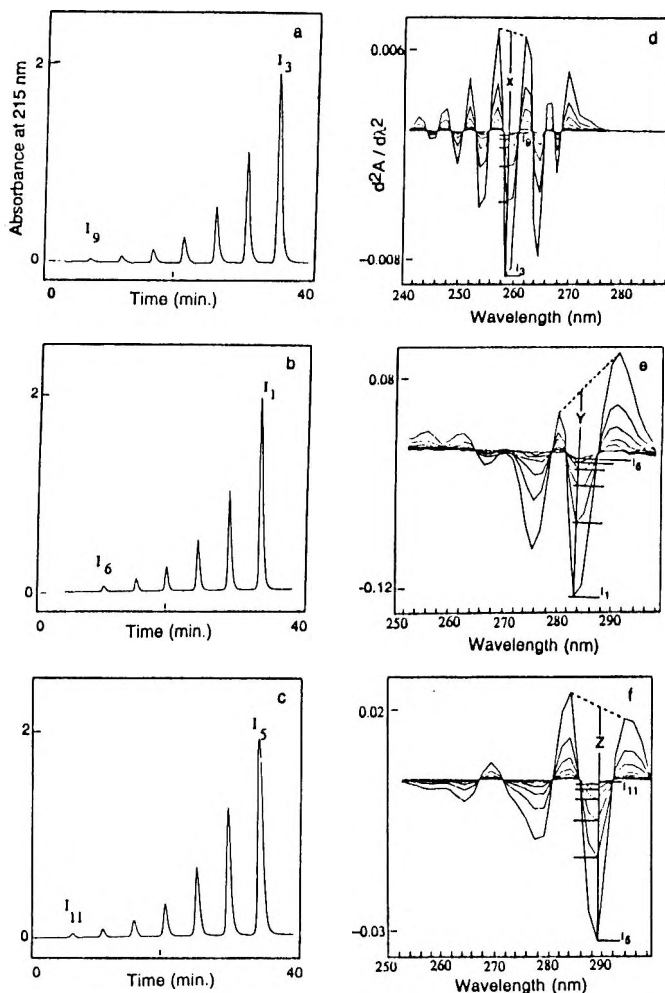
Figure 1. The chromatographic profiles and the second order derivative spectra of phenylalanine (a,d), tyrosine (b,e) and tryptophan (c,f) obtained in SE-HPLC system under the conditions described in experimental section.   The amounts and the volume of injection were as follows: I_1 : 1000 nmoles / 20 μL, I_2 : 500 nmoles / 10 μL, I_3 : 250 nmoles / 20 μL, I_4 : 125 nmoles / 10 μL, I_5 : 62.5 nmoles / 20 μL, I_6 : 31.25 nmoles / 10 μL, I_7 : 15.6 nmoles / 20 μL, I_8 : 7.8 nmoles / 10 μL, I_9: 3.9 nmoles / 20 μL, I_{10} : 1.95 nmoles / 10 μL, I_{11} : 0.975 nmoles / 20 μL. X, Y, Z represented the amplitude of Phenylalanine (I_3), Tyrosine (I_1) and tryptophan (I_5).

On-line instantaneous UV absorbance spectral scans were performed between 200 nm and 300 nm with a rate of one spectrum/second for all chromatographic acquisitions. The resolution was 1.2 nm. The results of chromatographic analyses were completed by using Millennium software.

RESULTS AND DISCUSSION

The chromatographic behavior of free aromatic amino acids was investigated firstly. Under our chromatographic conditions, the retention times for the three aromatic amino acids were 31 (Tyr), 32 (Phe) and 35 minutes (Trp) (not shown). Consequently, for each amino acid, series of injections were carried out at the rate of one injection every four minutes. After six or seven injections, the chromatographic and spectral acquisition was started and lasted 40 minutes.

As an example, the peaks corresponding to the increasing amounts injected are displayed in Figure 1 (a,b,c). Their second order derivative spectra between 240 nm and 300 nm are presented on Figure 1 (d,e,f). This indicated that even when the amount of aromatic amino acids changed, the wavelength of inflection point did not vary. This phenomenon was observed and used to determining of aromatic residues in denatured proteins by second order derivative spectrometry.[11]

The same process was repeated to cover ranges between 0.03 and 1000 nmoles (10 or 20 µL injected). As described previously,[14] in second order derivative spectra, X, Y and Z represented the amplitudes of minima at their specific wavelength for Phe (258.5nm), Tyr (283.5nm) and Trp (289.5nm). The amplitudes at their specific wavelength were directly proportional to the aromatic amino acids content. In our chromatographic system (SE-HPLC), free aromatic amino acids were used as standards for calibration curve.

Very good response patterns (Figure 2) are illustrated by the correlation factors r: 0.999 (Phe), 1.000 (Tyr) and 0.996 (Trp). Linear responses were observed from 4 to 1000 nmoles (Phe), 1 to 1000 nmoles (Tyr) and 0.25 to 250 nmoles (Trp) (Figure 2 A, B, C). Identical response patterns for low concentration were displayed in Figure 2 (a, b, c). The slope of the three curves were 6.52×10^{-5} (Phe), 1.60×10^{-4} (Tyr) and 7.26×10^{-4} (Trp) $d^2A/d\lambda^2$ (nmole)$^{-1}$. Both linear responses and curve slopes indicated that the detection sensibility and accuracy for tryptophan is about 4.5 times higher than for Tyr and 10 times higher than for Phe. This is in good agreement with the relative values of the molar extinction coefficient of three aromatic amino acids ($\varepsilon_{Trp} >$ $\varepsilon_{Tyr} > \varepsilon_{Phe}$). These results were very similar to that obtained in simple second order derivative spectrometry.[11]
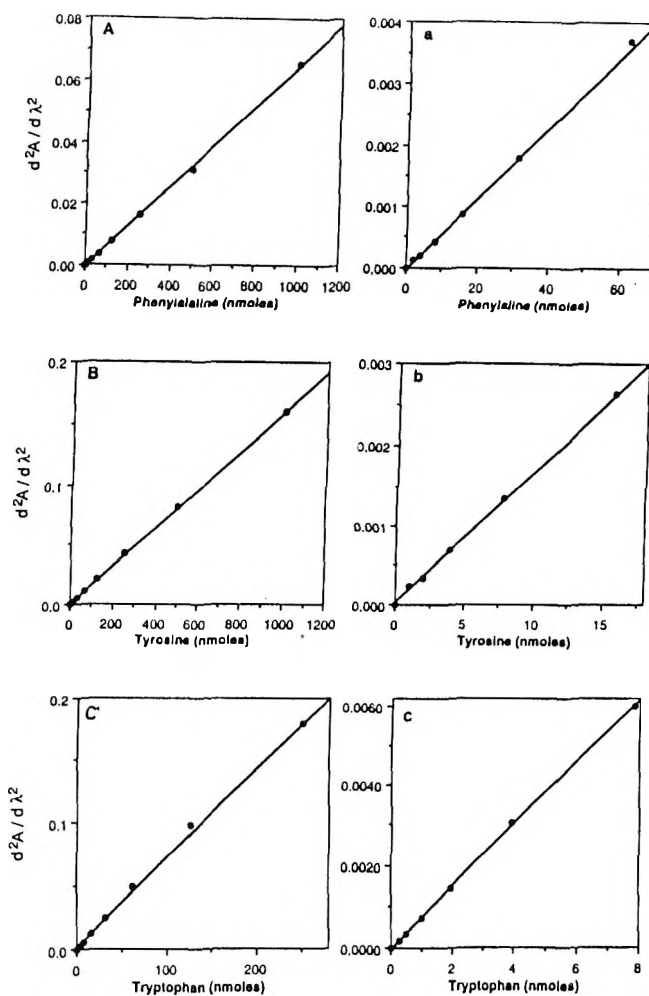
Figure 2. Linear plots of second order derivative absorbances obtained from the analysis on a TSK G2000 SWG column of free aromatic amino acids in SE-HPLC system. The amplitude at 258.5 nm (phe), 283.5 nm (tyr) and 289.5 nm (trp) in great and small quantitiy ranges were displayed for phenylalanine (A, a), tyrosine (B, b) and tryptophan (C, c).

As far as the injection volume is concerned its influence towards chromatographic resolution was demonstrated.[1] In the above results, the volumes of injection varied from 10 μL to 20 μL. Figure 3 (A, B, C) presents
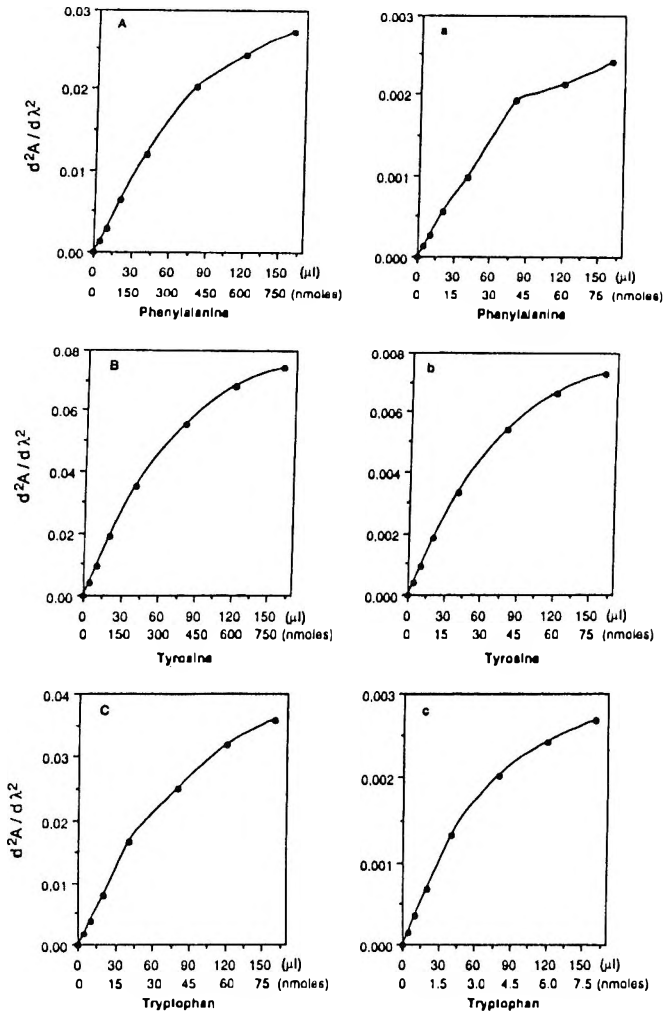
Figure 3. The response pattern between second order derivative absorbances at 258.5 nm (phe), 283.5 nm (tyr) , 289.5 nm (trp) and the injection volume, obtained from the analysis on a TSK G2000 SWG column of free aromatic amino acids in SE-HPLC system. The concentration were 5.00×10^{-3} M for A and B, 5.00×10^{-4} for a, b, C, and 5.00×10^{-5} M for c.

the same calibration curve as in Figure 2 except for the injection volumes varying from 5 μL to 160 μL. The quantities of aromatic amino acids in these

volumes were roughly the same as in Figure 2. For injection volume over 60 µL, the linear relation between injected volume of 5.00 X 10^{-3}M (Phe and Tyr) and 5.00 X 10^{-4}M (Trp) solution and amplitudes was no longer verified. This was also observed for ten times lower concentration solutions of aromatic amino acids (Figure 3 a,b,c). As a result to obtain linear response, the calibration must be carried out with small injected volume (below 60 µL).

These optimal conditions for aromatic amino acids were further applied to their determination in native proteins. In this work, acetate ammonium buffer (10 mM, pH 6) was used as mobile phase and gave good resolutions for tuna myoglobin, horse myoglobin and bovine carbonic anhydrase as described below.

The investigation was firstly performed with tuna myoglobin which was extracted from the red skeletal muscle under conditions described in experimental section. Tuna myoglobin which is a heme metalloprotein offered an interesting test case for the second order derivative spectrophotometric analyses, since it showed non-zero absorption in the near UV region.[11] This absorption interferred with the application of the normal absorbance method of Edelhoch[18] for determining tryptophan residues by having broad absorption bands from the visible to UV region.[19]   Second order derivative spectrophotometry appeared to resolve these difficulties. Series of injections (5µL to 40µL) of a prepared tuna myoglobin solution (8.28 X 10^{-4}M) were performed on a TSK G2000SWG column. Figure 4 (a) shows one of the chromatographic profiles. Prior to spectral investigations, the purity of tuna myoglobin was checked. A peak integration gave 93% purity for myoglobin. Taking into accounts this results, the real myoglobin concentration was rectified to 7.70 X 10^{-4}M (Table 1).

The known tuna myoglobin molecular sequence comprise one tryptophane, two tyrosine and six phenylalanine residues.[20] Consequently when all aromatic amino acids could be totally detected, the following molar ratios should be verified: Myoglobin/Trp/Tyr/Phe = 1/1/2/6.

Figure 4 (d) shows one second order derivative spectrum of tuna myoglobin. The amplitudes at specific wavelengths allowed us to calculate the amounts of Phe and Trp using free aromatic amino acids calibration curves. The amount of tyrosine was specifically determined by the method previously described.[14] Figure 5 shows the proportionality between myoglobin amount injected and aromatic amino acids quantities detected. The molar ratios for Myoglobin/ Trp/ Tyr/ Phe were determined as: 1.00/1.00/0.57/2.98 [Calculated as follows: $(7.70 \times 10^{-4}/7.70 \times 10^{-4}) / (7.63 \times 10^{-4}/7.70 \times 10^{-4}) / (4.42 \times 10^{-4}$

Table 1

Determination of Aromatic Amino Acids at Protein Surface

		Proteins		
		Tuna Myoglobin	**Horse Myoglobin**	**Carbonic Anhydrase**
Protein concentration $(10^{-4}M)$		7.7	20.1	3.88
Aromatic amino acids concentration determined by second derivative spectra $(10^{-4}M)$	Phe	23	30.7	17.0
	Tyr	4.42	0.0	0.0
	Trp	7.63	1.17	7.87
Mole of aromatic amino acids for one mole of protein (Theoretical)	Phe	6	6	19
	Tyr	2	2	8
	Trp	1	2	7
Mole of aromatic amino acids for one mole of protein (Experimental)	Phe	2.98	1.4	4.38
	Tyr	0.57	0	0
	Trp	1	0.53	2.03
Exposure degree of aromatic amino acids at protein surface (%)	Phe	49.7	25.5	23.1
	Tyr	29.0	0.00	0.00
	Trp	100	28.2	29.0
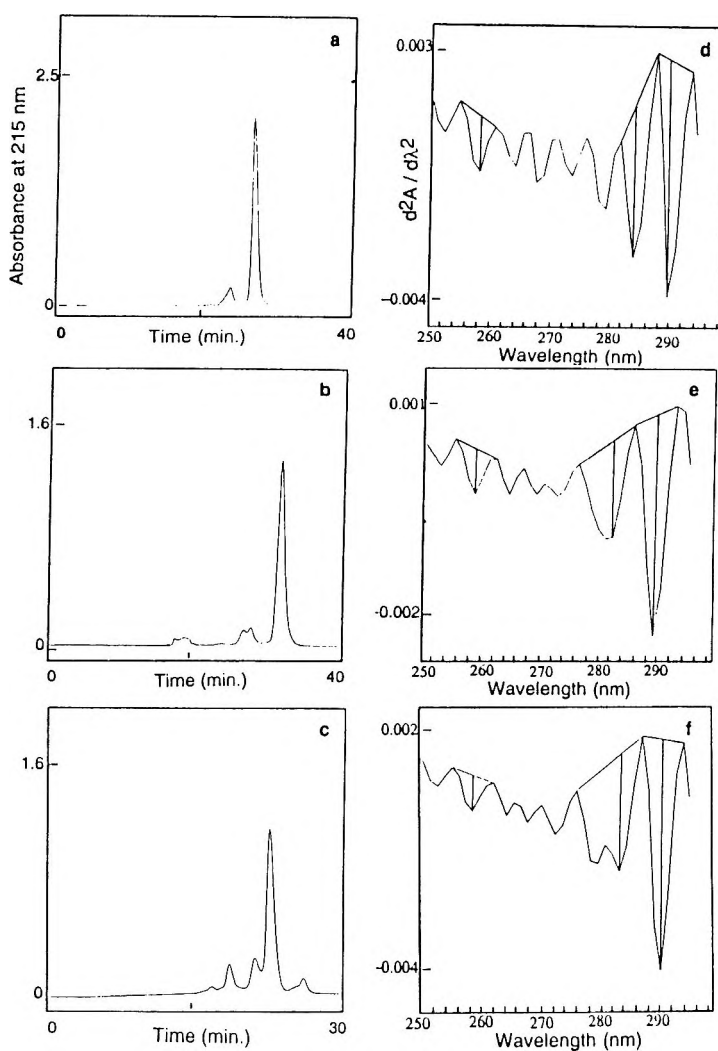
Figure 4. The chromatographic profiles and the second order derivative spectra of 10 μL (prepared concentration: 8.28 x 10^{-4} M) tuna myoglobin (a,d), 5 μL (prepared concentration: 2.19 x 10^{-3} M) horse myoglobin (b,e) and 10 μL (prepared concentration: 4.66 x 10^{-4} M) carbonic anhydrase (c,f) obtained in SE-HPLC system under the conditions described in experimental section.

/ 7.70×10^{-4}) / ($23.00 \times 10^{-4}/7.70 \times 10^{-4}$)]. The comparison of theoretical and experimental molar ratios allowed us to conclude that the aromatic amino acids were not fully accessible to this detection method. Indeed some aromatic amino acids residues were buried inside the protein and not detected, thus the degree of exposure of aromatic amino acids at surface of native proteins could be calculated.[13] Whenever 100% Trp could be detected, the percentage for Tyr and Phe were 28.96% (0.57/2) and 49.67% (2.98/6) respectively (Table 1). Consequently, it could be concluded that the accessibility of aromatic amino acid to the detection method is related to their spacial position in the protein. Thus the more aromatic amino acids are exposed at the protein surface, the more they are detected. On the other hand, the more aromatic amino acids are buried inside the protein, the less they are detected. As far as the tuna myoglobin is concerned, the tryptophan residue is fully exposed at the molecule surface under our non-denaturing conditions. In the same way, globally 28.96% of Tyr and 49.67% of Phe residues are exposed at the surface.

The localisation of aromatic residues within the crystallographic structure of tuna myoglobin[21] confirmed that the aromatic cycle of tryptophan in position 14 was totally situated at the myoglobin molecule surface. The aromatic cycle of tyrosine 21 was partly exposed at the surface whereas Tyr 146 was buried inside myoglobin molecule. As far as phenylalanine is concerned, the classification of the residues with regard to their exposition degree, from totally exposed at the surface to fully buried, was the following: Phe 7 and Phe 151 (100% exposed) > Phe 46 > Phe 43 and Phe 33 > Phe 104 (0% exposed). This information was in very good agreement with the results obtained by our determination (Table 1).

A similar protein, horse myoglobin was then investigated. It contains two tryptophan, two tyrosine and six phenylalanine residues giving a molar ratio for myoglobin/Trp/Tyr/Phe of 1/2/2/6.[22] Figures 4-b and 4-e show the chromatographic profile and second order derivative spectrum. Impurity was calculated by area integration as 8.30% giving a real myoglobin concentration of 7.70×10^{-4}M (Table 1). As for tuna myoglobin, the ratios for myoglobin/Trp/Tyr/Phe were measured as 1.00/0.53/0.00/1.40 [Calculated as following: ($20.10 \times 10^{-4}/20.10 \times 10^{-4}$) / ($11.70 \times 10^{-4}/20.10 \times 10^{-4}$) / ($0.00/20.10 \times 10^{-4}$) / ($30.70 \times 10^{-4}/20.10 \times 10^{-4}$)]. The aromatic amino acids exposure degrees at the molecule surface were then calculated and displayed in Table 1. It indicated that the two tyrosine residues were completely buried inside the molecule. The two tryptophan residues were globally exposed at 28.51% and the six phenylalanine residues at 25.46%. The crystal structure of horse myoglobin indicated that the localisation of aromatic residue within this molecule[23] had a very good correspondance with our calculated results.
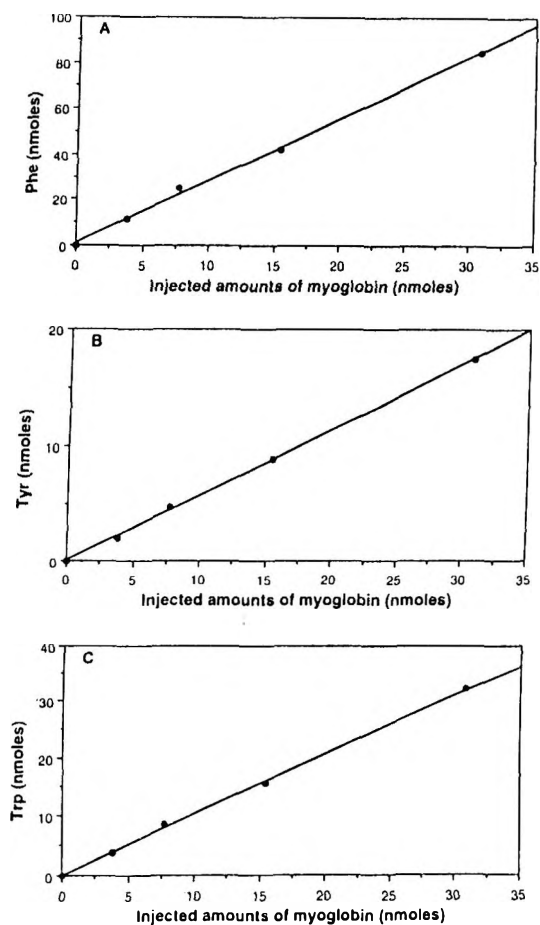
Figure 5. Relation between aromatic amino acid amounts and the different injection quantities of tuna myoglobin in SE-HPLC system under the conditions described in experimental section. The amounts of Phe (A), Tyr (B) and Trp (C) were determined by their second order derivative spectra using free aromatic amino acids calibration curve in Figure 2.

It can be seen that the investigation of horse and tuna myoglobin in SE-HPLC system gave a great difference in exposure degrees of aromatic amino acids at the surface of the molecules. Consequently, these two similar myoglobins could be easily distinguished by the above characteristics.

Carbonic anhydrase (MW: 29000 Dalton) was selected arbitrarily. It contains 7 Trp, 8 Tyr and 19 Phe residues giving a molar ratio for carbonic anhydrase/Trp/Tyr/Phe of 1/7/8/19.[24]   Figures 4-c and 4-f show its chromatographic profile and second order derivative spectrum. Impurity was calculated as 16.7% giving a real concentration of 3.88×10^{-4}M. According to their second derivative spectra, the ratio for carbonic anhydrase/Trp/Tyr/Phe were measured as 1.00/2.03/0.00/4.38 [Calculated as following: (3.88×10^{-4} /3.88×10^{-4}) / (7.87×10^{-4}/3.88×10^{-4}) / ($0.00/3.88 \times 10^{-4}$) / ($17.00 \times 10^{-4}/3.88 \times 10^{-4}$)]. Exposure degrees of aromatic amino acids at surface of this molecule were calculated as 23.05% (Phe), 0.00% (Tyr) and 28.96% (Trp) (Table 1).

From all above results, the molar ratio between aromatic amino acids at surface of proteins was investigated These calculated ratios are presented in Table 1. These results indicated a conformational state of these proteins in our non denaturing conditions. So it could be postulated that under defined conditions, these ratios were constant and constitute parameter termed as "apparent aromatic amino acid composition" (A.A.A.A.C.) useful for further protein characterization. This parameter is furthermore easily accessible by second order derivative spectroscopy. The fluctuation of this "A.A.A.A.C." for one given protein might indicate a conformational change.[25] It could also be used as a "marker" to identify precisely and follow a protein during a purification process, and assess a protein purity. For example, in spite of very similar amino acid composition and molecular weights, horse and tuna myoglobin are definitely and unambigously distinguishable.

In conclusion, these studies appear to indicate the important role of aromatic amino acid in proteins identification. A method was developed here to determine the A.A.A.A.C. of a protein and characterize it. The conformational change of proteins resulting in aromatic amino acid exposure modification could also be detected by this method. In conclusion, it could be very useful in protein conformation research and for protein structure-function investigation.

REFERENCES

1. G. D. Swergold, S. R. Charles, Anal. Biochem., **131**, 295-300 (1983).

2. G. B. Irvine, C. Shaw, Anal. Biochem., **155**, 141-148 (1986).

3. E. Stellwagen, W. Shalongo, in **High Performance Liquid Chromatography of Peptides and Proteins**, C. T. Mant, R. S. Hodges, eds, CRC Press, pp 599-604, 1991.

4. S. Wu, B. L. Karger in **High Performance Liquid Chromatography of peptides and proteins,** C. T. Mant, R. S. Hodges, eds, CRC Press, pp 613-621, 1991.

5. B. Grego, E. Nice, R. Simpson, J. Chromatogr., **352,** 359-368 (1986).

6. F. Nyberg, C. Pernow, U. Moberg, R. Eriksson, J. Chromatogr., **359,** 541-551 (1986).

7. A. Fell, B. Clark, H. Scott, J. Chromatogr., **297,** 203-214 (1984).

8. D. E. H. Palladino, K. A. Cohen, J. Chromatogr. Sci., **29,** 91-97 (1991).

9. P. Zavitsanos, P., H. Goetz, in **High Performance Liquid Chromatography of Peptides and Proteins**, C. T. Mant, R. S. Hodges, eds, CRC Press, pp. 553-562, 1991.

10. J. A. Black, R. S. Hodges, in **High Performance Liquid Chromatography of Peptides and Proteins**, C. T. Mant, R. S. Hodges, eds, CRC Press, pp. 563-570, 1991.

11. Y. Nozaki, Arch. Biochem. Biophys., **277(2)**, 324-333 (1990).

12. T. Ichikawa, H. Terada, Biochim. Biophys. Acta., **671**, 33-37 (1981).

13. R. Ragone, G. Colonna, C. Balestri, L. Servillo, G. Irace, Biochemistry, **23**, 1871-1875 (1984).

14. Q. Y. Zhao, I. Garreau, F. Sannier, J. M. Piot, J. Liq. Chromatogr., **18**, 1077-1092 (1995).

15. H. Mach, C. R. Middaugh, Anal. Biochem., **222**, 323-331 (1994).

16. T. Suzuki, Y. Sugawara, Y. Satoh, J. Chromatogr., **195**, 277-280 (1980).

17. W. D. Brown, J. Biol. Chem., **238(8)**, 2238-2240 (1961).

18. H. Edelhoch, Biochemistry, **6**, 1948-1954 (1967).

19. Y. Nozaki, Arch. Biochem. Biophys., **249**, 437-446 (1990)

20. D. A. Watts, R. H. Rice, W. D. Brown, J. Biol. Chem., **255**, 10916-10924 (1980).

21. G. I. Birnbaum, D. R. Rose, M. Przybylska, to the PDB DATA BANK, 1993.

22. G. D. Fasman, in **Handbook of Biochemistry and Molecular Biology**, 3rd ed., Vol. 3, CRC Press, pp. 437-440, 1976.

23. S. V. Evans, G. D. Brayer, J. Mol. Biol., **213**, 885-897 (1990).

24. J. M. Gulian, N. Limozin, B. Mallet, J. Di Costanzo, M. Charrel, Biochimie, **59**, 293-302 (1977).

25. J. A. Kornblatt, M. J. Kornblatt, G. H. B. Hoa, Biochemistry, **34**, 1218-1223 (1995).

CHIRAL SEPARATION OF REDUCED HALOPERIDOL BY CAPILLARY ZONE ELECTROPHORESIS WITH HEPTAKIS (2,6-DI-O-METHYL)-β-CYCLODEXTRIN

H. L. Wu*, K. Otsuka#, S. Terabe#

* Graduate Institute of Pharmaceutical Sciences
Kaohsiung Medical College
Kaohsiung, Taiwan 807, ROC

Department of Material Science
Faculty of Science
Himeji Institute of Technology
Kamigori, Hyogo, 678-12, Japan

ABSTRACT

A simple capillary zone electrophoresis was developed for the chiral separation of reduced haloperidol, a chiral metabolite of antipsychotic drug, haloperidol. Reduced haloperidol was separated in a phosphate buffer (pH 2.5) using heptakis (2,6-di-O-methyl)-β-cyclodextrin as a chiral selector. Several parameters such as type of cyclodextrin, pH and concentration of buffer, applied voltage, concentration of chiral selector and detection wavelength that affected the chiral separation and detection of reduced haloperidol were discussed.

1567
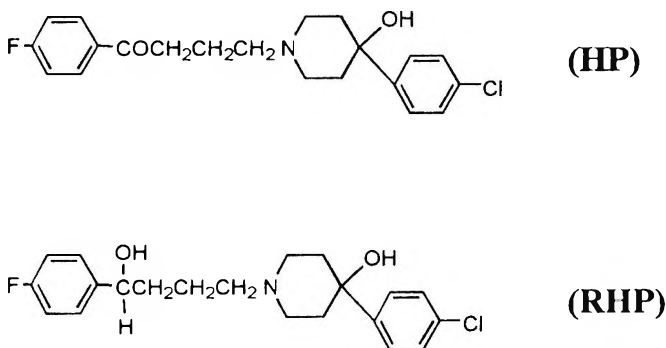
Figure 1. Chemical structures of haloperidol (HP) and reduced haloperidol (RHP).

INTRODUCTION

Haloperidol (HP) is one of the most widely used drugs for the treatment of schizophrenia and related psychotic disorders. After administration of HP, it is partly biotransformed to reduced haloperidol (RHP), a chiral metabolite as shown in Fig. 1.

Monitoring the plasma levels of both HP and RHP has been suggested as a better therapeutic indicator for patients undergoing HP treatment, but there are inconsistent reports[1-4] that a higher RHP to HP ratio in plasma is good or bad for therapeutic response. Since RHP is an optically active species, the enantiomeric composition of RHP and its possible role in HP therapy is of great interest.

A variety of liquid chromatographic (LC) methods[5-30] have been used for the analysis of HP/RHP in various samples, but only limited method[31] demonstrated the separation of synthetic RHP by LC with chiral column. In this report a preliminary work on the chiral separation of RHP by capillary electrophoresis (CE) with neutral cyclodextrin was performed.

The results indicated that the enantiomers of RHP can be simply resolved by CE in acidic phosphate buffer with heptakis (2,6-di-O-methyl)-β-cyclodextrin (dimethyl-β-CD) as a chiral selector. This may be a favorable step to investigate the chiral profile of RHP in HP therapy.

METHODS

Apparatus

A Beckman P/ACE system 2000 (CA, USA) equipped with a filtered UV detector and with a liquid-cooling device was used. Capillary zone electrophoresis was performed in a neutral coated capillary (Beckman) of 37 cm X 50 μm I.D. (effective length, 30 cm). Samples were injected by pressure for 1 s, equivalent to a volume of about 1.78 nL (according to the specification of the manufacturer) and the applied voltage was 22 kV. Separations were achieved at about 21°C with phosphate buffer (40 mM, pH 2.5) including dimethyl-β-cyclodextrin (10mM). The above-mentioned CE conditions were used for the general experiment unless stated otherwise.

Chemicals and Solutions

RHP (Janssen, Olen, Belgium), HP (Aldrich, WI, USA), dimethyl-β-cyclodextrin (dimethyl-β-CD), β-cyclodextrin (β-CD), γ-cyclodextrin (γ-CD) and hydroxypropyl β-cyclodextrin (HP-β-CD) (Beckman), α-cyclodextrin (α-CD), phosphoric acid (H_3PO_4) and disodium hydrogen phosphate (Na_2HPO_4) (Nacalai, Osaka, Japan), heptakis (2,3,6-tri-O-methyl)-β-cyclodextrin (TM-β-CD), 6-O-α-maltosyl-α-CD, sodium dihydrogen phosphate (NaH_2PO_4) and hydrochloric acid (Wako, Osaka, Japan) were used without further treatment. Milli-Q (Millipore, CA, USA) treated water was used for the preparation of buffer and related aqueous solutions.

Solutions of various phosphate buffers at pH 2.5 or 4.5 were obtained by neutralizing related NaH_2PO_4 solution with H_3PO_4 solution, each at same concentration; solutions of phosphate buffer at pH 6.5 were prepared by neutralizing Na_2HPO_4 solutions with H_3PO_4 solution, each at same concentration. Stock solutions of RHP (1.0 mM) and HP (1.0 mM) were prepared in 0.1 M HCl and suitably diluted with phosphate buffer (40 mM, pH 2.5) as working solution.

RESULTS AND DISCUSSION

Optimal parameters for the chiral separation and detection of RHP at 66 μM were studied, including the wavelength for absorption, the neutral CD as chiral selector, pH and concentration of phosphate buffer, applied voltage and concentration of dimethyl-β-CD. It was found simple in the present study to
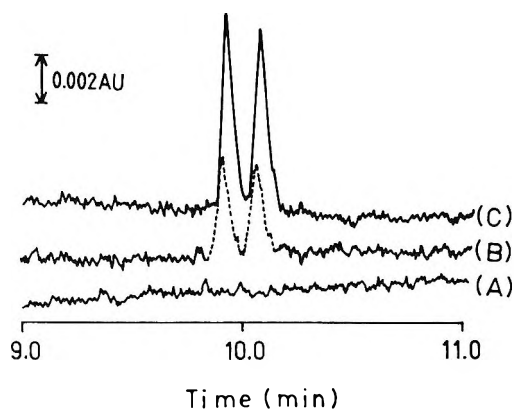
Figure 2. Composite electropherograms of RHP detected at (A) 254 nm, (B) 214 nm and (C) 200 nm. Conditions: buffer, 40 mM phosphate (pH 2.5) with 10 mM dimethyl-β-CD; capillary electrophoresis at 22 kV; sample, RHP at 66 mM; see text for other conditions.

use the resolution[32] (R) stated below for screening the parameters for the separation of RHP, i.e., $R = (h_m - h_v) / h_m$, where h_m is the mean peak height and h_v is the height of the valley. This gives the values of R between 0 and 1 (as baseline resolution).

Effect of Wavelength for Detection

After chiral separation of RHP in phosphate buffer (40 mM, pH 2.5) with 10 mM dimethyl-β-CD as a chiral selector, RHP was monitored at 200, 214 or 254 nm. The results in Fig. 2 indicated that a higher response can be obtained with RHP detected at 200 nm, due mainly to a larger molar absorptivity obtained from favorable excitation of RHP at the lower UV irradiation.

Effect of Neutral CD

Several neutral CDs were tested as chiral selector for the separation of RHP in phosphate buffer (40 mM, pH 2.5) at 22 kV. The results in Table 1 indicated that the enantiomeric resolution of RHP is better when dimethyl-β-CD, α-CD or 6-O-α-maltosyl-α-CD was used as a chiral selector. Dimethyl-β-
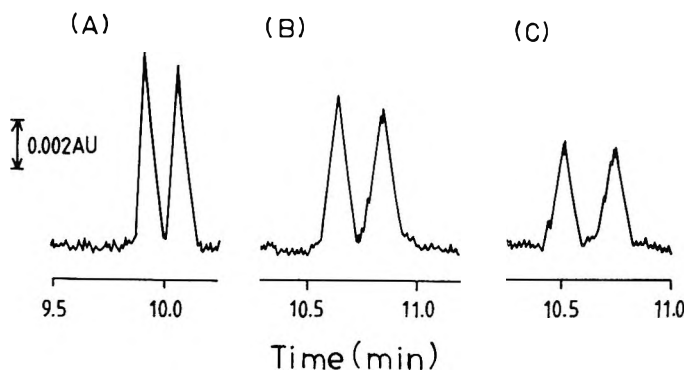
Figure 3. Electropherograms of RHP separated with (A) dimethyl-β-CD (10 mM), (B) α-CD (10 mM) and (C) 6-O-α-maltosyl-α-CD (10 mM). See text for conditions.

Table 1

**Resolution Values for RHP Enantiomers
Separated with Neutral Cyclodextrins**

Cyclodextrin	Resolution*	
	5mM	**10mM**
α-CD	0.86	0.97
β-CD	0	0
γ-CD	0	0
DM-β-CD	0.81	0.99
HP-β-CD	0.12	0.45
TM-β-CD	0	0.40
6-O-α-Maltosyl-α-CD	0.91	0.97

* Resolution (R) of RHP in phosphate buffer (40 mM, pH 2.5) with cyclo-dextrins each at 5 and 10mM; R, expressed as $(h_m = h_v)h_m$, where h_m for the mean peak height and h_v for the height of the valley. See text for conditions.
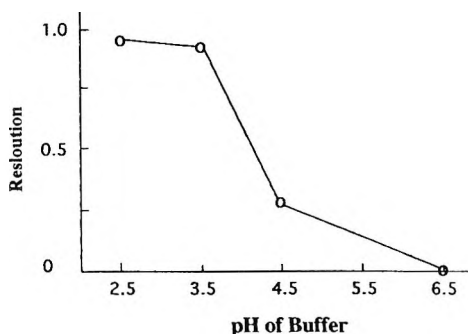
Figure 4. Effect of the pH of phosphate buffer (40 mM) on the resolution of RHP. See text for conditions.

CD was selected as the chiral additive in phosphate buffer for the separation of RHP, because it gave sharper peaks of RHP as shown in Fig. 3 . It is interesting to observe that α-CD and its derivative are also able to recognize the enantiomers of RHP. This reveals that the chiral moiety of RHP including the lipophilic 4-fluorophenyl group may do good fit in the cavity of α-CD.

The potential use of α-CD as a chiral selector for RHP seems to be very attractive.

Effect of pH of the Buffer

Fig. 4 indicated that chiral separation of RHP at higher pH resulted in poor resolution of the enantiomers of RHP. As a consequence, separation of RHP in phosphate buffer (40 mM) at pH 2.5 was performed.

Effect of the Applied Voltage

Resolution of RHP at a voltage range of 14-26 kV was studied. The results in Fig. 5 indicated that there are no apparent change of resolution (an R range of 0.93-0.98) except that a higher applied voltage definitely led to a shorter migration time (t_m) of RHP (a t_m range of about 8.6 to 16.3 min).
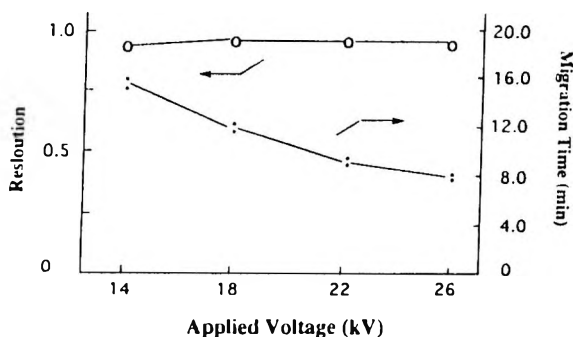
Figure 5. Effect of applied voltage on the resolution and migration of RHP. See text for conditions.
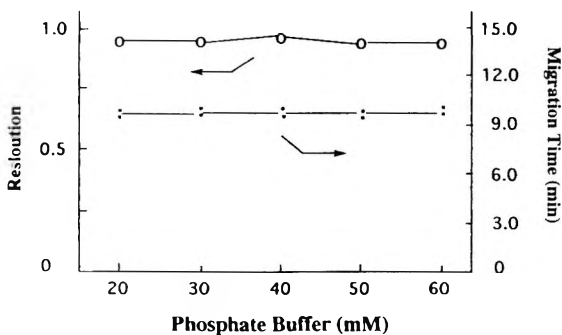
Figure 6. Effect of buffer's concentration on the resolution and migration of RHP. See text for conditions.

Effect of the Buffer Concentration

Chiral separation of RHP in phosphate buffer (pH 2.5) at concentration range of 20-60 mM with constant dimethyl-β-CD (10 mM) was examined. The results in Fig. 6 showed that there are no apparent change of resolution (an R range between 0.94-0.98) and migration time (a t_m range of about 9.6-10.0). Increasing the concentration of the buffer usually results in a higher viscosity of
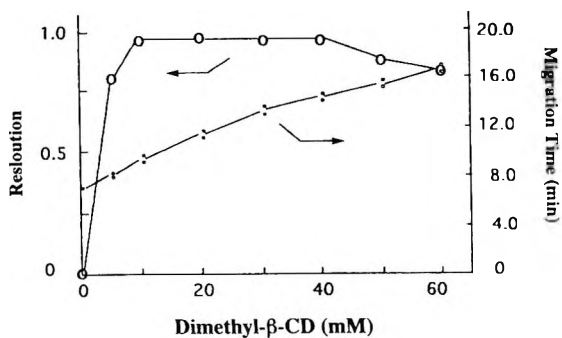
Figure 7. Effect of the concentration of chiral selector on the resolution and migration of RHP.
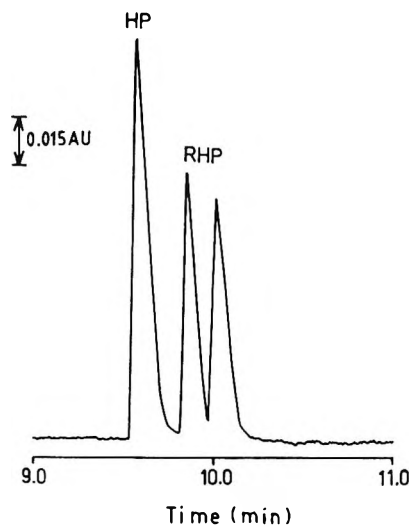
Figure 8. Electropherogram for a standard mixture of HP (0.27 mM) and RHP (0.26 mM). See text for conditions.

the buffer, in turn, leads to a larger Joule's heat in electrophoresis that interactively offsets the viscosity effect. This may partially explain that only minute variation of migration time was observed in CE of RHP at elevated buffer concentrations.

Effect of the Concentration of Dimethyl-β-CD

Optimal concentration of a chiral selector may exist for the resolution of certain enantiomers.[33] Therefore, the selected chiral selector, dimethyl-β-CD, at concentrations between 0-60 mM in phosphate buffer (40 mM, pH 2.5) was investigated for the separation of RHP. The results in Fig. 7 indicated that the concentrations of dimethyl-β-CD at 10-30 mM gave better resolution of RHP. A typical electropherogram for a standard mixture of RHP and HP was illustrated in Fig. 8, indicating the minimally acceptable resolution of RHP enantiomers and the full separation of RHP from its parent drug, HP.

In conclusion, a simple capillary zone electrophoresis is established for the chiral separation of RHP in phosphate buffer (40 mM, pH 2.5) using dimethyl-β-CD (10 mM) as the chiral selector. Coupled with a preconcentration treatment of RHP from biological sample, the present CE method seems to be a potential approach to study the chiral profile of RHP from patients undergoing HP therapy; namely, the metabolic form of RHP appears as an enantiomer, a racemate or other enantiomer mixture can be investigated.

ACKNOWLEDGMENT

REFERENCES

1. A. C. Altamura, M. C. Mauri, R. Cavallaro, Lancet, **1**, 814 (1987).

2. W. H. Chang, T. Y. Chen, C. F. Lee, W. H. Hu, E. K. Yeh, Biol. Psychiatry, **22**, 1406 (1987).

3. W. H. Chang, S. K. Lin, M. W. Jann, Y. W. F. Lam, T. Y. Chen, C. T. Chen, W. H. Hu, E. K. Yeh, Biol. Psychiatry, **26**, 239 (1989).

4. L. Ereshefsky, C. M. Davis, C. A. Harrington, M. W. Jann, J. L. Browning, S. R. Saklad, N. R. Burch, J. Clin. Psycho-pharmacol., **4(3)**, 138 (1984).

5. K. Miyazaki, T. Arita, I. Oka, T. Koyama and I. Yamashita, J.Chromatogr., **223**, 449 (1981).

6. P. I. Jatlow, R. Miller, M. Swigar, J. Chromatogr., **227**, 233 (1982).

7. M. J. Kogan, D. Pierson, K. Verebey, Ther. Drug Monit., **5**, 485 (1983).

8. M. Larsson, A. Forsman, R. Ohman, Curr. Ther. Res., **84**, 999 (1983).

9. J. L. Meek, R. J. Wyatt, Clin. Chem., **29**, 624 (1983).

10. A. K. Dhar, H. Kutt, Clin. Chem., **30**, 1228 (1984).

11. A. McBurney, S. George, J. Chromatogr., **308**, 387 (1984).

12. D. Hequet, C. Jarry, C. Rouguette , A. Brachot-Liermain, Ann Biol. Clin., **43**, 739 (1985).

13. R. L. Miller, C. L. Devane, J. Chromatogr., **374**, 405 (1986).

14. K. K. Midha, J. K. Cooper, E. M. Hawes, J. W. Hubhard, E. D. Korchinski, G. Mckay, Ther. Drug. Monit., **10**, 177 (1988).

15. M. Hayakari, Y. Hashimoto, T. Kita, S. Murakami, Forensic Sci. Int., **35**, 73 (1987).

16. L. B. Nilsson, J. Chromatogr., **431**, 113 (1988).

17. G. T. Vatassery, L. A. Herzan, M. W. Dysken, J. Chromatogr., **433**, 312 (1988).

18. N. D. Eddington, D. Young, J. Pharm. Sci., **77**, 541 (1988).

19. M. Harihram, E. K. Kindt, T. Van Noord, R. Tandon, Ther.Drug Monit., **11**, 701 (1989).

20. G. T. Vatassery, L. A. Herzan, M. W. Dysken, J. Anal.Toxicol., **14**, 25 (1990).

21. D. Wilhelm, A. Kemper, J. Chromatogr., **525**, 218 (1990).

22. C. Cahard, P. P. Pop, T. Conquy, A. Viala, J. Chromatogr., **532**, 193 (1990).

23. K. H. Park, M. H. Lee, M. G. Lee, J. Chromatogr., **572**, 259 (1991).

24. T. Uematsu, H. Matsuno, H. Sato, H. Hirayama, K. Hasegawa, M. Nakashima, J. Pharm. Sci., **81(10)**, 1008 (1992).

25. D. W. Eyles, H. A. Whiteford, T. J. Stedman , S. M. Pond, Psychopharmacology, **106**, 269 (1992).

26. K. Igarashi. N. Castagnoli Jr., J. Chromatogr., **579**, 277 (1992).

27. J. Fang, J. W. Gorrod, J. Chromatogr., **614**, 267 (1993).

28. A. J. Tomlinson, L. M. Benson, K. L. Johnsm, S. Naylor, J.Chromatogr., **621**, 239 (1993).

29. A. J. Tomlinson, L. M. Benson, J. P. Landers, G. F. Scanlan, J. Fang, J. W. Gorrod, S. Naylor, J. Chromatogr., **652**, 417 (1993).

30. M. Aravagiri, S. R. Marder, T. Van Putten, B. D. Marshall, J. Chromatogr. B, **656**, 373 (1994).

31. J. C. Jaen, B. W. Caprathe, S. Priebe, L. D. Wise, Pharmaceu. Res., **8(8)**, 1002 (1991).

32. M. Z. El Fallah, M. Martin, Chromatographia, **24**, 115 (1987).

33. S. A. C. Wren and R. C. Rowe, J. Chromatogr., **603**, 235 (1992).

HPLC VERSUS SFC FOR THE DETERMINATION OF SALBUTAMOL SULPHATE AND ITS IMPURITIES IN PHARMACEUTICALS

J. L. Bernal, M. J. del Nozal, H. Velasco, L. Toribio

Department of Analytical Chemistry
Faculty of Sciences
University of Valladolid
E-47005 Valladolid, Spain

ABSTRACT

A method to determine salbutamol sulphate and six impurities: 5-formyl-saligenin, salbutamol ketone, salbutamol bis ether, isopropyl salbutamol, desoxysalbutamol sulphate and salbutamol aldehyde, using reverse phase high performance liquid chromatography (RP-HPLC) with diode array detection (DAD) is proposed. The best separation was achieved using a gradient of 0.1 M ammonium acetate pH 3.0 and acetonitrile.

When the procedure was applied to the analysis of tablets and cough syrups, the versatility of the HPLC method was higher than one based on supercritical fluid chromatography (SFC). When using the later method the excipient difficulted the identification and quantification of some compounds in cough syrup samples.

INTRODUCTION

Salbutamol sulphate is a bronchodilator widely used for asthma treatment, which is sold under the Glaxo trade mark of Ventolin.

Until now, most of the papers published in relation to salbutamol analyses described its determination and quantification in tissues and biological fluids of animals under treatment with this drug. Usually, the methods employed were based on HPLC techniques using detectors of high sensitivity such as fluorescence[1-3] and electrochemical.[4-6]

It is known that there are some impurities which could be produced during the synthetic process or during an unsuitable storage of the drug being their analysis important. HPLC[7] or capillary electrophoresis[8] methods have been used to determine these compounds, but only two of the impurities were analysed. Recently, in a work done by our group[9] salbutamol and six impurities were separated satisfactorily in a short time by employing packed column supercritical fluid chromatography, although the method provided good results in the analysis of Ventolin tablets, some problems appeared with excipient peaks when analysing Ventolin cough syrups.

The aim of this work has been to establish the best chromatographic conditions to separate and determine salbutamol sulphate and the six related impurities using RP-HPLC with diode array detection, trying to obtain a method useful to analyse both kind of samples: tablets and cough syrups and using a sample treatment as simple as possible. For this purpose the variables affecting most the separation have been studied. The method has been applied to the analysis of Ventolin (Glaxo trade mark) tablets and cough syrups, and the results have been compared to those obtained in the SFC analysis of the same samples.

EXPERIMENTAL

Reagents

Ammonium acetate and n-propylamine were purchased from Sigma Aldrich Quimica (Madrid, Spain). Acetonitrile and methanol HPLC grade were obtained from Lab-Scan (Dublin, Ireland). Samples and drug standards were kindly supplied by Glaxo S.A. (Aranda de Duero factory, Burgos, Spain), the stock solutions were prepared in methanol. SFC grade carbon dioxide was purchased from Carburos Metálicos (Barcelona, Spain).
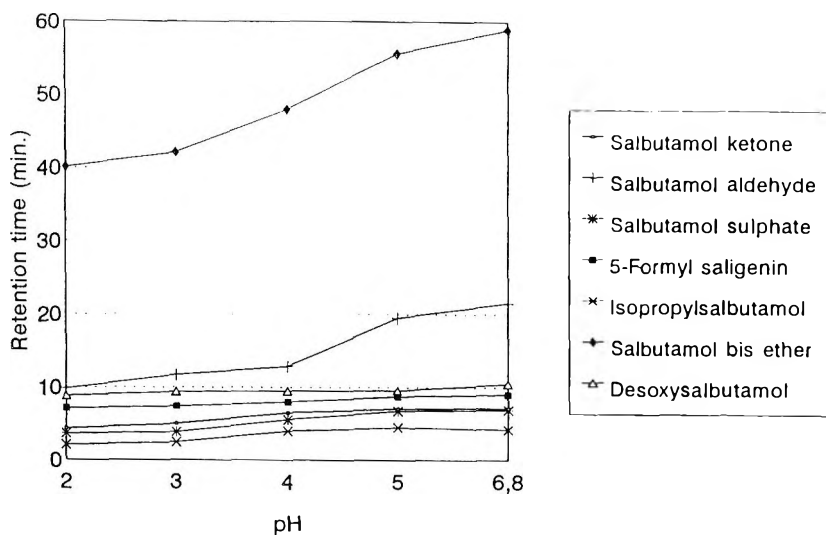
Figure 1. Variation of the retention time with the pH of the mobile phase in HPLC.

Apparatus and Chromatographic Conditions

HPLC : A Philips PU4100 liquid chromatograph (Cambridge, GB) equipped with a PU 4021 diode array detector was used. The column employed was a 200 x 2.1 mm, 5μm Hypersil ODS (Phenomenex, Torrance CA, USA). The elution was carried out employing a gradient of acetonitrile/0.1 M ammonium acetate pH=3.0. The flow-rate was set at 0.3 mL min^{-1}. and the injection volume was 20 μL.

The compounds were determined at 227 nm which was the wavelength where they presented the highest absorbance.

SFC : A Hewlett-Packard G1205A supercritical fluid chromatograph (Palo Alto, CA) with a diode array detector was used. The instrument was operated in the downstream mode, the pressure and temperature were fixed at 300 bar and 70°C respectively, the flow-rate was 1.5 mL min^{-1} and a gradient of modifier (methanol with 0.5% n-propylamine) was used. The injection volume was 5 μL (full loop). The column employed was a 250 x 4.6 mm, 5 μm Lichrosphere Diol column (Phenomenex, Torrance CA, USA).

Table 1

Gradient Employed in HPLC

Time (min)	% 0.1 M AcNH$_4$, pH 3	% Acetonitrile
0	96	4
5	96	4
8	88	12
30	88	12

Sample Treatment

To analyse Ventolin cough syrups, 1 mL of the sample was diluted to 10 mL with nanopure water and then passed through an 0.45 μm filter.

To analyse Ventolin tablets, 5 tablets of 4 mg were mixed with 20 mL of nanopure water and sonicated for 10 minutes, then the solution was centrifuged and the liquid was passed through an 0.45 μm filter.

RESULTS AND DISCUSSION

HPLC Procedure:

Effect of pH

Figure 1 shows the results obtained for a mixture of 30 μg mL^{-1} of each compound, working at ambient temperature (20°C) and using different mobile phases where the percentage of acetonitrile was fixed at 8% and the pH of the 0.1 M ammonium acetate was varied between 2 and 6.8. As can be seen, a pH increase caused an increase of the retention especially in the case of the late eluted compounds: salbutamol aldehyde and salbutamol bis ether. The selectivity of the separation did not change. Taking into account that, at pH 3, the compounds were separated and the retention time of salbutamol bis ether was the lowest, this pH was selected.
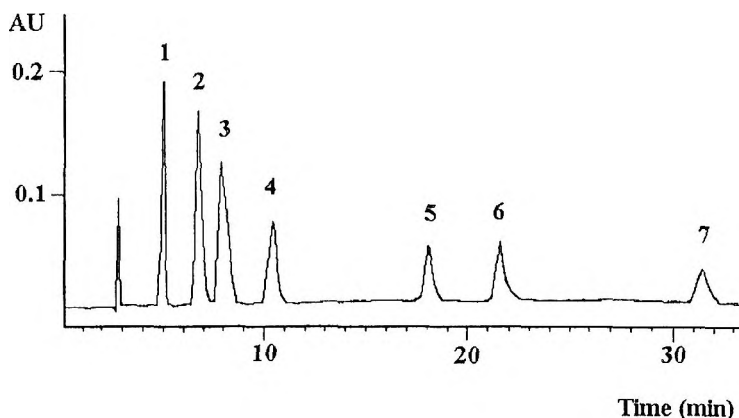
Figure 2. HPLC Chromatogram of a mixture of 30 μg mL^{-1} of the compounds. Peak labels are the same as in table 2.

Effect of Acetonitrile Percentage

The retention decreased as expected when the percentage of acetonitrile was increased. Isocratic conditions failed to provide a good separation in a short time. For optimum performance in terms of resolution and analysis time, several gradients of acetonitrile were tested. The best results were obtained with the gradient listed in Table 1. Working under these conditions the seven compounds were separated in 32 minutes (Figure 2).

Sensitivity

The detection limits obtained using as mobile phase the 0.1 M ammonium acetate pH=3/acetonitrile gradient schedule, listed in Table 1, are given in Table 2. They were calculated according to the IUPAC[10] recommendations and ranged from 0.60 μg mL^{-1} to 0.70 μg mL^{-1}, except for salbutamol bis ether, for which the detection limit was 3.50 μg mL^{-1}.

This also shows that they are similar to those obtained with SFC, but somewhat higher due to the fact that the efficiency of HPLC is lower than that of SFC and so the HPLC peaks are wider.

Table 2

Detection Limits

Compound	Detection Limit (μg mL^{-1})	
	HPLC	SFC
(1) Isopropyl salbutamol	0.6	0.5
(2) Salbutamol sulphate	0.6	0.5
(3) Salbutamol ketone	0.7	0.5
(4) 5-Formyl-saligenin	0.7	0.2
(5) Desoxysalbutamol	0.7	0.3
(6) Salbutamol aldehyde	0.7	0.5
(7) Salbutamol bis ether	3.5	1.3

Table 3

Efficiency and Resolution in the HPLC Separation

Compound	Number of Plates	Resolution
Isopropyl salbutamol	249	
Salbutamol sulphate	554	193
Salbutamol ketone	508	0.99
5-Formyl-saligenin	892	1.83
Desoxysalbutamol	1975	4.60
Salbutamol aldehyde	1263	1.73
Salbutamol bis ether	2625	3.92

SFC Procedure:

The SFC working conditions were as described in a previous paper.[9]

Application To Pharmaceutical Samples Analysis

Both SFC or HPLC methods gave a good resolution for the impurities and salbutamol sulphate at relative levels present in a typical salbutamol sample (Figure 3). The determination of 4 μg mL^{-1} salbutamol bis ether and 1 μg mL^{-1} of
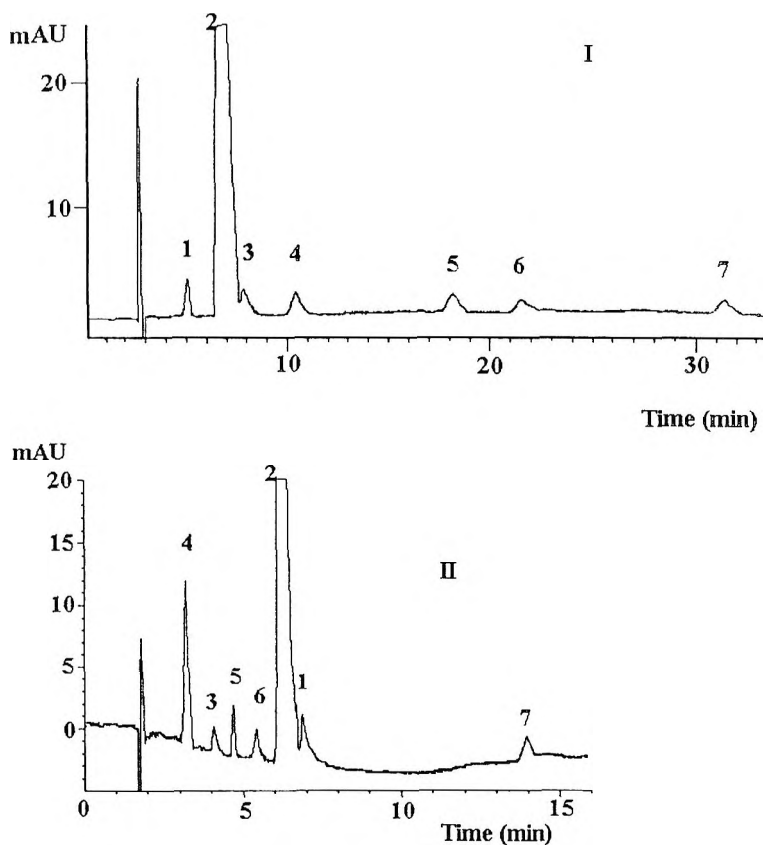
Figure 3. Chromatogram of a mixture of 1 µg mL^{-1} 5-formyl-saligenin, 1 µg mL^{-1} salbutamol ketone, 1 µg mL^{-1} desoxysalbutamol, 1 µg mL^{-1} salbutamol aldehyde, 1000 µg mL^{-1} salbutamol sulphate, 1 µg mL^{-1} isopropyl salbutamol and 3 µg mL^{-1} salbutamol bis ether.
Peak labels are the same as in Table 2.
(I) Using the HPLC method..
(II) Using the SFC method.

the other impurities in the presence of 1000 µg mL^{-1} salbutamol sulphate was possible. It should be noted that using the SFC method the efficiency and resolution of the separation was much better than using the HPLC one (Tables 3 and 4), and the analysis time was shorter in SFC than in HPLC.
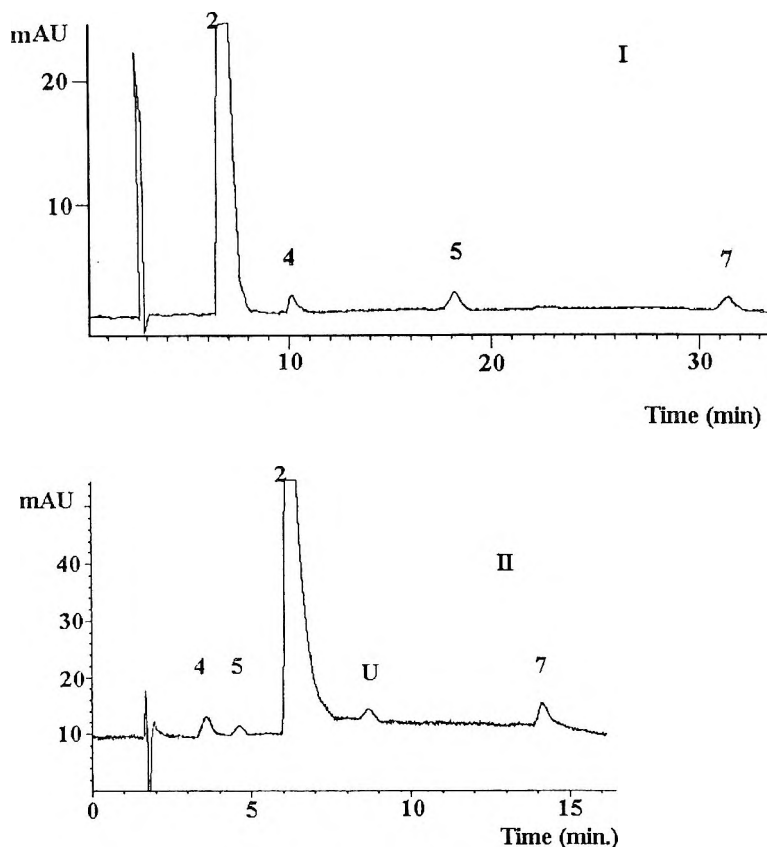
Figure 4. Chromatogram of a sample of Ventolin tablets degraded at 37°C and 70% of humidity for a year. (I) Using the HPLC method. (II) Using SFC method.(U) Unknown peak. Peak labels are the same as in table 2.

In Figure 4 the chromatogram of a sample of Ventolin tablets which was degraded, at 37°C and 70% of humidity for a year, is shown. There is no interference of the matrix in the analysis of that kind of pharmaceutical preparations, neither using the SFC method nor using the HPLC one, and the impurities could be perfectly quantified. Nevertheless, when a sample of undegraded Ventolin syrup and spiked with the impurities at the concentration levels of 4 μg mL^{-1} salbutamol bis ether and 1 μg mL^{1} for the other compounds, was analysed (Figure 5), the correct determination and quantification of these compounds was only possible in the case of the HPLC method. As can be seen in Figure 5 when using the SFC method, there were some problems with the peaks
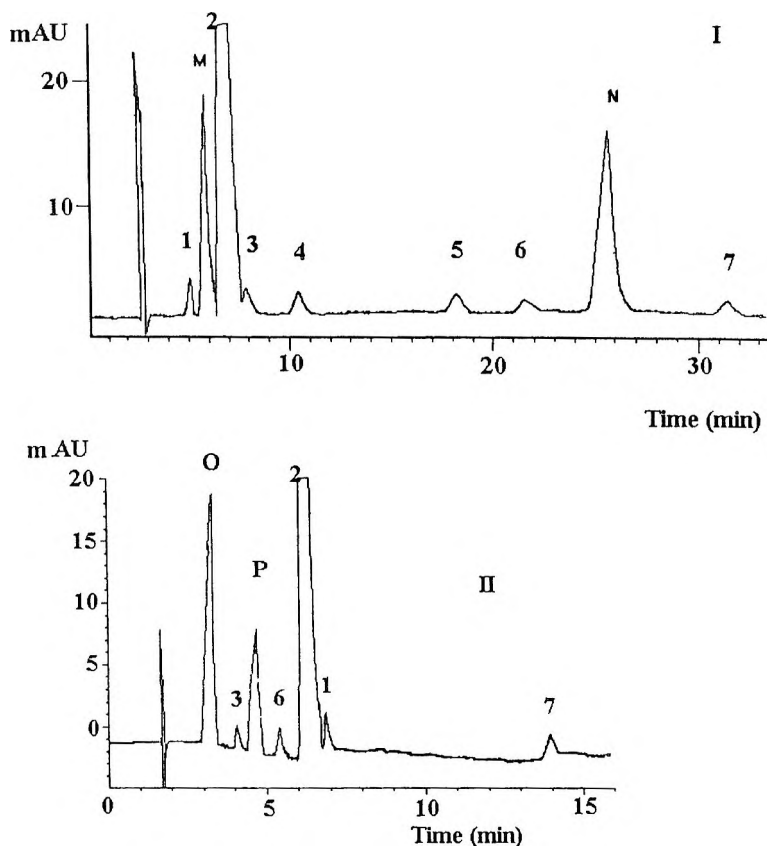
Figure 5. Chromatogram of a sample of Ventolin cough syrup spiked with the impurities at the concentration levels of figure 3. (I) Using the HPLC method, saccharine (M), benzoate (N). (II) Using the SFC method, benzoate and 5-formyl-saligenin (O), saccharine and isopropyl salbutamol (P). Peak labels are the same as in Table 2.

due to the excipient (benzoate and saccharine) : 5-formyl-saligenin coeluted with benzoate and isopropylsalbutamol co-eluted with saccharine. This shortcoming could be circumvented introducing some clean-up procedures, but this would complicate sample treatment and result in a longer analysis time.

The HPLC method could be considered more useful in this particular case, because of the two kinds of pharmaceutical preparations, tablets and syrups, can be analysed and their impurities quantified without interferences, in spite of the fact that the analysis take 30 minutes.

Table 4

Efficiency and Resolution in the SFC Separation

Compound	Number of Plates	Resolution
5-Formyl-saligenin	2440	
Salbutamol ketone	3047	3.05
Desoxysalbutamol	12159	2.66
Salbutamol aldehyde	8333	3.65
Salbutamol sulphate	8216	3.10
Isopropyl salbutamol	7817	2.25
Salbutamol bis ether	10128	16.31

CONCLUSIONS

Salbutamol sulphate and six related impurities are separated, and can be quantified, in Ventolin tablets and cough syrup samples, by employing RP-HPLC and DAD detection without no interferences of the matrix.

Efficiency and resolution of the separation as well as the analysis time, were better using SFC than HPLC. Nevertheless the analysis of cough syrup samples using SFC presented some problems related to the excipient interferences, which provoked an incorrect identification and quantification of the salbutamol related impurities. Using SFC these compounds could only be analysed in tablets samples, while using HPLC the two kind of samples could be analysed perfectly.

ACKNOWLEDGEMENTS

REFERENCES

1. J. M. Degroodt, B. W. Debukanski, S. Srebrnik, Z. Lebens., 6, 566-568, (1992).

2. P. T. Mccarthy, S. Atwal, A. P. Sykes, J. G. Ayres, Biomed. Chromatogr., 7, 25-28, (1993).

3. R. N. Gupta, H. D. Fuller, M. B. Dolovich, J. Chromatogr., **B, 654,** 205-211, (1994).

4. K. A. Sagar, C. Hua, M. T. Kelly, M. R. Smyth, Electroanalysis, **4,** 481-486, (1992).

5. K. A. Sagar, M. T. Kelly, M. R. Smyth, Biomed. Chromatog., **7,** 29-33, (1993).

6. F. Ramos, M. C. Castihlo, M. I. N. Dasilveira, J. A. M. Prates, J. H. R. Correira, Anal. Chim Acta., **275,** 279-283, (1993).

7. M. Mulholland, J. Waterhouse, Chromatographia, **25,** 769-773, (1988).

8. K. D. Altria, J. Chromatogr., **634,** 323-328, (1993).

9. J. L. Bernal, M. J. Del Nozal, J. M. Rivera, M. L. Serna, L. Toribio, Chromatographia, (1996) (in press).

10. G. L. Long, J. D. Winefordner, Anal. Chem., **55,** 712A-716A, (1983).

MOLECULAR CHARACTERIZATION OF POLYMERIC ANTITUMOR DRUG CARRIERS BY SIZE EXCLUSION CHROMATOGRAPHY AND UNIVERSAL CALIBRATION

R. Mendichi,[1] V. Rizzo,[2] M. Gigli,[2]
A. Giacometti Schieroni[1]

[1]Istituto di Chimica delle Macromolecole (CNR)
via Bassini 15
20133, Milan, Italy.

[2]Pharmacia
via Papa Giovanni XXIII 23
20014, Nerviano, Italy.

ABSTRACT

The development of a Size Exclusion Chromatography (SEC) method for the molecular characterization of FCE 28068, a conjugate between a synthetic polymeric carrier and the antitumor drug doxorubicin is presented. The aim was an accurate and reproducible, yet relatively simple and rapid method for the routine quality control of production batches. A standard SEC method that utilizes just a refractive index detector and relies upon universal calibration with commercial narrow standards was found suitable. The development of this method implied the following steps: test of universal calibration in the chosen experimental conditions with commercial narrow

1591

standards; fractionation of FCE 28068; test of compliance for the FCE 28068 fractions to universal calibration conditions; test of accuracy and reproducibility of the SEC measurement. The use of off-line light scattering and viscometry for the molecular characterization of standards and of FCE 28068 is discussed.

INTRODUCTION

Synthetic polymers are commonly used in many different biomedical applications, including prostheses, contact lenses, plasma expanders, wound dressing and pharmaceutical excipients.[1] The acquired knowledge about their biocompatibility and the experience gained in producing materials that comply with requests of regulatory authorities have encouraged studies about polymeric drug delivery systems, mainly in cancer chemotherapy.[2] Polymer-based drug delivery systems are usually designed to improve the pharmacokinetic profile of an antitumor agent. Compared to other macromolecular carriers (immunoconjugates, natural polymers), synthetic polymers are structures that can be tailor-made to optimize features such as molecular weight and inclusion of targeting moieties.

Poly-N-(2-hydroxypropyl)methacrylamide (PHPMA) is a biocompatible polymer, originally developed at the Prague Academy of Sciences as a plasma expander[3] and used later on for the preparation of a variety of water-soluble coniugates with antitumor agents (doxorubicin, daunorubicin, melphalan).[4-10] Generally, antitumor agents have been covalently bound to HPMA via a peptidyl spacer designed to be stable in bloodstream,[11] but cleavable by lysosomal enzymes inside the cells.[12] FCE 28068 is a PHPMA copolymer containing as a comonomer methacrylamide bound to doxorubicin via a tetrapeptidyl spacer (Gly-D,L-Phe-L-Leu-Gly).[4]

Doxorubicin, an antibiotic of the anthracycline group, is a well known antineoplastic agent used in the clinical treatment of leukemias, lymphomas, soft tissue and osteogenic carcinomas and solid tumors.[13,14] Nevertheless, its efficacy is restricted by a range of toxic side-effects, including cumulative cardiotoxicity.[15]

Improved antitumor activity of FCE 28068, compared to free drug, has been demonstrated preclinically, especially in solid tumor models.[16] Moreover, the stability of the linkage in the bloodstream reduces general toxicities such as cardiotoxicity in animal studies.[17] At present, the compound is under phase I clinical evaluation, where no cardiotoxicity has been observed, even at high drug-equivalent doses.[18]

The molecular weight of a drug-carrier conjugate and its molecular size under physiological conditions are important for effective function. They influence the accessibility of polymer to target cells other than phagocytes.[19] Besides, synthetic polymers are often non-degradable, therefore their molecular weight must be lower than the renal excretion threshold, otherwise they will be retained in the body.[20] The effect of molecular weight on plasma clearance makes the determination of the average molecular weight and of its distribution an important part of the analytical characterization of FCE 28068. Here, a conventional Size Exclusion Chromatography (SEC) method for such a characterization is presented: this method utilizes refractive index detection, and relies upon universal calibration with commercial narrow standards.

The aim was a relatively simple and fast procedure, complying with the batch quality control needs, for the accurate and reproducible determination of weight average-molecular weight (Mw) and of true molecular weight distribution (MWD). The study implied the following steps: choice of mobile phase and columns; check of universal calibration in the chosen experimental conditions, with narrow standards as polyethylenglycol/polyethylenoxide (PEG/PEO) and polymethylmethacrylate (PMMA); fractionation of PHPMA and of FCE 28068; check of universal calibration also for the narrow fractions of PHPMA and FCE 28068; check of the SEC measurement accuracy by comparison with results of independent light scattering determinations; check of the SEC measurement reproducibility. The study utilized some classic analytical techniques for the characterization of macromolecules in solution, such as multi-angle laser light scattering (MALLS) and viscometry both off- and on-line with the SEC system.

MATERIALS AND METHODS

Source of Polymers

PEO standards were purchased by Shove Denko. PEG and PMMA standards were provided by Polymer Laboratories. Both PHPMA and FCE 28068 fractions were obtained as described below.

PHPMA and FCE 28068 Fractionation.

Fractions of PHPMA prepared by chromatography on a 5x100 cm column containing a 1:1 mixture of Sepharose 4B and 6B (Pharmacia Biotech), were provided by Dr. K. Ulbrich, Institute of Macromolecular Chemistry, Academy of Sciences of the Czech Republic, Prague.   FCE 28068 was fractionated on a

5x100 cm column containing Sephacryl S-200 (Pharmacia Biotech); each fraction was further chromatographed on a 5x30 cm column filled with Sephacryl S-100 (Pharmacia Biotech). For both polymers the eluent was 0.1 M phosphate buffer, 0.5 M NaCl, pH 6.0; flow-rate: 1 mL/min for PHPMA and 5 mL/min for FCE 28068; temperature 22 °C; loaded sample concentration 1g/30 mL. For PHPMA a refractive index detector was used, whereas FCE 28068 elution peak was monitored off-line by optical density measurement at 480 nm on a 8451A UV-Visible detector (Hewlett Packard) after proper dilution.

The chromatographic peak of FCE 28068 was integrated and the integrated surface divided into 6 fractions of similar area. Tubes corresponding to each fraction were pooled and concentrated in an Amicon 8050 ultrafiltration cell on a Diaflo YM10 membrane (cut-off 10000) under nitrogen pressure. Eventually, fractions were desalted on a 2.6x14 cm column filled with Sephadex G-25 fine (Pharmacia Biotech), by elution at 1 mL/min and 22 °C, evaporated to dryness and dried in oven under vacuum at 50 °C for 3 hr.

Chromatographic Systems

Generally, for analytical purposes, a 150CV (Waters) system, composed by a liquid chromatograph equipped with an on-line single-capillary viscometer and a refractive index detector was used. Both detectors were exploited for the viscometric characterization, whereas just the latter was utilized for standard SEC analyses.

The "Expert Easy" software, version 2.0, was used for data acquisition and analysis. In some cases also a UV-visible photometer was used. Some experimental data were obtained with a 1090A chromatograph (Hewlett-Packard) equipped with an HP 1047A refractive index detector. For semi-preparative purposes, a Waters 625 chromatograph was utilized.

Chromatographic Experimental Conditions.

Two column sets were tested. The first one was composed by two identical PLgel Mixed C (Polymer Laboratories) columns in series. The second set was made by a Styragel HR4 and a Styragel HR3 column (Waters) in series.

Both sets were filled with a polystyrene/divinylbenzene matrix (5 μm particle size). Theoretical plate number was calculated with 1 % ethylene glycol as flow-marker. In spite of a lower efficiency (35,000 vs 40,000 plates/linear meter) the Waters Styragel columns were preferred for the higher reproducibility of chromatographic data.

A ternary mobile phase was used.   N,N-dimethylformamide (DMF, Aldrich) was chosen on the basis of the polymer solubility and of the compatibility with commercially available columns; 0.01 M LiBr (Sigma) was added to avoid molecular aggregation, whereas 0.05 M acetic acid (Carlo Erba Analyticals) was necessary in order to prevent anthracycline chelation of metallic ions released by the chromatographic system.   Flow-rate was 0.8 mL/min; column and detector temperature were 50 °C; the eluent was degassed with helium.

Light Scattering

Even though measurements were performed with a multiangle laser light scattering photometer (MALLS) Dawn DSP-F (Wyatt Technology Co.) in the static mode, a flow-cell (F2) was utilized to reduce the scattering volume. The MALLS instrument measures, through 15 detectors, the scattered light intensity over a broad range of angles (from $7°$ to $173°$ in methanol). The light source is a vertically polarized 5 mW He-Ne laser tuned at 632.8 nm. Data were analyzed by the software Dawn, version 2.04. More details on the instrument and data analysis are described elsewhere.[21,22]

Instrument calibration was carried out with toluene as a standard, assuming the Raileygh ratio value $R = 1.406 \ 10^{-5}$. The angular normalization of photodiodes was obtained using an almost uniform low molecular weight PEG standard (Mp = 12,600 g/mol; dispersity, D = 1.04), assumed as isotropic scatterer. Light scattering of FCE 28068 in DMF is affected by luminescence phenomena, thus the used solvent for MALLS measurements was methanol (Baker) containing 0.05 M acetic acid. This solvent is incompatible with SEC columns, therefore light scattering measurements were performed only in batch mode. The refractive index increments, dn/dc, for PHPMA and FCE 28068 were determined with a Brice-Phoenix BP-2000-V differential refractometer at 25 °C in the above cited solvent.

Viscometry

Intrinsic viscosity ($[\eta]$) was generally determined on-line with the viscometer included in the Waters 150CV SEC system. Hardware and software data analysis of a SEC-viscometry system have been extensively reported in literature.[23,24] For some standards and polymer fractions, with $[\eta]$ near the detector lower sensitivity threshold (≈ 0.1 dL/g), measurements were carried out in static mode, with an Ubbelhode capillary viscometer.   The Mark-Houwink constants "k"and "a" of the narrow polymer fractions and of the SEC
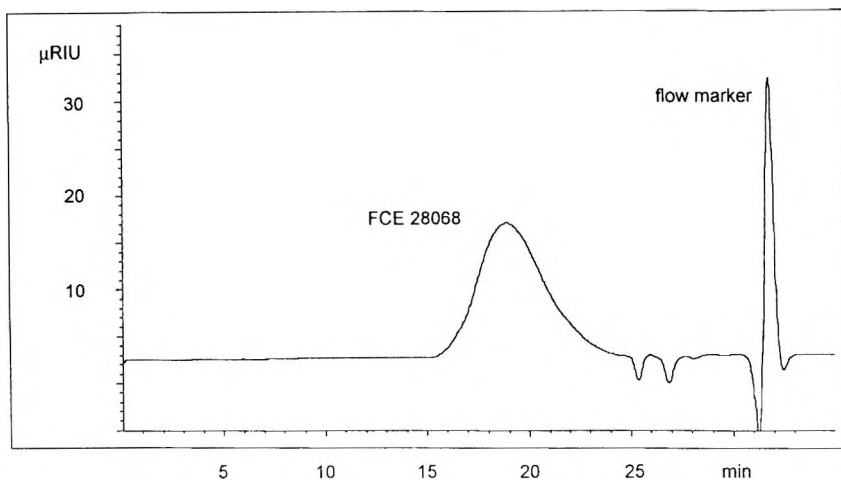
Figure 1. Size exclusion chromatogram of FCE 28068 (lot 0122; 2 mg/mL; injection volume 200 µl; filtered on Millipore 0.22 µm PTFE membrane) as obtained with a refractive index detector. Experimental conditions: see Materials and Methods. With a set of just two columns (Waters Styragel HR4 and HR3) impurity peaks (25-28 min), due to residual solvents, are completely resolved from the polymer peak ($\approx$19 min). The peak at about 32 min is due to toluene, added as a flow marker.

standards were calculated by least squares fitting of $[\eta]$ versus weight average molecular weight (Mw), as obtained from MALLS in batch mode. For SEC standards, only the molecular weight at peak apex (Mp) and dispersity were known. Still, for such narrow standards (D < 1.1), a log normal MWD can be assumed, and thus Mw could be calculated from Equation 1.

$$M_w = M_p \sqrt{D} \qquad\qquad\qquad (1)$$

RESULTS AND DISCUSSION

A typical chromatogram of a FCE 28068 sample, obtained as described in "Materials and Methods", is shown in Figure 1: the signal to noise ratio is quite high and the polymer peak ($\approx$19 min) is well separated from peaks of low molecular weight contaminants (residual solvents: 25-28 min). The peak at about 32 min is due to toluene added as a flow marker.

Table 1

**Manufacturer* Data and Viscometric Characterization of
PEG/PEO and PMMA Narrow Standards**

	PEG/PEO			PMMA		
#	Mp (g/mol)	D	[η] (dl/g)	Mp (g/mol)	D	[η] (dl/g)
1	860,000	1.17	4.2821	496,000	1.07	1.0250
2	570,000	1.10	3.0774	216,600	1.05	0.5465
3	270,000	1.09	2.0037	100,250	1.05	0.3390
4	160,000	1.07	1.3189	68,000	1.07	0.2438
5	85,000	1.06	0.8210	48,600	1.05	0.2040
6	45,000	1.07	0.5075	29,400	1.06	0.1431
7	21,000	1.12	0.3208	17,000	1.06	0.1002
8	12,600	1.04	0.2146	9,400	1.10	0.0679
9	4,100	1.05	0.1105	4,700	1.07	0.0503
10	1,470	1.05	0.0596	2,010	1.10	0.0386
11	960	1.03	0.0469	1,140	1.11	0.0320

* see Materials and Methods

Table 2

**Mark-Houwink Equation Constants of PEG/PEO and PMMA Narrow
Standards and of PHPMA and FCE28068 in SEC Mobile Phase at 50 °C**

Polymer	$k \bullet 10^4$ (dl/g)	a
PEG/PEO	4.33	0.666
PMMA	1.12	0.692
PHPMA	1.46	0.650
FCE 28068	2.21	0.652

Viscometric Characterization of PEG/PEO and PMMA Standards

Seven PEO, four PEG ($960 < \text{Mp} < 8.6 \; 10^5$ g/mol) and eleven PMMA narrow standards ($1140 < \text{Mp} < 4.96 \; 10^5$ g/mol) were utilized for the universal calibration. Standard Mp and dispersity values (as reported by the manufacturer) are summarized in Table 1, together with intrinsic viscosity values, as measured with the SEC on-line viscometer. These values are in good agreement with the corresponding off-line measurements (not shown). The Mark-Houwink constants "k" and "a" for PEG/PEO and PMMA standards, in the chosen mobile phase at 50 °C were calculated from the data of Table 1, and are reported in Table 2.

Characterization of PHPMA and FCE 28068 Fractions

The refractive index increments, dn/dc, for PHPMA and FCE 28068 were 0.202 and 0.212 mL/g, respectively. The six PHPMA fractions (see Materials and Methods) showed a broad molecular mass range ($8.3 \; 10^3 < \text{Mw} < 3.5 \; 10^5$ g/mol) and a low dispersity ($1.13 < D < 1.3$). On the contrary, six FCE 28068 fractions covered a limited molecular mass range ($2.2 \; 10^4 < \text{Mw} < 4.8 \; 10^4$) and dispersity varied from 1.18 to 1.51. Every fraction was accurately characterized as far Mw and [η] are concerned. Corresponding values are reported in Table 3. In the same table, dispersity values are reported, as obtained with SEC. Values for the Mark-Houwink constants for PHPMA and FCE 28068 in the chosen SEC mobile phase at 50 °C were obtained from data in Table 3 and are reported in Table 2.

Check of Universal Calibration for PHPMA and FCE 28068

The universal calibration holds when polymers elute as a function of their hydrodynamic volume, that is proportional to the product between molecular mass and intrinsic viscosity.[25] Thus, to check the universal calibration validity means to verify that the calibration function log ($M[\eta$]) = $f(V)$ (where V is the elution volume) is common to all the utilized polymers: PEG/PEO, PMMA, PHPMA, and FCE 28068.

If the universal calibration holds, a true (not nominal) MWD can be obtained, also when used standards are different from the analyzed polymer. In Figure 2, experimental data of the above cited polymers are reported, as obtained with the SEC described system, together with a 3rd degree polynomial data fitting (the calibration function). Deviation from the fitting function is evident for some of the data on low molecular weight samples: this is likely to be due to errors in the determination of
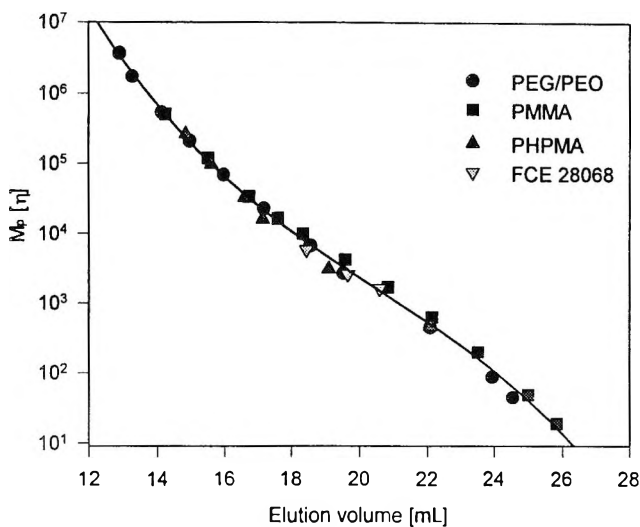
Figure 2. Test of universal calibration. Log (M_p [η]) values of four sets of polymers (PEG/PEO, PMMA, PHPMA, FCE 28068) are plotted versus their retention times: all these values are described with the same curve (a 3rd order polynomial), thus universal calibration holds in the chosen experimental conditions.

Table 3

Characterization of PHPMA and FCE 28068 Fractions

	PHPMA			FCE 28068		
#	Mp (g/mol)	D	|η| (dl/g)	Mp (g/mol)	D	|η| (dl/g)
1	349, 500	1.15	0.8138	48,200	1.51	0.1651
2	188,300	1.17	0.5585	45,500	1.36	0.1567
3	99,450	1.16	0.3539	37,300	1.38	0.1398
4	65,300	1.13	0.2637	32,400	1.24	0.1259
5	25,600	1.23	0.1349	28,200	1.20	0.1151
6	8,300	1.30	0.0637	22,000	1.18	0.0988

correspondingly low intrinsic viscosity values. Both the PHPMA and the FCE 28068 fractions follow the calibration function (as calculated with the narrow PEG/PEO and PMMA standards), thus it is true that these polymers elute accordingly to their hydrodynamic volume, and therefore they can be characterized by conventional SEC and universal calibration.

Characterization of Unfractioned FCE 28068 Polymer

Off-line characterization (by MALLS in static mode) of FCE 28068 (lot 0122) gave the following average values: weight average molecular weight Mw $= (3.84 \pm 0.04) \, 10^4$ g/mol; radius of gtyration $<s^2>_z$ 8.8 ± 1.4 nm. The radius of gyration value is near the low sensitivity limit of a MALLS instrument equipped with a He-Ne laser, and thus the datum precision is low. On the other hand, the Mw value is obtained with high precision. Data fitting was performed with the traditional Zimm graphic procedure, as shown in Figure 3.

SEC Measurement Accuracy

Comparison between "true" off-line determined Mw and [η] values, and the corresponding SEC on-line values for FCE 28068 (lot 0122) is reported in Table 4. The good agreement among these data confirms the validity of universal calibration for FCE 28068 polymer. Generally, improved accuracy of Mw values of FCE 28068 fractions, as determined with PEG/PEO standards (see Figure 4) led us to prefer this set of standards for the quality control method.

Heterogeneity in a copolymer composition can affect the MALLS determined Mw value, if the dn/dc value is not constant for all the sample molecules. In the FCE 28068 copolymer, the doxorubicin content was found to vary between about 6 % (in the lowest Mw fraction) and about 12 % (in the highest Mw fraction). Nevertheless, when two chromatograms are acquired for the same FCE 28068 sample, with two different detectors (RI for the whole copolymer and UV-visible tuned at 480 nm, the maximum wavelength for the doxorubicin chromophore), they are perfectly superposable.

Thus, by taking into account this identity, the low average molar fraction of doxorubicin in FCE 28068 and finally the relatively low difference between the dn/dc values of the polymeric carrier alone (PHPMA), and of the [drug-polymeric carrier] conjugate (FCE 28068) respectively, we can assume that the modest observed composition heterogeneity does not significantly affect the MALLS determined Mw value.
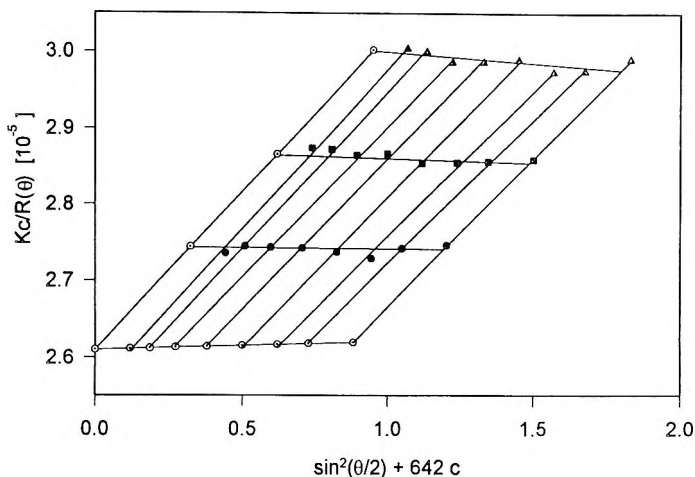
Figure 3. Zimm plot of a FCE 28068 sample (lot 0122), as obtained by MALLS in static mode. Solvent: methanol, 0.05 M acetic acid. Temperature: 25 °C.

Table 4

Accuracy of SEC Characterization of a FCE 28068 Sample (lot 0122)

$Mw^{(1)}$ (g/mol)	$Mw^{(2)}$ (g/mol)	$Mw^{(3)}$ (g/mol)	$[\eta]^{(4)}$ (dl/g)	$[\eta]^{(2)}$ (dl/g)	$[\eta]^{(3)}$ (dl/g)	$D^{(2)}$	$D^{(3)}$
38,400	37,200	40,850	0.1331	0.1286	0.1372	1.74	1.62

(1) as obtained by MALLS
(2) as obtained by SEC with PEG/PEO calibration
(3) as obtained by SEC with PMMA calibrations
(4) as obtained off-line with the Ubbelhode capillary viscometer

SEC Measurement Reproducibility

SEC measurement reproducibility was determined by analysing twice per week along one month a freshly prepared solution of FCE 28068 (lot 0120). Every time, a calibration curve with PEG/PEO standards was calculated. Average values of Mw and D, as obtained from 10 measurements, are 38,800
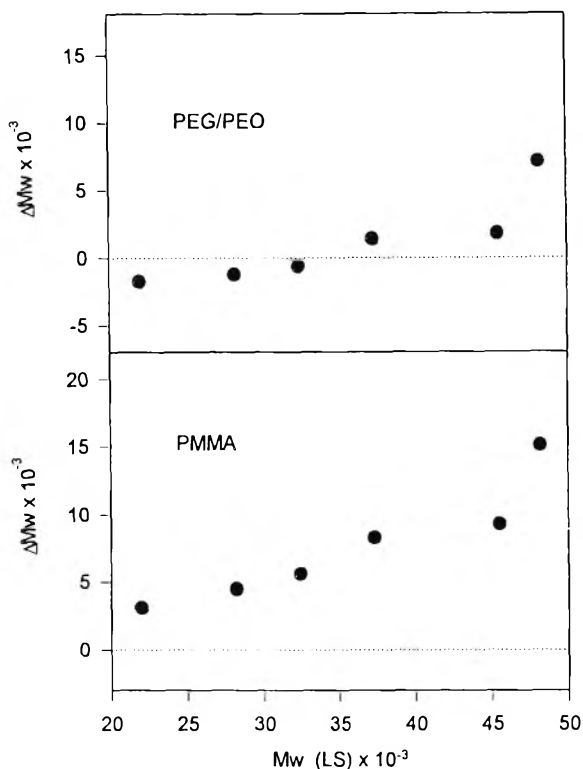
Figure 4. Test of method accuracy as a function of the used calibration standards. For six FCE 28068 fractions the difference between Mw obtained with SEC and the light scattering values (ΔMw) is plotted as a function of Mw. The two panels display results obtained with two sets of calibration standards.

and 1.84, respectively. The relative standard deviation (RSD% = 1.52 % for Mw and 1.38 % for dispersity) are well within the typical range for SEC determinations, and confirm the very good reproducibility of the method.

CONCLUSIONS

For routine Mw and MWD analysis on a given polymer, a two-step process works often well. In the first step, a commercial set of standards with known Mw value of each component is selected, the intrinsic viscosity of these standards in the chromatographic mobile phase is determined, and the universal calibration is checked.

In the second step, the universal calibration is used to analyze all the samples by a conventional SEC approach using only the refractive index detector. In the described work, the considerable amount of data obtained with several techniques (SEC, SEC-viscometry, MALLS, off-line viscometry) led to some meaningful conclusions. It is possible to characterize the FCE 28068 copolymer and the PHPMA homo-polymer through conventional SEC in organic mobile phase after calibration with commercial standards. Chromatographic separation of FCE 28068 and of PHPMA in the specified experimental conditions is fundamentally based on their hydrodynamic volume, thus universal calibration operates. The SEC method is rapid: forty minutes are needed for one chromatogram with a set of just two high-efficiency columns (35-40,000 theoretical plates). Both PEG/PEO and PMMA calibration give Mw and [η] values close to those measured by light scattering in static mode and by off-line viscometry respectively. PEG/PEO calibrated SEC generally gives more accurate Mw values. Finally, reproducibility of the described SEC method (RSD % < 2 %) is very high, thus the method is suitable for quality control.

REFERENCES

1. C. G. Gebelein, **Advances in Biomedical Polymers,** New York, Plenum Press, 405, (1987).

2. R. Duncan, Anti-Cancer Drugs, **3**, 175-210, (1992).

3. L. Sprincl, J. Exner, O. Sterba, J. Kopecek, J. Biomed. Mater. Res., **10**, 953-63 (1976).

4. J. Kopecek, H. Bazilova, Eur. Polym. J., **9**, 7-14 (1978).

5. J. Strohalm, J. Kopecek, Angew. Makrom. Chem., **70**, 109-18 (1978).

6. P. Rejmanova, J. Labsky, J. Kopecek, Makromol. Chem., **178**, 2159-68 (1977).

7. K. Ulbrich, E.I. Zacharieva, B. Obereigner, Biomaterials, **1**, 199-204 (1980).

8. J. Kopecek, R. Duncan, J. Controlled Rel., **6**, 315-327 (1987).

9. B. Rihova, K. Ulbrich, J. Strohalm, V. Vetvicka, M. Bilej, R. Duncan, J. Kopecek, Biomaterials, **10**, 335-42 (1989).

10. J. Kopecek, J. Controlled Rel., **11**, 279-90 (1990).

11. P. Rejmanova, J. Kopecek, R. Duncan, J. B. Lloyd, Biomaterials, **6**, 45 (1985).

12. P. Rejmanova, J. Pohl, M. Baudys, V. Kostka, J. Kopecek, Makromol. Chem., **184**, 2009 (1983).

13. F. Arcamone. **Doxorubicin, Anticancer Antibiotics: Medicinal Chemistry,** a series of monographs, Vol. 17, Academic press, New York, 1981.

14. J. R. Brown, S. Heider Imam, in **Progress in Medicinal Chemistry**, G. P. Ellis, G.B. West Eds., Vol. 21, 196-236, Elsevier, Amsterdam, 1984.

15. C. Myers, **Anthracyclines in Cancer Chemotherapy**, H. Pinedo, B. Chabner Eds., Vol. 8, 52-64. Elsevier Science Publishers, Amsterdam, 1986.

16. L. W. Seymour, K. Ulbrich, P. S. Steyger, M. Brereton, V. Subr, J. Strohalm, R. Duncan, Br. J. Cancer, **70**, 636-641 (1994).

17. T. K. Yeung, J. W. Hopewell, R. Simmonds, L. W. Seymour, R. Duncan, O. Bellini, M. Grandi, F. Spreafico, J. Strohalm, K. Ulbrich, Cancer Chemother. Pharmacol., **29**, 105-111 (1994).

18. P. A. Vasev, R. Duncan, S. B. Kaye, J.Cassidy, Communication to the 8th European Conference on Clinical Oncology Cancer Research and Cancer Nursing, Paris, 29-10-1995.

19. R. Duncan, M. K. Pratten, H. C. Cable, H. Ringsdorf, J. B. Lloyd, Biochem. J, **196**, 49 (1981).

20. L. W. Seymour, R. Duncan, J. Strohalm, J. Kopecek, J. Biomed. Mater. Res, **21**, 1341-58 (1987).

21. P. J. Wyatt, I. Izisel, R. G. Parker, G. K. Wyatt, Proc. Int. GPC Symp., Itasca, IL, 168 (1987).

22. L. Nilsson, C. Jackson, P. J. Wyatt, Proc. Int. GPC Symp., Newton, MA, 166 (1989).

23. J. L. Ekmanis, Proc. Int. GPC Symp., Newton, MA, 1 (1989).

24. Y. Kuo, T.Provder, M. E. Koehler, Proc. Int. GPC Symp., Newton, MA, 54 (1989).

25. Z. Grubisic, P. Rempp, H. Benoit, J. Polymer Sci. B, **5**, 753 (1967).

DETERMINATION OF THE ANTIPARASITIC DRUG IVERMECTIN IN LIVER, MUSCLE AND FAT TISSUE SAMPLES FROM SWINE, CATTLE, HORSES AND SHEEP USING HPLC WITH FLUORESCENCE DETECTION

Guglielmo Dusi, Michele Curatolo,
Antonio Fierro, Elena Faggionato

Department of Chemistry
Istituto Zooprofilattico Sperimentale
della Lombardia e dell'Emilia
25124 Brescia, Italy

ABSTRACT

A rapid and very effective analytical procedure for the isolation, derivatization and fluorescence HPLC determination of Ivermectin (IVM) residues in all the animal tissues and organs listed in the EEC Regulation 2901/93 has been developed and tested. First, the drug is extracted from the samples with acetonitrile. Then, the IVM extracts, mixed with water and triethylamine, are cleaned up on and eluted with terbutylmethylether from SPE C_{18} columns. Prior to the derivatization step, the IVM eluates are purified from the interfering lipophilic substances through a liquid-liquid partition step. Finally, IVM is derivatized and analyzed by HPLC

with fluorescence detection. The mean recoveries from IVM fortified samples were 76% for liver and 77% for fat tissue in a concentration range of 10-120 ng/g. The limit of determination was 2 ng/g.

This paper also reports the results of a short trial on the pharmacokinetics of the IVM depletion in guinea pigs dosed with the drug.

INTRODUCTION

Ivermectin (IVM) is a broad-spectrum antiparasitic drug of the chemical family of Avermectins, used against Nematodes and Arthropods in food-producing animals.[1] IVM is a mixture of two homologs, not less than 80% of 22,23 - dihydroavermectin B_{1a} (H_2B_{1a}) and not more than 20% of 22,23 - dihydroavermectin B_{1b} (H_2B_{1b}). H_2B_{1a}, the component in the largest amount in the mixture, is metabolized more slowly than the other drug component H_2B_{1b} and therefore is considered to be a satisfactory marker compound for measuring total residues.[2]   IVM displays a prolonged persistence in the animal and its pharmacological action has been reported to be effective at very low dosage levels.[3]

With its Regulation 2901/93 the EEC[4] definitively fixed the MRL's for IVM in tissues from several food-producing animal. The animal species included were swine, cattle, horses and sheep and the tissues recommended for the analysis were liver and fat. A number of analytical methods for the determination of IVM in animal tissues has been published, by Tway et al.,[2] Markus et al.,[5] Salisbury[6] and Degroodt et al.[7] In general, all these procedures involve a liquid-liquid extraction step of the drug from the samples, followed by a clean-up step of the resulting IVM extracts, either with liquid-liquid purifications or with SPE column technique.

Recently, Schenk et al.[8] and Iosifidou et al.[9] have reported an extension of the matrix solid phase dispersion (MSPD) technique to the determination of IVM in tissues. To perform the quantification of the drug by fluorescence detection, nearly all the authors use, except Stong,[10] the same chemical derivatization step of the IVM extracts.

Before the quantification of IVM by fluorescence-HPLC, the method we report employs sequentially two very effective clean-up procedures for the IVM extracts from the tissues: an SPE column extraction step and a very fast liquid-

liquid partition step. This makes the method suitable for the routine analysis of IVM in all the tissues from all the animal species listed in the EEC Regulation 2901/93. This paper also reports the results of a short trial on the pharmacokinetics of the IVM depletion in guinea pigs dosed with the drug.

MATERIALS

Reagents and Equipment

Acetonitrile, methanol (HPLC grade), hexane, chloroform, triethylamine and terbutylmethylether were obtained from Merck. Water for LC analysis was prepared with a Nanopure Ultrapure Water System of Barnstead. 1-Methylimidazole, acetic anhydride and N,N- dimethylformamide were obtained from Sigma.

C_{18} Bakerbond SPE columns, each with 500 mg of stationary phase and a 6-mL volume were obtained from J.T. Baker (code no. 7020-06). Silica SPE columns were obtained from Waters (code no. WAT051900). The columns were connected to an SPE vacuum manifold block, obtained from Supelco Inc.

The HPLC system consisted of a Model 9010 ternary pump from Varian, equipped with a loop injector with a 100 μL loop from Rheodine Corp. A Model 9070 fluorescence detector from Varian and a Model 561 recorder from Perkin-Elmer (chart speed: 0.5 cm/min) was used for fluorimetric detection. The HPLC separation was carried on a 5 μm Supelcosil LC - 18 150 x 4.6 mm column at room temperature, with a 5 μm Supelguard LC - 18 20 x 4.6 mm guard column (both the columns from Supelco Inc.).

The operating conditions for fluorescence-HPLC were: mobile phase 95:5 v/v methanol:water, flow 1.8 mL/min, injection volume 20 μL, chart speed 5 mm/min, excitation wavelength 360 nm, emission wavelength 470 nm, absorbance units of full scale (AUFS) 0.2-0.5.

Standard and Standard Solutions

The IVM (Reference standard L-640.471 - 076P005) standard solution at a concentration of 1.39 % w/w, stored at -20° C, was a generous gift of Merck Sharp and Dohme (Research Laboratory) of Germany. IVM stock solution was prepared in methanol at a concentration of 13.9 μg/mL.

The IVM working solutions at concentrations of, respectively, 0.35, 0.69, 1.39, 2.78 and 5.56 μg/mL, were prepared in methanol on the day of use from the stock solution and were employed to fortify the samples for the recovery study, giving IVM concentrations in the 10-120 ng/g range.

Aliquots of these solutions (100 μL) were derivatized according to the procedure described below. A standard curve was prepared with each batch of samples.

EXPERIMENTAL

Extraction and Clean-up Procedure

5.00 g minced tissue sample (liver, muscle or fat) was weighed into a 50 mL polypropylene centrifuge tube; 15 mL acetonitrile was added and the mixture was homogenized with an Ultraturrax homogenizer at high speed for 3 min. The homogenizer rod and blades were rinsed into the tube with 2 mL acetonitrile and the tube was placed into an ultrasonic bath for 15 min.

After centrifugation for 5 min at 3000 rpm, the supernatant layer was poured from the tube, through a folded paper filter, into a 100 mL flat-bottomed flask. The samples were re-extracted as previously described, again with 10 mL acetonitrile, the two acetonitrilic portions were combined, and the filter was washed with 3 mL acetonitrile. 70 mL distilled water and 0.1 mL triethylamine (TEA) were then added to the flask and the resulting mixture was throughly stirred.

A C_{18} SPE column was placed on the vacuum manifold block, and a 75 mL reservoir was attached to its top. Before the extraction step, the column was activated with, respectively, 3 x 5 mL methanol, 5 mL acetonitrile and 3 x 5 mL 70:30 v/v water:acetonitrile mixture containing 0.1% TEA. The sample extract was added into the reservoir and passed through the SPE column. The eluate was discarded. The column was washed with 2 x 5 mL v/v 50:50 water:acetonitrile mixture. IVM was eluted with 7 mL terbutylmethylether from the column into a 10 mL glass centrifuge tube.

To obtain the best IVM recoveries, the elution flow rate should be of about 2 mL/min. The tube was stocked overnight in a refrigerator at -20°C.

The cool, clear supernatant etheric layer was throughly decanted to another 10 mL centrifuge glass tube, after discarding the lower frozen water layer. Then the etheric layer was reduced to dryness under N_2 at 50 °C. 3 mL methanol and then 0.1 mL bidistilled water were added to the tube and the resulting solution was washed with 2 x 3 mL hexane, vortex-mixing after every addition. The two hexanic washings were re-extracted with 1 mL methanol and this methanolic portion was combined with the hydromethanolic layer in the tube. The mixture was reduced to dryness under N_2 at 50°C. Finally, all the traces of the solvents were exhaustively removed from the sample extract by heating the tubes for 30 min in a vacuum oven at 50°C.

Derivatization

150 μL freshly prepared derivatizing reagent (1-methylimidazole-acetic anhydride-dimethylformamide, 2+3+9 v/v) was added to the tube, then it was tightly capped, vortex-mixed for 30 sec, and heated for 60 min in an oven at 100°C. Then the tube was removed and cooled, and 1 mL chloroform was added. After vortex-mixing, the dark brown solution was transferred onto a silica SPE column, previously activated with 8 mL chloroform and placed on the vacuum manifold block. The tube was rinsed with 3 x 3 mL chloroform. The rinses were loaded onto the column and eluted into a 10 mL centrifuge glass tube.

The chloroformic eluate in each tube was reduced to dryness under N_2 at 50°C. The residue was dissolved in 0.4 mL methanol. After vortex-mixing, 20 μL derivatized IVM solution was injected onto the fluorescence-HPLC system, operating as previously described.

Trial in Guinea Pigs

Eight guinea pigs (approximately 500 g body weight) were administered a pharmaceutical preparation containing IVM, namely Ivomec®, from Merck Sharp and Dohme, i.e. 0.2 mg/kg b.w., injected subcutaneously in the retroscapular region. The animals were fed ad libitum both before and during the experiment.

Groups of two animals were sacrificed at 2, 4, 6 and 13 days after dosing and samples of liver, muscle and fat tissue were collected from each of the two animals, combined and frozen at -20 °C until analysis was performed. The samples were analyzed in duplicate according to the procedure described below, in order to study the "in vivo" IVM depletion profile and, also, to further validate the analytical procedure of IVM determination.
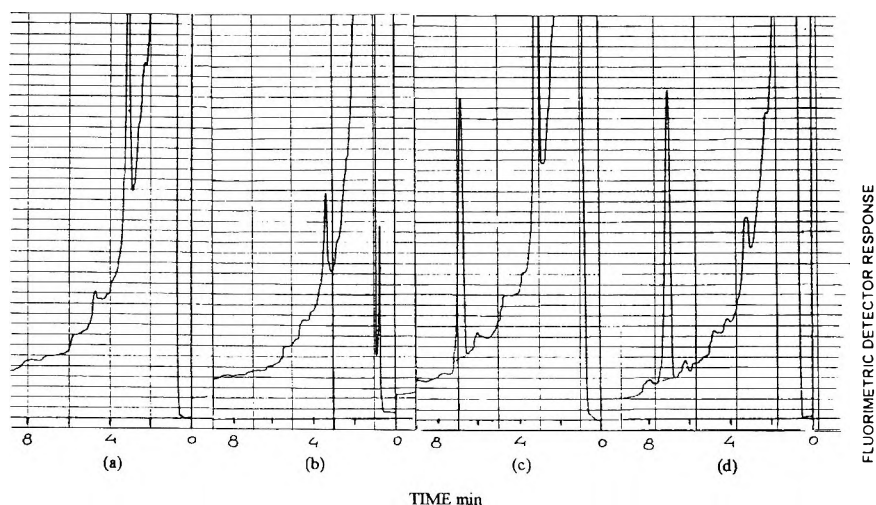
Figure 1. Representative chromatograms of IVM: - (a), (b) blank control samples of sheep liver and fat tissue respectively - (c), (d) IVM-fortified (20 ng/g) sheep liver and fat tissue respectively.
Conditions: mobile phase, methanol-water (95+5 v/v); column, 150 x 4.6 mm, C_{18}; flow rate, 1.8 mL/min; recorder sensitivity, 0.5 AUFS; chart speed, 0.5 cm/min; and injection volume, 20 μL from a final volume of 400 μL.

RESULTS AND DISCUSSION

Several papers are available in the scientific literature on the determination of IVM in different animal matrices and tissues, mostly in milk,[11] plasma,[12] muscle and liver.[6-9] However, only very few studies report reliable analytical procedures to be contemponeously applied both to liver and fat tissues,[2,5] which represent the two matrices recommended for the IVM analysis in the EEC Regulation 2901/93.

Compared to the methods of this kind published so far, this analytical procedure has a major advantage in its extremely effective clean-up procedure. Carried out with an SPE C_{18} extraction, followed by a very fast liquid - liquid partition, this method can actually yield sample extracts with a minimum of interfering substances. This improvement makes the present method suitable for the analysis of IVM, not only in derivatized liver and fat tissue extracts by fluorescence - HPLC, but also, as reported by Dickinson,[13] in non-derivatized muscle tissue extracts by HPLC - UV.

Table 1

Average IVM Recoveries of Six Replicates (% - ± Standard Deviation) From Spiked Samples of Blank control Fat and Liver Tissue of Cattle, Horse, Swine, and Sheep

Added IVM (ng/g)	Swine Fat	Swine Liver	Sheep Fat	Sheep Liver	Horse Fat	Horse Liver	Cattle Fat	Cattle Liver
10	88 ± 4	74 ± 8	70 ± 5	76 ± 4	84 ± 5	77 ± 7	---	---
20	77 ± 1	77 ± 4	79 ± 9	78 ± 3	77 ± 6	78 ± 5	71 ± 8	---
30	77 ± 3	78 ± 4	73 ± 5	73 ± 5	76 ± 9	82 ± 6	75 ± 8	---
40	71 ± 4	76 ± 7	70 ± 4	77 ± 7	76 ± 9	82 ± 9	82 ± 4	---
60	---	---	---	---	---	---	79 ± 4	73 ± 3
80	---	---	---	---	---	---	---	68 ± 7
100	---	---	---	---	---	---	---	74 ± 5
120	---	---	---	---	---	---	---	75 ± 3

The present procedure was also applied to the fat samples without performing the liquid-liquid partition step, but our results suggest that, in these conditions, the derivatization of the fat extracts was not successful. Also, the procedure was carried through omitting the final silica SPE clean-up, but, in these conditions, the derivatized extracts were not purified enough, so that their injection dramatically shortened the life of the HPLC column.

Fig. 1 shows the chromatograms of a blank sheep liver tissue extract (a), of a sheep liver tissue extract, fortified with 20 ng/g IVM (b), of a blank sheep fat tissue extract (c), and of a sheep fat tissue extract fortified with 20 ng/g IVM (d). The response of the fluorimetric detection is linear in the working range of 2-120 ng/g IVM concentrations in tissue. The limit of determination of IVM is 2 ng/g for both tissues.

The chromatographic profiles of the liver and fat tissue extracts from the other animal species listed in the EEC Regulation 2901/93 (cattle, horses and swine) are practically identical to those shown in Fig. 1. In Table 1 are listed the recovery and standard deviation percentages of IVM of liver and fat tissue samples from different animal species, fortified to give IVM concentrations of 10, 20, 30, 40, 60, 80, 100, 120 ng/g. The overall recovery percentages of IVM from fortified samples are 76% with SD 6% for liver and 77% with SD 7% for fat samples.
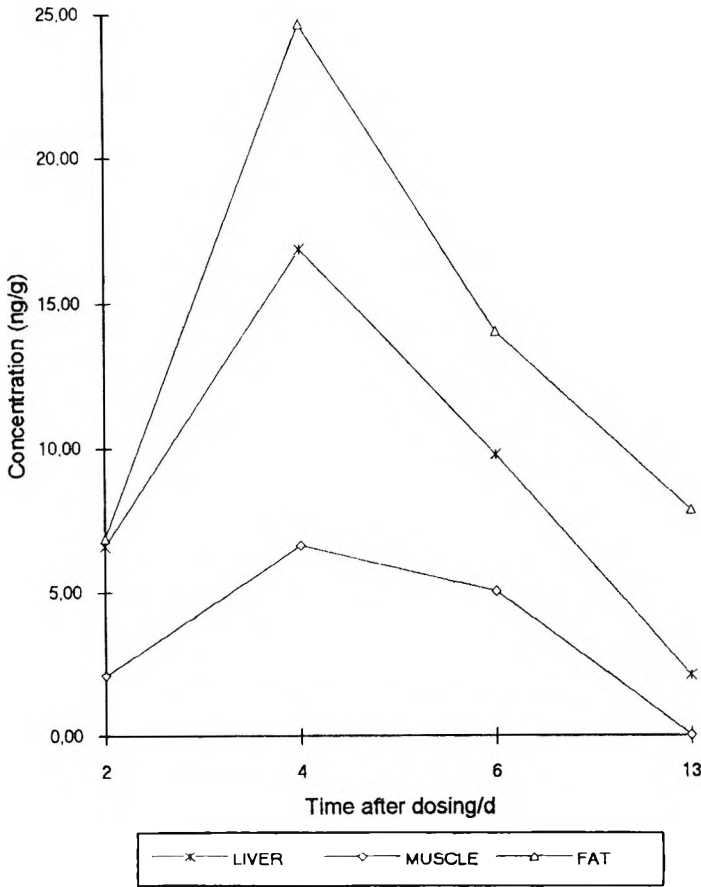
Figure 2. Residual concentration of IVM in muscle, liver and fat tissue of guinea pig following a single subcutaneously dose (0.2 mg/kg body weight). Data represent the mean for two guinea pigs at each time point.

In order to further validate this procedure, and also to study the pharmacokinetics and the depletion features of the drug in guinea pigs administered IVM, a short trial has been carried out. Its results, shown in Fig. 2, confirm the findings of other authors on the depletion of IVM in guinea pigs[14] and in pigs.[15] IVM concentrations increased to reach, after 4 days, their maximal levels of, respectively, 7, 17 and 25 ng/g in muscle, liver and fat. Then

they slowly decreased thereafter. This short study demonstrates that liver and fat tissues are the preferred matrices for IVM accumulation in guinea pigs, as in other animals.[2,15] Moreover, as the intra-assay variation for IVM determinations in duplicate is less than 5 % on all the samples from the treated animals, it can be concluded that this method is effective not only on fortified samples, but also on incurred ones.

This method provides a protocol for IVM determination on food-producing animals, which is in full agreement with the recommendations of the European Community. In fact, it completely fulfils the most important analytical requirements of EEC Regulation 2901/93, both in terms of the IVM limit of determination, and of the animal tissues and species to which IVM analysis should be extended.

ACKNOWLEDGEMENT

REFERENCES

1. W. C. Campbell, M. H. Fisher, E. O. Stapley, G. Albers-Schonberg, T. A. Jacob, Science, **221**, 823-828 (1983).

2. P. C. Tway, J. S. Wood, G. V. Downing, J. Agric. Food Chem., **29**, 1059-1063 (1981).

3. J. A. Bogan, Q. A. McKellar, Vet. Pharmacol. Therap., **11**, 260-268 (1988).

4. Council Regulation N° 2901/93 of 18 October 1993 on **The Determination of Residues in Foodstuffs of Animal Origin**, Off. J. of the Eur. Comm. N° L 246/1 of 23.09.1993.

5. J. Markus, J. Sherma, J. Assoc. Off. Anal. Chem., **75**, 757-767 (1992).

6. C. D. C. Salisbury, J. Assoc. Off. Anal. Chem., **76**, 1149-1151 (1993).

7. J. M. Degroodt, B. Wyhowski De Bukanski, S. Srebrnik, J. Liquid Chrom., **17**, 1419-1426 (1994).

8. F. J. Schenck, S. A. Barker, A. R. Long, J. Assoc. Off. Anal. Chem., **75**, 655-658 (1992).

9. E. Iosifidou, P. Shearan, M. O'Keeffe, Analyst, **119**, 2227-2229 (1994).

10. J. D. Stong, Anal. Chem., **59**, 266-270 (1987).

11. M. Alvinerie, J. F. Sutra, P. Galtier, P. L. Toutain, Ann. Rech. Vet., **18**, 269-274 (1987).

12. R. Chiou, R. J. Stubbs, W. F. Bayne, J. Chromatogr., **416**, 196-202 (1987).

13. C. M. Dickinson, J. Chromatogr., **528,** 250-257 (1990).

14. Q. A. McKellar, D. M. Midgley, E. A. Galbraith, E. W. Scott, A. Bradley, The Vet. Rec., **130**, 71 -73 (1992).

15. S. V. Prabhu, T. A. Wehner, P. C. Tway, J. Agric. Food Chem., **39**, 1468-1471 (1991).

RETENTION OF AROMATIC SULFUR-CONTAINING COMPOUNDS ON RP-HPLC: CORRELATION WITH PARTITION COEFFICIENTS AND MOLECULAR CONNECTIVITY INDICES

Hui Hong, [†][*] Dai Zhou,[†] Shuokui Han,[†] Liansheng Wang,[†]
Zheng Zhang,[‡] Gongwei Zou[‡]

[†]Department of Environmental Science & Engineering
and
[‡]Department of Chemistry
Nanjing University
Nanjing, P. R. China 210093

ABSTRACT

The partition coefficients (log K_{ow}) in n-octanol/water, together with the HPLC capacity factors (k') measured on a C_{18} column, using methanol-water mobile phase of different compositions, were determined for 27 aromatic sulfur-containing compounds. The linear relationship between the log k' values and the percentage of the methanol in the eluent was tested for each compound. The best percentage of methanol (61%), by which the chromatographic partition system became the best model of the n-octanol/water partition system, was determined.

Various molecular connectivity indices (MCI's) were calculated for the compounds and good correlations were established between MCI's and log K_{ow} and log k'. The present correlations can be used to predict partition coefficients and HPLC retention values for other derivatives.

1617

INTRODUCTION

With the development of industry, sulfur-containing compounds, especially aromatic sulfur-containing compounds, are being used more widely and extensively. These compounds are primarily used as intermediates in the manufacture of pesticides, herbicides and anthelmintics.[1] The n-octanol/water partition coefficient (K_{ow}) is critical, both in medical chemistry and in environmental research.[2-5]

As the determination of lipophilicity by the traditional shake-flask method has certain limitations, reverse phase, high performance liquid chromatography (RP-HPLC) has increasingly been used as an alternative method for rapidly measuring the hydrophobicity. Most RPLC methods use C_{18} modified stationary phase and methanol-water mixtures as the mobile phase.[6,7,8] However, the relationship between log k' and log K_{ow} is influenced by the mobile phase composition.[9,10]

Many investigations have reported that the log k'_w values, which can be obtained by extrapolation from the linear portion of the plot of log k' against the percentage, by volume, of methanol in the eluents to 100% water, correlate better with their log K_{ow} values than log k' in mixed eluent.[6,8] But, there are also papers showing different results. Yamagami and co-workers,[11-13] in their series studies on the estimation of heterocyclic hydrophobicity parameters, showed that good linear correlations between log K_{ow} and log k' were obtained with eluents containing 50-70% of methanol, and deviations from linearity were observed with water-rich eluents.

In order to gain more information about this problem, studies of the relationship between log k' and log K_{ow}, at different mobile phase compositions for a variety types of compounds, are required.

While interest in aromatic sulfur-containing compounds has been increasing, little has been studied comprehensively except for the investigations of Han et al.[1] and He et al.[14] In this paper, we determined the K_{ow} values by the traditional shake-flask method and examined the relationships between log K_{ow} and log k', measured under various mobile phase compositions and calculated the percentage of organic modifier in the eluent by which the chromatographic partition system became the best model of the n-octanol/water partition system.

We also investigated the quantitative relationships between molecular connectivity indices and log K_{ow} and log k'.

Table 1

Chemical Structures
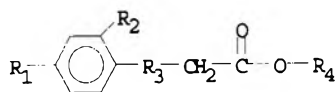
No.	R_1	R_2	R_3	R_4
1a	NO_2	H	S	CH_3
1b	NO_2	H	S	$CH(CH_3)_2$
1c	NO_2	Cl	S	CH_3
1d	NO_2	Cl	S	$CH(CH_3)_2$
1e	H	NO_2	S	CH_3
1f	H	NO_2	S	$CH(CH_3)_2$
1g	Cl	NO_2	S	CH_3
1h	Cl	NO_2	S	$CH(CH_3)_2$
1i	NO_2	NO_2	S	CH_3
1j	NO_2	NO_2	S	$CH(CH_3)_2$
2a	NO_2	H	SO	CH_3
2b	NO_2	H	SO	$CH(CH_3)_2$
2c	NO_2	Cl	SO	CH_3
2d	NO_2	Cl	SO	$CH(CH_3)_2$
2e	H	NO_2	SO	CH_3
2f	H	NO_2	SO	$CH(CH_3)_2$
2g	Cl	NO_2	SO	CH_3
2h	Cl	NO_2	SO	$CH(CH_3)_2$
2i	NO_2	NO_2	SO	CH_3
2j	NO_2	NO_2	SO	$CH(CH_3)_2$
3a	NO_2	H	SO_2	CH_3
3b	NO_2	H	SO_2	$CH(CH_3)_2$
3c	NO_2	Cl	SO_2	CH_3
3d	NO_2	Cl	SO_2	$CH(CH_3)_2$
3e	H	NO_2	SO_2	CH_3
3f	H	NO_2	SO_2	$CH(CH_3)_2$
3g	Cl	NO_2	SO_2	CH_3
3h	Cl	NO_2	SO_2	$CH(CH_3)_2$

MATERIALS AND METHODS

Instruments

The HPLC system (Shimadzu, Kyoto, Japan) consisted of a SCL-8A system monitor, a LC-8A pump, a C-R4A integrator and a SPD-6AV ultraviolet spectrophotometer as the detector. A C_{18} reverse phase Nucleosil 7 (Dalian Institute of Chemical Physics, Academic Sinica) (15 cm x 4.6 mm i.d.) column was used.

Materials

The compounds which were studied are shown in Table 1. These compounds, which are phenylthio, phenylsulfinyl and phenylsulfonyl acetates, were synthesized in our laboratory. Their purities were monitored by HPLC to assure high purity. The water used as a mobile phase component was double-distilled. Methanol was analytical grade and was redistilled before use. Sodium nitrate and n-octanol were also analytical grade.

Methods

The log k' values were determined for each compound. The mobile phases were made by mixing methanol with water in the proportions 100:0, 90:10, 85:15, 80:20, 75:25 and 70:30 (v/v). The flow rate was 0.8 mL/min. All measurements were made at least in duplicate. The average reproducibility of each determination was better than 1.0% relative. The capacity factors (k') were determined using $k' = (t_r - t_0)/t_0$, where t_r is the retention time of the compound, and t_0 is the void volume or the dead time. Aqueous solution of sodium nitrate was used for the measurement of t_0.[15]

The n-octanol/water partition coefficients were determined by shake-flask method, as described by OECD Guideline for Testing of Chemicals, at 25°C, followed by centrifuging and analysis of the compound in the aqueous phase with a UV spectrophotometer against a water blank.

The molecular connectivity indices (MCI's) were calculated according to Kier and Hall.[16] The calculation was performed with an AST 386 computer.

The regression analyses were performed using the "Statgraphics" program (STSC, Inc.; 1987).

Table 2

Slope & Intercept Values of the Log k' vs OP% Straight Lines Measured in Various Compositions of Methanol

No.	Slope	Log k'$_w$	Corr. Coeff.
1b	-4.3866	3.5217	0.999
1c	-4.0966	3.3447	0.998
1d	-4.8403	4.1696	0.997
1e	-3.2507	2.2814	0.994
1f	-4.0279	3.1399	0.995
1g	-3.8686	3.1098	0.996
1h	-4.6978	3.9944	0.995
1i	-3.8370	2.8392	0.992
1j	-4.6216	3.6981	0.993
2a	-2.4484	1.1556	0.990
2b	-3.3513	2.1306	0.985
2c	-2.9856	1.8731	0.985
2d	-3.8653	2.8306	0.995
2e	-2.2803	1.0951	0.975
2f	-3.3452	2.2285	0.957
2g	-3.0988	1.9930	0.985
2h	-3.8492	2.8675	0.995
2i	-2.5911	1.3085	0.980
2j	-3.3090	2.1766	0.991
3a	-4.3534	2.5766	0.990
3b	-4.6980	3.1919	0.995
3c	-3.9539	2.5675	0.985
3d	-4.6605	3.3681	0.995
3e	-3.4937	1.8633	0.975
3f	-4.2896	2.8329	0.991
3g	-4.0939	2.7119	0.990
3h	-4.7195	3.4724	0.995

RESULTS AND DISCUSSION

Determination of the Best Composition of Mobile Phase for K_{ow} Estimation

There have been numerous studies on the estimation of log K_{ow} from HPLC log k' data. But, which log k' values, determined under various chromatography conditions, best correlate with the log K_{ow} values. Valko[17]

established a general approach for the estimation of K_{ow} by RP-HPLC. In his work, the following regression equation was used to obtain the best percentage of organic modifier in the eluent for modeling the n-octanol/water partition system:

$$\log K_{ow} = a \text{ 'slope'} + b \log k'_w + c \tag{1}$$

where 'slope' and log k'_w are, respectively, the slope and intercept value of log k' vs. OP% (percentage of organic phase in the eluent) straight line. a, b and c were constants obtained by a least squares method. The quotient of the values of a and b gave the percentage of organic modifier in the eluent by which the chromatographic partition system became the best model of the n-octanol/water system.

The value of the log k' for each studied compound was correlated with OP% and yielded the values of 'slope', log k'_w and the correlation coeffcients of the compounds. These values are shown in Table 2.

Substituting the obtained values of the 'slope' and log k'_w into Eq. 1, and by applying a least square method, the following equation was obtained:

$$\log K_{ow} = 1.031 \text{ 'slope'} + 1.682 \log k'_w + 1.262 \tag{2}$$

$$R = 0930; SE = 0.196; F = 174.62; n = 27$$

The relationship described by Eq. 2 is statistically significant at the level better than 0.01: $F = 174.62 > F(2,24,0.01) = 5.16$.

The quotient of the regression coefficients of the 'slope' and the log k'_w values gives 0.613. This means that the chromatographic partition system containing 61% methanol and 39% water mixture, with an RP-C_{18} column shows the greatest similarity to the n-octanol/water partition system for these aromatic sulfur-containing compounds. The observed and calculated log K_{ow} values, according to Eq. 2, are listed in Table 3. It is clear that K_{ow} values of the other derivatives of aromatic sulfur-containing compounds can be estimated by RP-HPLC at a methanol level of 61 % and RP-C_{18} column.

The observed values of log Kow were also correlated with log k'_w and the following equation was obtained:

$$\log K_{ow} = 0.817 \log k'_w - 0.354 \tag{3}$$

$$R = 0.815; SE = 0.325; F = 110.53; n = 27$$

Table 3

**Observed and Calculated Log K_{ow} Values
for the Studied Compounds**

Compound	Exptl[a]	Calcd[b]	Log K_{ow} Diff[b]	Calcd[c]	Diff[c]
1b	2.79	2.66	0.13	2.81	-0.02
1c	2.26	2.66	-0.40	2.10	0.16
1d	3.20	3.29	-0.09	3.00	0.20
1e	1.88	1.75	0.13	1.80	0.08
1f	2.76	2.39	0.37	2.70	0.06
1g	2.24	2.50	-0.26	2.42	-0.18
1h	3.00	3.14	-0.14	3.32	-0.32
1i	2.05	2.08	-0.03	1.80	0.25
1j	2.81	2.72	0.09	2.69	0.12
2a	0.80	0.68	0.12	0.78	0.02
2b	1.64	1.39	0.25	1.68	-0.04
2c	1.35	1.33	0.02	1.12	0.23
2d	2.01	2.04	-0.03	2.01	0.00
2e	0.74	0.75	-0.01	0.68	0.06
2f	1.59	1.56	0.03	1.57	0.02
2g	1.29	1.42	-0.13	1.30	-0.01
2h	2.22	2.12	0.10	2.19	0.03
2i	0.63	0.79	-0.16	0.68	-0.05
2j	1.61	1.51	0.10	1.57	0.04
3a	0.78	1.11	-0.33	0.94	-0.16
3b	1.80	1.79	0.01	1.83	-0.03
3c	1.45	1.50	-0.05	1.48	-0.03
3d	2.40	2.12	0.28	2.37	0.03
3e	0.78	0.79	-0.01	0.92	-0.14
3f	1.72	1.60	0.12	1.81	-0.09
3g	1.30	1.60	-0.30	1.54	-0.24
3h	2.45	2.24	0.21	2.44	0.01

[a] Determined by shake-flask method. [b] Calculated according to Eq. 2 (RP-HPLC method). [c] Calculated according to Eq. 4 (MCI's method).

Comparing the R values of Eq. 2 and 3, it is obvious that log k'_w is less powerful for the estimation of log K_{ow} values of these studied compounds. Valko[18] also suggested that the correlation coefficients for the variable of 'slope' and log k'_w was a quantitative measure of structural similarities with regard to

the compounds' behavior in a RPLC system. The intercorrelation of the two variables in Eq. 2 is 0.94; this suggests that the studied compounds behave similarly in the RP-HPLC system. This partition similarity is important in Quantitative Structure-Activity Relationship (QSAR) investigations. It means that, although the degree of oxidation of sulfur atoms in phenylthio, phenylsulfinyl and phenylsulfonyl are different; these three sets of compounds will show similar partition behavior in the biological system.

Correlation Between MCI's and Log K_{ow} and Log k'

Molecular connectivity is a method of deriving topological indices from the hydrogen suppressed skeleton of a molecule. A detailed calculation method is provided by Kier and Hall;[19] only a brief description of the procedure used to calculate MCI's will be presented here. To calculate MCI's of a molecule, first, each non-hydrogen atom is assigned a delta value. For simple indices, each nonhydrogen atom is assigned a delta value (δ) which is equal to the number of atoms to which it is bonded. Valence indices are obtained by assigning atom δ values based on the number of valence electrons not involved in bonds to hydrogen atoms. Simple and valence indices of different orders and types can be calculated for a given molecule. The order refers to the number of bonds in the skeletal substructure or fragment used in computing the index: zero order defines individual atoms, first order uses individual bond lengths, second order uses two adjacent bond combinations, and so on. The type refers to the structural fragment (path, cluster, path/cluster or chain) used in computing the index. Only path indices are possible for orders less than 3. The symbol $^1\chi^v$ represents a first order valence index while $^2\chi$ represents a simple second order index. Each index is computed by an algorithm introduced by Randic[20] which sums the reciprocal square roots of the assigned δ values over all molecular fragments as illustrated below for zero, first, and second order indices:

$$\chi = \sum (\delta_i)^{-1/2} \text{ for all atoms}$$

$$\chi = \sum (\delta_i \delta_j)^{-1/2} \text{ for all bonded pairs of atoms}$$

$$\chi = \sum (\delta_i \delta_j \delta_k)^{-1/2} \text{ for all bonded pairs of atoms}$$

There have been many papers concerning the utility of molecular connectivity indices for describing partition coefficients and HPLC retention parameters.[21-23] Since the MCI's can be calculated quickly and accurately, only based on the structure of a chemical and with no experimental requirements, they are becoming more and more of interest. In molecular connectivity

Table 4

Selected Molecular Connectivity Indices for the Studied Compounds

No.	$^0\chi(R_4)$	$^3\chi^v_c(Ph)$	$^2\chi^v(Ph)$	$^1\chi^v(Ph)$	$^3\chi_c(Ph)$	$^5\chi_{pc}(Ph)$
1b	2.5774	0.2787	2.0824	2.8888	0.3042	0.3715
1c	1.0000	0.4185	2.5843	3.3716	0.4327	0.6487
1d	2.5774	0.4185	2.5843	3.3716	0.4327	0.6487
1e	1.0000	0.2459	2.0325	2.8948	0.2784	0.5629
1f	2.5774	0.2459	2.0325	2,8948	0.2784	0.5629
1g	1.0000	0.4347	2.6123	3.3716	0.4451	0.7399
1h	2.5774	0.4347	2.6123	3.3716	0.4451	0.7399
1i	1.0000	0.3480	2.4290	3.3429	0.4648	0.8083
1j	2.5774	0.3480	2.4290	3.3429	0.4648	0.8083
2a	1.0000	0.2466	2.1480	3.1464	0.2697	0.4081
2b	2.5774	0.2466	2.1480	3.1464	0.2697	0.4081
2c	1.0000	0.3906	2.6574	3.6292	0.4028	0.7502
2d	2.5774	0.3906	2.6574	3.6292	0.4028	0.7502
2e	1.0000	0.2181	2.1056	3.1524	0.2485	0.5727
2f	2.5774	0.2181	2.1056	3.1524	0.2485	0.5727
2g	1.0000	0.4068	2.6854	3.6292	0.4152	0.7534
2h	2.5774	0.4068	2.6854	3.6292	0.4152	0.7534
2i	1.0000	0.3202	2.5021	3.6005	0.4349	0.8219
2j	2.4774	0.3202	2.5021	3.6005	0.4349	0.8219
3a	1.0000	0.2551	2.1756	3.1645	0.3564	0.5052
3b	2.5774	0.2551	2.1756	3.1645	0.3564	0.5052
3c	1.0000	0.4048	2.6949	3.6473	0.4917	0.9403
3d	2.5774	0.4048	2.6949	3.6473	0.4917	0.9403
3e	1.0000	0.2323	2.1430	3.1705	0.3373	0.6833
3f	2.5774	0.2323	2.1430	3.1705	0.3373	0.6833
3g	1.0000	0.4210	2.7229	3.6473	0.5043	08656
3h	2.5774	0.4210	2.7229	3.6473	0.5043	08656

indices calculation, if the studied compounds have a common parent structure, molecular fragment connectivity indices are calculated instead of calculating the whole molecular connectivity indices. Kier and Hall,[19] and Kaliszan[24] had used this sort of partial molecular connectivity indices in their work.

The structures of the compounds investigated in this study are shown in Table 1. An examination of the general structures of the studied compounds suggests that the structure can be divided into two areas. One is the ester alkyl R_4 of CH_3 or $CH(CH_3)_2$, the other is the substitution pattern of R_1, R_2 and R_3 on

the benzene ring. Since the two areas occupy sites at opposite ends of the molecule, it would not be surprising if these two parts exert independent influences on their physicochemical properties and biological activities. For this reason, molecular connectivity indices were calculated for truncated portions of the molecule.

For the ester alkyl group R_4, the simple zero order index $^0\chi(R_4)$ was calculated. It was enough, by using $^0\chi(R_4)$ to discriminate CH_3 and $CH(CH_3)_2$. For the substituted phenyl part Ph, $^0\chi(Ph)$, $^1\chi(Ph)$, and simple path indexes $^2\chi(Ph)$ through $^7\chi_p(Ph)$, simple third-order cluster $^3\chi_c(Ph)$, simple fourth- and fifth-order path/cluster indexes $^4\chi_{pc}(Ph)$ and $^5\chi_{pc}(Ph)$, as well as the corresponding valence indices were calculated. All of the 23 calculated connectivity indexes were stored as variables in the data file.

By stepwise regression, the statistically significant variables were chosen for log K_{ow} and log k'_w. High quality regression equations were obtained. The selected MCI's of the studied compounds are listed in Table 4.

$$\log K_{ow} = 0.568 \, (0.036) \, ^0\chi(R_4) + 22.953 \, (1.275) \, ^3\chi^v_c(Ph)$$
$$- 6.878 \, (0.479) \, ^2\chi^v(Ph) + 1.549 \, (0.325) \, ^5\chi_{pc}(Ph)$$
$$+ 8.698 \, (0.639) \tag{4}$$

$r = 0 \, 980; \, s = 0.146; \, F = 162.90; \, n = 27$

$$\log k'_w = 0 \, 547 \, (0 \, 053) \, ^0\chi(R4) + 6.868 \, (1.079) \, ^3\chi^v_c(Ph)$$
$$- 3.414 \, (0.293) \, ^1\chi^v(Ph) + 7.333 \, (1.127) \, ^3\chi_c(Ph)$$
$$+ 7.995 \, (0.740) \tag{5}$$

$r = 0.964; \, s = 0 \, 217; \, F = 87 \, 07; \, n = 27$

Eq. 4 and 5 are both highly significant at the level better than 0.01: $F = 162.90 > F(4,22,0.01) = 4.31$; $F = 87.07 > F(4, 22, 0.01) = 4.31$. The student t value for each coefficient also is very large: 15.897, 18.009, -14.356 and 4.761 for Eq. 4 and 15.897, 18.009, -14.357 and 4.761 for Eq. 5. The observed and calculated log K_{ow} values according to Eq. 4 are also listed in Table 3. Figure 1 shows the correlation between the extrapolated values of log k'_w and the values calculated by Eq. 5.

The results show that calculation of the connectivity indices may provide a method for the prediction of HPLC retention values and MCI's can be used successfully in QSAR and QSRR (Quantitative StructureRetention Relationship).
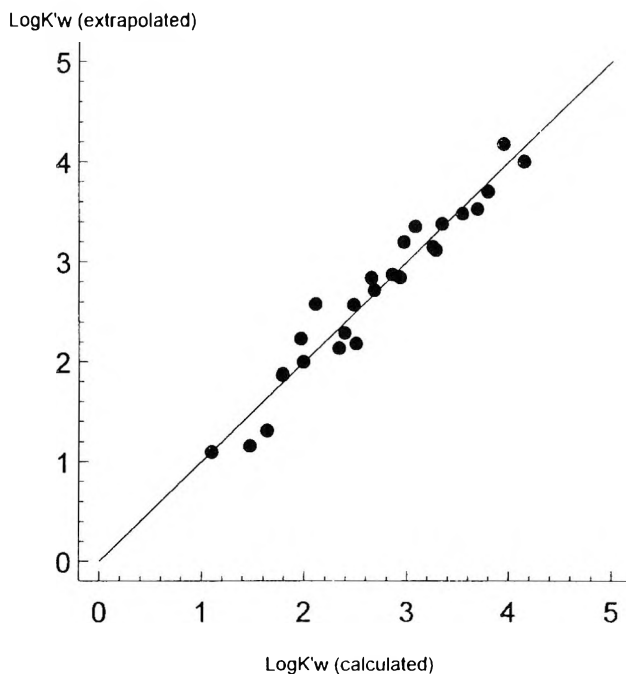
Figure 1. Plot of the extrapolated and the calculated log k'_w values according to Eq. 5.

REFERENCES

1. S. K. Han, L. Q. Jiang, L. S. Wang, Z. Zhang, Chemosphere, **25**, 643-649 (1992).

2. C. Hansch, A. Leo, **Substitutent Constants for Correlation Analysis in Chemistry and Biology**, John Wiley & Sons, New York, 1979.

3. D. Mackay, A. Bobra, W. Y. Shiu, S. H. Yalkowsky, Chemosphere, **9**, 701-711 (1980).

4. G. G. Briggs, J. Agric. Food Chem., **29**, 1050-1059 (1981).

5. W. B. Neely, D. R. Branson, G. E. Blau, Environ. Sci. Technol., **8**, 1113
    1115 (1974).

6. Th. Braumann, J. Chromatogr., **373**, 191-225 (1986).

7. C. Yamagami, H. Takami, K. Yamamoto, K. Miyoshi, N. Takao, Chem.
    Pharm. Bull., **32**, 4994-5002 (1984).

8. D. J. Minick, J. H. Frenz, M. A. Patrick, D. A. Brent, J. Med. Chem., **31**,
    1923-1933 (1988).

9. J. G. Dorsey, M. G. Khaledi, J. Chromatogr. **A656**, 485-499 (1993).

10. B. McDuffie, Chemosphere, **10**, 73-83 (1981).

11. C. Yamagami, T. Ogura, N. Takao, J. Chromatogr., **514**, 123-136 (1990).

12. C. Yamagami, N. Takao, Chem. Pharm. Bull., **39**, 2924-2929 (1991).

13. C. Yamagami, N. Takao, Chem. Pharm. Bull., **40**, 925-929 (1992).

14. Y. B. He, L. S. Wang, S. K. Han, Y. H. Zhao, Chemosphere, **30**, 117-125
    (1995).

15. C. Horvath, W. Melander, I. Molnar, Anal. Chem., **49**, 142-154 (1977).

16. L. B. Kier, L. H. Hall, **Molecular Connectivity in Chemistry and Drug
    Research**, Academic Press, New York, 1976.

17. K. Valko, J. Liq. Chromatogr., **7**, 1405-1424 (1984).

18. K. Valko, J. Liq. Chromatogr., **10**, 1663-1686 (1987).

19. L. B. Kier, L. H. Hall, **Molecular Connectivity in Structire-Activity
    Analysis**, Research Studies Press, John Wiley & Sons, Inc., New York,
    1986.

20. M. Randic, J. Amer. Chem. Soc., **17**, 6609-6615 (1975).

21. W. G. Murray, L. H. Hall, J. Pharm. Sci., **64**, 1978-1981 (1975).

22. K. Jinno, K. Kawasaki, Chromatographia, **18**, 90-95 (1984).

23. J. Bojarski, L. Ekiert, Chromatographia, **15**, 172-176 (1982).

24. R. Kaliszan, H. Foks, Chromatographia, **10**, 346-349 (1977).

HIGH PERFORMANCE LIQUID CHROMATOGRAPHIC METHOD FOR THE DETERMINATION OF DULOXETINE AND DESMETHYL DULOXETINE IN HUMAN PLASMA

Jason T. Johnson, Samuel W. Oldham,
Ronald J. Lantz, Allyn F. DeLong

Lilly Research Laboratories
Lilly Laboratory for Clinical Research
Eli Lilly and Co.
Indianapolis, IN 46202, USA.

ABSTRACT

A high performance liquid chromatographic (HPLC) method was developed and validated for the analysis of duloxetine and desmethyl duloxetine in human plasma. Plasma was adjusted to pH 10 with 1.0 M sodium carbonate and extracted with hexane which contained 2% isopropyl alcohol. The concentrated extract was derivatized with dansyl chloride (500 μg/mL). A Phenomenex Primesphere 5 C_{18} HC column provided chromatographic separation of the analytes followed by fluorescence detection with excitation and emission wavelengths at 285 nm and 525 nm respectively. The linear dynamic range for both analytes was 2 ng/mL to 64 ng/mL with precision and accuracy of <10%.

INTRODUCTION

Animal models of pharmacologic activity demonstrated that duloxetine hydrochloride is a potent and selective mixed serotonin (5-HT) / norepinephrine (NE) reuptake inhibitor.[1-3] After single and multiple once a day dose administration of 5 mg to 40 mg in volunteers, duloxetine blocked the uptake of serotonin in human platelets and was well tolerated by the subjects. Duloxetine hydrochloride is currently being evaluated in depression and other disease states for which alteration of serotonergic and noradrenergic neurotransmission may produce beneficial therapeutic effects.

A high performance liquid chromatographic (HPLC) assay was developed to monitor duloxetine and desmethyl duloxetine during clinical trials and to determine the pharmacokinetics of duloxetine and metabolite.

EXPERIMENTAL

Chemicals and Reagents

Desmethyl duloxetine, 210980 (I), duloxetine hydrochloride, LY248686 (II), and internal standard, 113821 (III), were synthesized at Lilly Research Laboratories (Eli Lilly and Co., Indianapolis, IN, USA (Fig. 1, structures, base forms). HPLC quality water was prepared from a Millipore Milli-Q System (Marlborough, MA, USA). Acetone, acetonitrile, and methanol were HPLC grade and purchased from Mallinckrodt, Paris, KY, USA.   Hexane and isopropyl alcohol were purchased from Baxter Scientific, USA. Ammonium acetate was purchased from EM Science, USA. Dansyl chloride was purchased from Sigma, USA.   Sodium carbonate anhydrous was purchased from Mallinckrodt. Drug free (blank) heparinized human plasma was purchased from Biological Specialty Corporation, Colmar, PA, USA.

High Performance Liquid Chromatography

The HPLC system consisted of a Waters 715 Ultra WISP (Waters Associates, Millford, MA, USA), Beckman System Gold 126 binary pumping system (Beckman Instruments, Inc., San Ramon, CA, USA), Perkin Elmer LS40 Fluorescence detector (Perkin-Elmer Ltd., Beaconsfield, Buckinghamshire, England) and Perkin Elmer Access*Chrom data reduction system.   The guard column / analytical column combination was a Zorbax ODS, 4 mm x 1.25 cm,   5 μm (MAC - MOD, Chadds Ford, PA, USA) / Phenomenex

DULOXETINE (LY248686) FREE BASE

(II)

DES-METHYL METABOLITE (210980)

(I)

INTERNAL STANDARD (113821)

(III)
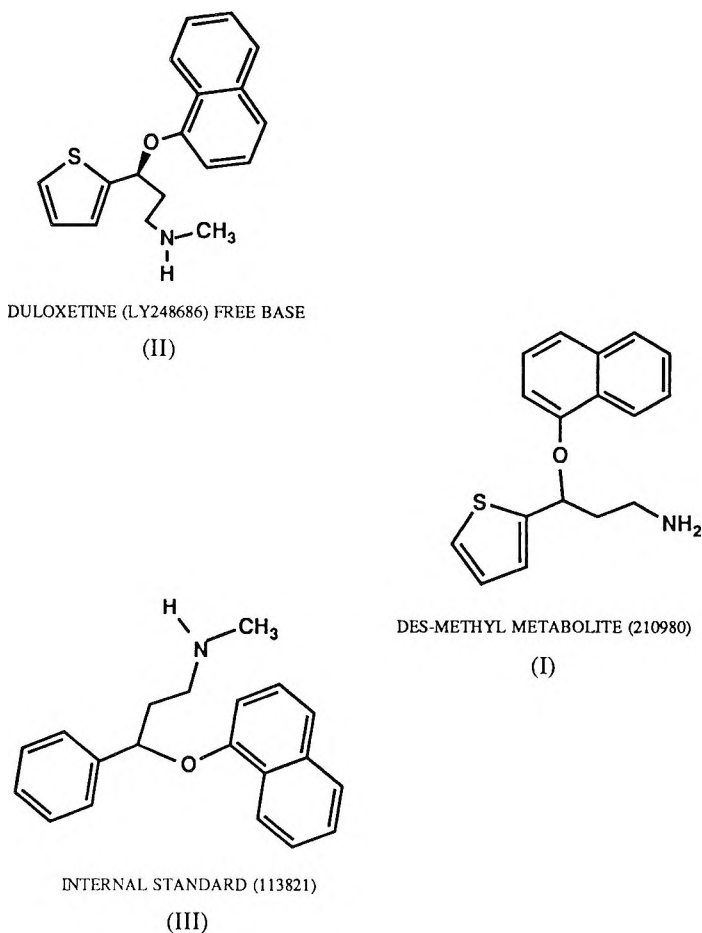
Figure 1. Structures (base form) of desmethyl duloxetine (I), duloxetine (II), and internal standard (III).

Primesphere 5 C_{18} HC, 25 cm x 4.6 mm, 5 μm (Phenomenex, Torrance, CA, USA). The mobile phase consisted of 21% 0.05 M ammonium acetate/79% acetonitrile which was filtered and degassed. The flow-rate was 2.0 mL/min and the column temperature was ambient. The chromatographic run required 20 minutes for completion.   The analytes were detected and quantified by fluorescence at excitation and emission settings of 285 nm and 525 nm, respectively.

Preparation of Standard Solutions

Silylated glassware and selected plasticware were used to prepare the samples and standards to minimize the nonspecific adsorption of the analytes to glassware. Stock solutions of I, II, and III were prepared in methanol at free base concentrations of 100 µg/mL. The plasma calibrators were prepared by spiking an appropriate amount of plasma with the standard stock to yield a 64 ng/mL sample. This sample was diluted with blank plasma to obtain calibrators of 32, 16. 8, 4, and 2 ng/mL.

Quality control samples at concentrations of 50, 25, and 5 ng/mL were prepared from a separate weighing of compound. A standard curve was prepared for each validation run in which 5 samples of each quality control concentration were analyzed. The quality control samples were stored at -20°C.

Sample Preparation Procedures

One mL aliquots of quality control samples and freshly prepared calibrators were placed in individual silylated 16 mm x 125 mm screw cap tubes with Teflon caps (Kimble Series 73750). After the addition of 1 mL of 1.0 M sodium carbonate buffer, pH 10, 200 µl of a 0.1 µg/mL internal standard solution, and 6 mL of a 98% hexane / 2% isopropyl alcohol solution, the tubes were tightly sealed with the screw cap. The samples were placed on a Labquake shaker (Labindustries Inc., Berkeley, CA, USA.) for 45 minutes. The samples were centrifuged at approximately 825 x g for 10 minutes and then placed in a methanol / dry ice bath to freeze the aqueous component.

The upper organic layer was decanted from the lower frozen aqueous layer and placed in 13 mm x 100 mm silylated culture tubes (Kimble Series 73500). The tubes containing the organic phase were placed in a Multivap (Organomation Associates, Berlin, MA, USA) sample concentrator at about 42°C for approximately 30 minutes or until dry.

The dried residue was then derivatized by adding 2 mL of acetone, 150 µl of 0.1 M sodium carbonate, pH 10, and 75 µl of 500 µg/mL dansyl chloride at 55°C for 30 minutes. The samples were reduced to dryness under nitrogen at 42°C and reconstituted with 200 µl of mobile phase. The samples were filtered using 10 µm filter tips (Zymark Corp., USA.) and 100 µl was injected onto the column. A typical chromatographic separation of desmethyl duloxetine, duloxetine, and internal standard from human plasma and a plasma standard can be seen in Fig. 2.
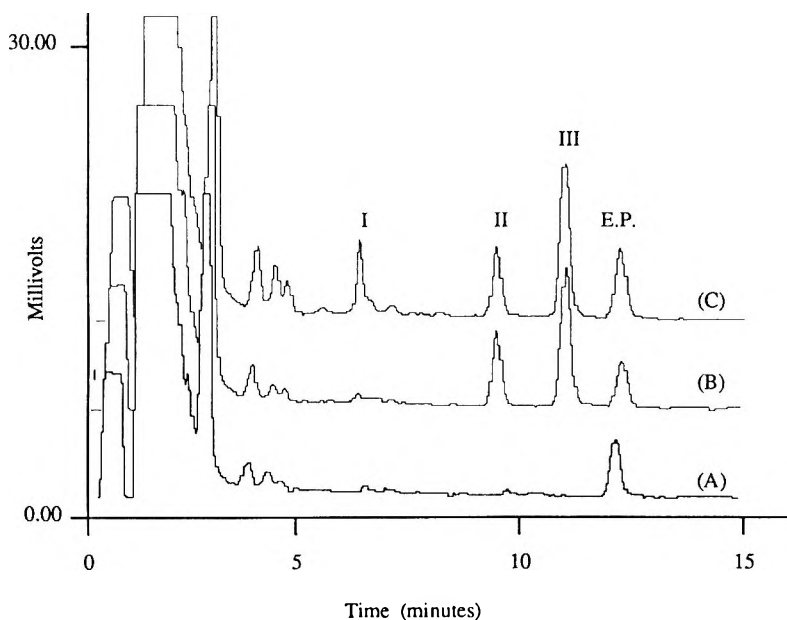
Figure 2. Representative chromatograms of blank human plasma (A), plasma sample with <LOQ (I) and 9.2 ng/mL (II) (B), and a plasma standard with 8 ng/mL (I) and 8 ng/mL (II) (C). Peaks: I = desmethyl duloxetine, II = duloxetine, III = internal standard. <LOQ represents below the limit of quantification which is 5 ng/mL. E.P. represents an endogenous peak.

Data Reduction / Data Acceptability Criteria

Data reduction/calculation was accomplished with an on line computer system (Perkin Elmer Access*Chrom). Calculation drug concentrations in unknown samples was based on a weighted $(1/x^2)$ least squares regression of plasma calibrator concentrations against the peak height ratios. The peak height ratios were obtained by dividing the peak heights of I and II by the peak height of the internal standard.

Each five (5) point calibration curve must have a coefficient of determination of at least 0.97. Both the relative error and the relative standard deviation of the control samples must be <15% of the theoretical value except for those at the limit of quantification which must be < 20%.

Determination of Standard Curve Characteristics, Precision and Accuracy

The regression coefficients for duloxetine and desmethyl duloxetine were greater than 0.99. The back calculated results for the standard curve demonstrated the precision and accuracy of the standard curves (Table 1). The precision and accuracy of the HPLC assay were evaluated by performing statistical analysis of 5 replicates of each quality control concentration during 3 days (Table 2). The statistical analysis of the precision and accuracy data demonstrate that the assay is suitable for quantifying the two analytes during clinical trials and/or pharmacokinetic studies to a limit of quantification of 5 ng/mL.

Determination of Drug/Metabolite Stability in Plasma

The stability of duloxetine and desmethyl duloxetine was determined at room temperature, -20°C, and -70°C. Also, the effects of freeze-thaw cycles were determined. At a minimum, replicate samples of known concentrations of the analytes were analyzed. Both analytes were stable at concentration ranges of 5 to 50 ng/mL at -20°C and -70°C for at least 2 months. The compounds were unaffected after three freeze-thaw cycles at -20°C. A sample with an approximate concentration of 30 ng/mL of each compound was stable at room temperature for at least 24 hours.

RESULTS AND DISCUSSION

Chromatography

The majority of the drug related analytes found in human plasma after administration of duloxetine hydrochloride was the parent drug. The desmethyl metabolite was seen in trace amounts. The retention times of the desmethyl metabolite, parent drug and internal standard were approximately 6.1, 9.3, and 10.9 minutes, respectively (Figure 2).

Assay Specificity

The specificity of the assay was determined by analyzing several lots of blank plasma for interferences. It was found that all plasma screened contained an endogenous peak with an approximate retention time of 12.2 minutes. This

Table 1

Standard Curve Characteristics

DULOXETINE					DESMETHYL DULOXETINE				
Target Value ng/mL	Mean ng/mL n = 5	S.D.	RE (%)	RSD (%)	Target Value ng/mL	Mean ng/mL n = 5	S.D.	RE (%)	RSD (%)
2	2.04	0.06	2.17	2.95	2	2.13	0.15	6.5	6.82
4	3.98	0.09	-0.42	2.14	4	4.05	0.07	1.17	1.79
8	7.98	0.06	-0.025	0.78	8	7.81	0.15	-2.38	1.91
16	15.78	0.17	-1.4	1.05	16	14.95	1.15	-6.65	7.68
32	31.68	0.34	-1.01	1.06	32	31.8	0.3	-0.62	0.95
64	64.54	0.32	0.84	0.5	64	65.28	1.24	2.01	1.9

LINEAR REGRESSION ANALYSIS[1]

Standard Curve Characteristics

Day	K0	K1	R2
1	-0.0116	0.09525	0.09996
2	-0.0148	0.057	0.9998
3	-0.0005	0.0589	0.9999

LINEAR REGRESSION ANALYSIS[1]

Standard Curve Characteristics

Day	K0	K1	R2
1	0.0135	0.06560	0.9944
2	-0.0178	0.0686	0.9993
3	-0.0136	0.0712	0.9999

[1] K0 = y-intercept of standard curve
K1 = slope of curve
R2 = caofficient of determination
RE = Relative Error
RSD = Relative Standard Deviation

endogenous peak did not interfere with the internal standard peak. There were no interferences in the resolution of the analytes in this chromatographic system.

Overall Analyte Recovery and Assay Linearity

The extraction recovery for duloxetine, desmethyl duloxetine, and internal standard was 27%, 58%, and 25%, respectively. The recovery was determined by measuring the peak height of extracted plasma samples vs. the peak height of neat standards in methanol.

As observed in blank plasma (Figure 2), hexane extraction provided minimal background from plasma components while providing consistent recovery of analytes. The standard curve characteristics and back calculated values of the standard curve samples are shown in Table 1. The assay was linear from 2 ng/mL to 64 ng/mL for both duloxetine and desmethyl duloxetine.

Precision, Accuracy, and Limit of Quantification

The determination of I and II was evaluated for precision and accuracy by replicate analysis of the quality control pools at three different concentrations within the standard curve range (Table 2). Both within-day and between-day precision and accuracy was found to be less than 10%. In addition, the limit of quantification (LOQ) was found to be 5 ng/mL.

Use of the Method During Patient Clinical Trials

The method was used to measure the concentration of the analytes in human plasma samples from clinical studies. Figure 3 displays plasma concentrations of duloxetine from a pilot bioequivalency study. The plasma concentrations of desmethyl duloxetine were mainly below the limit of assay quantification.

Conclusion

The three day validation data for this method shows that the relative error and relative standard deviation for both duloxetine and desmethyl duloxetine were < 10%. However, it has been found with application of this method that

Table 2

Precision and Accuracy for Duloxetine and Desmethyl Duloxetine

		DULOXETINE			DESMETHYL DULOXETINE		
		Target Concentration (ng/mL)			Target Concentration (ng/mL)		
		50.00	25.00	5.00	50.00	25.00	5.00
Day 1[1]	Mean	51.31	25.60	5.08	50.56	26.15	4.68
	S.D.	0.95	0.70	0.21	3.74	1.84	0.16
	RE (%)	2.62	2.40	1.52	1.12	4.58	-6.40
	RSD (%)	1.86	2.75	4.08	7.39	7.03	3.49
Day 2[1]	Mean	46.89	22.85	4.75	49.60	24.39	4.93
	S.D.	0.20	0.07	0.22	1.00	0.68	0.13
	RE (%)	-6.22	-8.60	-4.96	-0.79	-2.45	-1.32
	RSD (%)	0.43	0.29	4.72	2.02	2.78	2.62
Day 3[1]	Mean	45.68	21.97	4.51	49.75	24.21	5.10
	S.D.	0.56	0.14	0.12	2.18	0.78	0.19
	RE (%)	-8.63	-12.14	-9.80	-0.50	-3.14	2.04
	RSD (%)	1.22	0.64	2.60	4.38	3.23	3.78
Overall[2]	Mean	47.96	23.47	4.78	49.97	24.92	4.91
	S.D.	2.57	1.65	0.30	2.41	1.44	0.24
	RE (%)	-4.08	-6.11	-4.41	-0.06	-0.34	-1.89
	RSD (%)	5.37	7.02	6.22	4.83	5.80	4.79

(1) n = 5 determinations
(2) n = 15 determinations
S.D. = standard deviation
Accuracy expressed as %RE = relative error (%R.E. = ((mean/theoretical) -1)*100)
Precision expressed as %RSD = relative stadard deviation (%R.S.D. = (standard deviation/mean)*100)

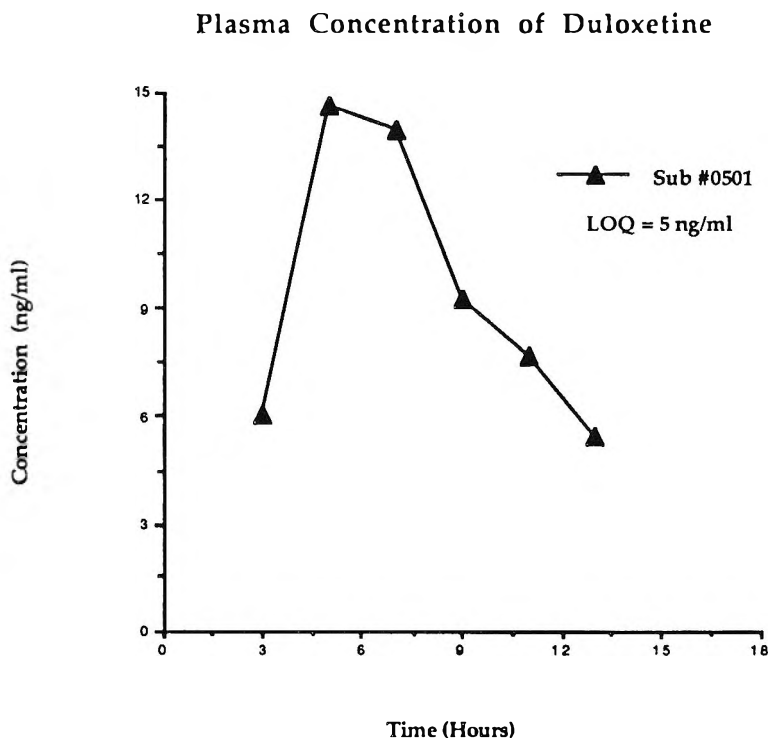## Plasma Concentration of Duloxetine

Time (Hours)

Figure 3. Plasma duloxetine in human subject #0501. Dose = 20 mg enteric coated tablet, fasted. morning.

the desmethyl duloxetine precision and accuracy data is sometimes > than 10%. The reason for the difference in the precision /accuracy of desmethyl duloxetine compared to duloxetine is unknown at this time.

This method has been used by our laboratory for bioavailability/bioequivalence studies and to monitor duloxetine plasma concentrations during clinical studies.

REFERENCES

1. D. R. Wong, F. P. Bymaster, D. A. Mayle, L. R. Reid, J. H. Krushinski, D. W. Robertson, LY248686, "A New Inhibitor of Serotonin and Norepinephrine Uptake," Neuropsychopharmacology **8**, 23, 1993.

2. R. W. Fuller, S. K. Hemrick-Luecke, H. D. Snoddy, "Effects of Duloxetine, an Antidepressant Drug Candidate, on Concentrations of Monoamines and their Metabolites in Rats and Mice, J. Pharmacol. Exp. Ther., **269**, 132, 1994.

3. T. Kihara, M. Ikeda, "Effects of Duloxetine, a New Serotonin and Norepinephrine Uptake Inhibitor, on Extracellular Monoamine Levels in Rat Frontal Cortex, J. Pharmacol. Exp. Ther., **272**, 177, 1995.

A RAPID QUANTITATIVE ANALYSIS OF THE β-BLOCKER TIMOLOL IN HUMAN URINE BY HPLC-ELECTROCHEMICAL DETECTION

M. Itxaso Maguregui, Rosa M. Alonso, Rosa M. Jiménez

Departamento de Química Analítica
Facultad de Ciencias
Universidad del País Vasco/EHU
Apdo. 644
48080 Bilbao, Spain.

ABSTRACT

A High Performance Liquid Chromatographic method with amperometric detection has been developed for the determination of the β-blocker 1-[(1, 1-dimethylethyl) amino]-3-[[4-(4-morpholinyl)-1, 2, 5-thiadiazol-3-yl] oxy], timolol.

The chromatographic separation was performed using a μ-Bondapak C_{18} column and a mobile phase of acetonitrile:water (30:70), containing 5mM KH_2PO_4/K_2HPO_4, pH 6.5 pumped at a flow rate of 1.3 mL/min. The amperometric detector equipped with a glassy carbon electrode was operated at +1000 mV. The method was applied to the determination of timolol in urine samples obtained from a hypertensive patient under medical treatment with the pharmaceutical formulation Blocadren 10 mg (timolol 10 mg). Using a simple liquid-liquid extraction procedure, a good recovery (93.25±2.5) and separation from the urine matrix is achieved. A good reproducibility, linearity and

accuracy are obtained, and the quantitation limit of 10 ng/mL, allows the method to be applied to doping analysis in human urine, and pharmacokinetic studies.

INTRODUCTION

Timolol maleate is a β-adrenergic blocker used for the treatment of hypertension, angina pectoris, and glaucoma. Due to its sedative effect, in January 1987 the use of this compound and other β-blockers was forbidden in sports such as pentathlon, shooting and billiards.[1]

This β-blocker has an oral bioavailability of about 75 % and undergoes oxidative biotransformation. About 20 % of the dose is excreted unchanged,[2-3] and the mean elimination half-life is 4 hours.

Methods for the detection and identification of timolol have been described using mainly gas chromatography (GC) with either electron capture detection (ECD),[4] flame ionization detection (FID) and mass spectrometry (MS) achieving detection limits as low as 0.5 ng/mL.[5-6] All these methods need the use of tedious extraction and back extraction procedures to minimize interferences from endogenous components of the matrixes (mainly plasma and serum).

There are several articles describing HPLC methods with different detection techniques such as UV detection[7] and atmospheric pressure chemical ionization mass spectrometry.[8] These determinations have been mainly done in plasma and serum matrixes and some of them in pharmaceutical formulations.[9-10] There is only one report dealing with urine matrixes: horse urine.[6]

With respect to the use of HPLC-electrochemical detection (ED) applied to the determination of timolol, Gregg et al.[11] describe a method for the determination of timolol in plasma and breast milk. The limits of detection given in this work are based only on signal-to-noise measurements (2 ng/mL) and should not be confused with the lower quantifiable limits.

On the other hand the extraction methods proposed are long and complicated. He et al.[12] report a determination of timolol in plasma monitored by coulometric detection, including also a complicated liquid-liquid extraction procedure.

Upon the basis of a recently developed method for the screening of several β-blockers using HPLC-ED,[13] and based on the good results obtained we are now developing methods for the quantitative determination of each β-blockers in human urine.

The aim of this paper is the application of a simple HPLC system with amperometric detection to the quantitation of timolol in human urine, preceded by a simple and fast liquid-liquid extraction procedure.

MATERIALS AND METHODS

Reagents, Chemicals and Standard Solutions

Timolol Maleate was supplied by Sigma (Bilbao, Spain). Potassium dihydrogenphosphate, and dipotassium hydrogenphosphate were Merck Suprapur (Bilbao, Spain).

HPLC grade solvents were purchased from Lab-Scan (Dublin, Ireland), and the water used was obtained from the Milli-RO and Milli-Q Millipore systems.

A stock solution of timolol (100μg/mL) was prepared in aqueous-acetonitrile mixture containing the same proportion of acetonitrile as used in the mobile phase, and stored at 4°C. Working solutions were obtained by appropriate dilution, just before use.

Procedure for Urine Samples

The clean-up procedure for urine samples was a simple liquid-liquid extraction : 0.5mL of NaOH (5M), 4mL of diethyl ether and 1g of Na_2SO_4 were mixed with 4mL of urine. The mixture was shaken mechanically for 15min and centrifuged for 5min at 734g.

The diethyl layer was separated and evaporated to dryness at 60°C under a gentle stream of nitrogen, using a Zymark TurboVap LV evaporator (Barcelona, Spain). The residue was dissolved in 2 mL of mobile phase and was measured under calibration conditions.

The reproducibility and efficiency of the extraction procedure was determined by extracting replicate spiked urine samples, doped with 2ppm of timolol. A quantitative recovery of (mean value±R.S.D%) 93.25±2.50% was achieved.

Chromatographic Conditions

The HPLC system consisted of a model 510-Waters pump (Waters Assoc., Barcelona, Spain), and a Rheodyne Model 7125 (Pharmacia, Barcelona, Spain) injector with a loop of 20µl.

The electrochemical detector (PAR Model 400) equipped with a glassy carbon cell (EG&G Princeton Applied Research, Madrid, Spain). It was operated at +1000mV vs a Ag/AgCl electrode, in the DC mode with a 5-s low pass-filter time constant, and a current range between 2 and 100nA. Chromatograms were recorded with the help of a computer and treated with the software Millenium 2010 Chromatography Manager from Waters.

The column used was a 30cm×3.9mm I.D., 10-µm, 125-Å µBondapack C_{18} column (Waters Assoc.). A µBondapack C_{18} guard column (Waters Assoc.) was used to prevent column degradation. The column was kept at constant temperature using a Waters TMC temperature control system.

The mobile phase was a mixture acetonitrile:water (30:70) containing 5mM potassium dihydrogenphosphate/dipotassium hydrogenphosphate. The pH was adjusted to 6.5 and the buffer served as supporting electrolyte. The µ Bondapack column head pressure was 1500PSI at a flow rate of 1.3mL/min. The injection volume was 20µL. The column was kept constant at 30±0.2°C.

RESULTS AND DISCUSSION

Hydrodynamic voltammetry of the compound was carried out in order to choose the optimum potential value for the amperometric detection of this β-blocker. An oxidative potential of 1000mV was chosen as the working potential, since it was the potential which provided the maximum sensitivity for timolol.

The study of the influence of pH and composition of the mobile phase gave an optimum value of pH 6.5 and a water:acetonitrile ratio of 70:30, which allowed the separation of timolol from the interfering endogenous compounds of the urine, keeping a low retention time.

Table 1

Determination of Timolol at Two Concentration Levels:μg/mL and ng/mL

β-Blocker: Timolol

Retention Time ± S.D. (min)	6.47 ± 0.03	
Linear Range	10 - 1000 ng/mL	0.5 - μg/mL
Slope of Calibration graph[a]	157412.1	15887.5
r^2	0.9996	0.9994
Repeatability Intraday R.S.D. (%)	6.16[b]	3.53[c]
Repeatability Interday R.S.D. (%)	---	3.37[d]
Experimental Quantitation Limit (ng/mL)	10	---

[a] Area/concentration
[b] Ten determinations at the 400 ppb level
[c] Ten determinations at the 4 ppm level
[d] Six determinations at the 4 ppm level
(For chromatographic conditions see the Experimental section)

The buffer potassium dihydrogenphosphate/dipotassium hydrogen-phosphate was used as supporting electrolyte since it gave the best signal to noise ratio at a concentration of 5mM.

An increase in the temperature caused a reduction of k´, without affecting the sensitivity. A temperature of 30±0.2°C was used throughout the work. A value of flow rate of 1.3mL/min was chosen as the optimum.

Once the optimum chromatographic conditions had been established, a quantitative method for the determination of timolol in urine samples was developed at two concentration levels: ppm and ppb (Table 1).

The relative standard deviation of the retention times is less than 1%, thus indicating high stability for the system.

Linearity ocurred at least from the limits of quantitation to 10ppm, with a good correlation.

The intra-day and inter-day repeatabilities were determined by injecting replicate samples (n=10 for the intra-day, and n=6 for the inter-day repeatability) at a 4 ppm and a 400 ppb level, and it is expressed as the relative standard deviation (R.S.D.) and listed in Table 1. The R.S.D is calculated by the formula R.S.D.=(standard deviation/mean of peak area)×100%.

The accuracy of the method was determined by the analysis of 5 control urine samples spiked with 2ppm of timolol. Acceptable accuracy, defined as mean (found concentration/actual concentration)×100, was achieved: 100.05 ± 8.6%.

The experimental quantitation limit, defined as the minimum concentration of timolol which gives rise to a signal able to be quantified by the computer program used, was 10 ng/mL, in spiked urine samples.

Analytical Applications

The method developed was applied to the determination of timolol in urine samples obtained from a patient suffering from hypertension and under medical treatment with the pharmaceutical formulation Blocadren 10mg (timolol maleate 10mg).

Urine was collected at different time intervals for the quantitative determination of the β-blocker: 0-2 hours, 2-4 hours and 4-12 hours.

The compound was easily detected at 0-2 and 2-4 hours intervals and the concentrations determinated, collected in Table 2, were in agreement with the pharmacokinetic data .[14] Timolol was not detectable at 4-12 hours interval. Urine samples were treated following the clean-up procedure described in the experimental section. Fig. 1 shows the chromatograms corresponding to a
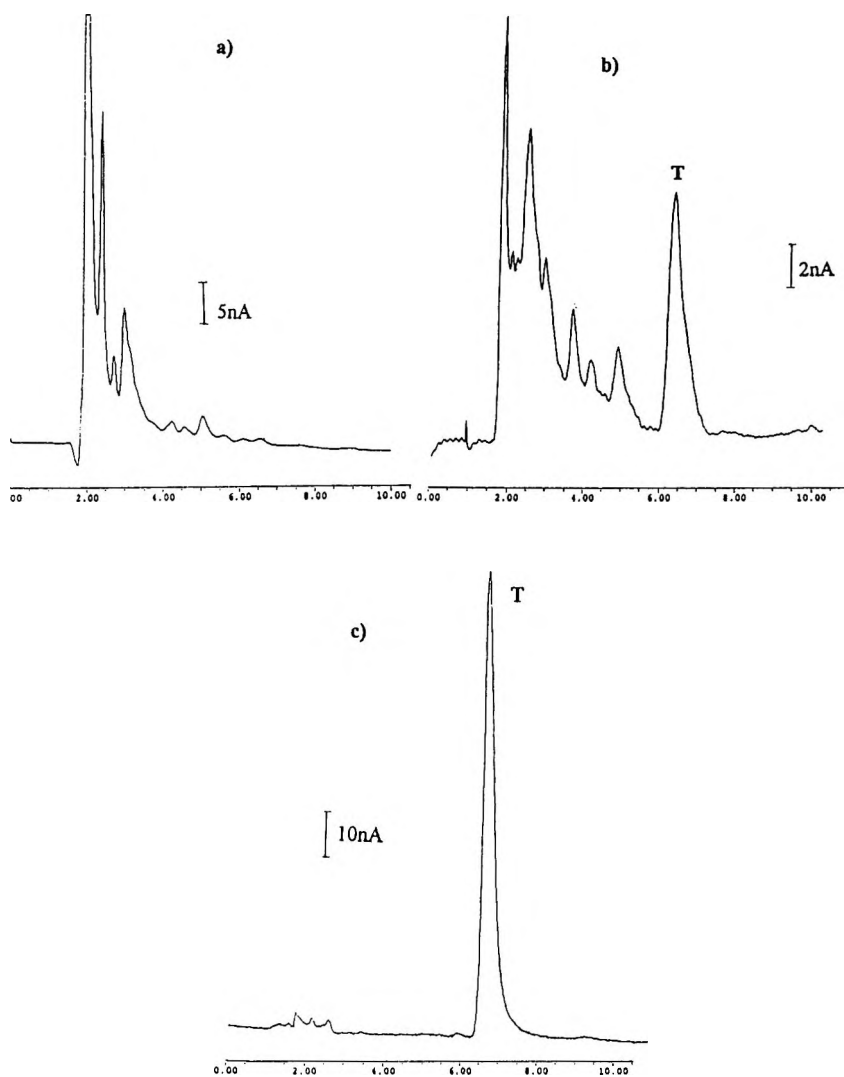
Figure 1. Chromatograms obtained from an extract of: a) blank urine sample, b) urine sample 0-2 hours after the oral administration of 1 tablet of timolol 10mg (Blocadren 10mg) to a hypertensive patient and c) a diluted solution of a tablet of Blocadren 10mg, containing 10 mg of timolol. For chromatographic conditions see experimental section.

Table 2

Determination of Timolol in Urine

Urine Samples

Time Interval	0-2 hours	2-4 hours	4-12 hours
Timolol conc. (μg/mL)	0.96	0.415	---

(Urine obtained from a hypertensive patient under treatment with
Blocadren 10 mg).

blank urine sample, a diluted solution of a tablet of Blocadren 10mg and a urine
sample 0-2 hours after the administration of a dose of Blocadren.

Discussion

Liquid chromatography with amperometric detection has been shown to be
a fast and powerful method for the identification and determination of timolol in
urine samples. The clean-up procedure is very simple with recoveries of 93.25
± 2.50%, and the chromatographic separation is made in less than 7 minutes.

The relatively low potential used in the detection +1000mV induces a low
background signal and provides high stability to the system. This fact constitute
an advantage with respect to the work done by Gregg et al.[11] who used
+1200mV as optimal potential for plasma and breast milk samples.

The limit of quantitation of 10ng/mL has proved to be sensitive enough for
the determination of the free timolol in urine samples of hypertensive patients in
the 0-2 and 2-4 hours intervals.

ACKNOWLEDGEMENTS

REFERENCES

1. E. G. de Jong, R. A. A. Maes, J. M. Van Rossom, Trends in Anal. Chem., **7(10)**, 375-382 (1988).

2. M. Litter, **Farmacología Experimental y Clínica**, "El Ateneo" Pedro García S.A., Buenos Aires, 1986.

3. V. Marko, **Determination of β-Blockers in Biological Material**, Elsevier, Amsterdam, 1989.

4. D. J. Tocco, F. A. Deluna, A. E. W. Duncan, J. Pharm. Sci., **64**, 1879-1881 (1975).

5. J. B. Fourtillan, M. A. Lefebvre, J. Girault, Ph. Courtois, J. Pharm. Sci., **70**, 573-575 (1981).

6. A. M. Duffield, S. Wise, J. Keledjian, C. J. Suann, J. Chromatogr., **518**, 215-220 (1990).

7. T. Kaila, L. Salminen, and R. Huupponen, J. Ocular Pharmacol., **1**, 79 (1985).

8. T. V. Olah, J. D. Gilbert, A. Barrish, J. Pharm. & Biomed. Anal., **11(2)**, 157-163 (1993).

9. M. I. R. M. Santoro, H. S. Cho, E. R. M. Kedor-Hackmann, Anal. Lett., **28(1)**, 71-81 (1995).

10. P. M. Lacroix, B. A. Dawson, R. W. Sears, D. B. Black, Chirality, **6**, 484-491 (1994).

11. M. R. Gregg, D. B. Jack, J. Chromatogr., **305**, 244-249 (1984).

12. H. He, T. I. Edeki, A. J. J. Wood, J. Chromatogr. B, **661**, 351-356 (1994).

13. M. I. Maguregui, R. M. Alonso, R. M. Jiménez, J. Chromatogr., **674**, 85-91 (1995).

14. D. J. Mazzo, A. E. Loper, Anal. Profiles Drug Subst., **16**, 641-692 (1987).

ENANTIOSELECTIVITY OF AZALANSTAT AND ITS KETAL TOSYLATE INTERMEDIATE IN CHIRAL HIGH PERFORMANCE LIQUID CHROMATOGRAPHY SEPARATIONS

Thomas V. Alfredson,[1,*] Robert Towne,[1] Michelle Elliott,[1]
Bruce Griffin,[1] Allassan Abubakari,[1]
Norman Dyson,[2] Denis J. Kertesz[2]

[1]Analytical Research
and
[2]Chemical Research and Development,
Syntex Research
3401 Hillview Avenue
Palo Alto, California 94304

ABSTRACT

Separation of the stereoisomers of azalanstat (RS-21607-197), a substituted imidazolyl-1,3-dioxolane which acts as a potent inhibitor of lanosterol 14α-demethylase in cholesterol bio-synthesis, and its ketal tosylate intermediate was achieved by chiral high performance liquid chromatography. Resolution of all four stereoisomers of azalanstat was accomplished by normal phase separation of the diastereomers on a short silica gel column coupled on-line to a Chiralpak AS amylose carbamate phase chiral column for resolution of the enantiomers.

A reversal in elution order of the *cis*-(2S,4S) and *cis*-(2R,4R) enantiomers of the ketal tosylate intermediate of azalanstat was exhibited by an Ultron ES-OVM ovomucoid protein bonded-

1653

phase column with a change in organic modifier from ethanol to
acetonitrile. This unusual enantioselectivity in the chiral reverse
phase separation of the ketal tosylate was attributed to a putative
change in binding domains or recognition sites on the ovomucoid
protein as a function of the organic modifier of the mobile phase.
Resolution of all four stereoisomers of the ketal tosylate was
achieved by use of a Chiralpak AD amylose carbamate phase
column in the normal-phase mode.

INTRODUCTION

Lanosterol 14α-demethylase is a cytochrome P_{450}-dependent enzyme that
catalyzes the first step in conversion of lanosterol to cholesterol in mammals.[1]
Selective inhibition of this enzyme represents a possible strategy for cholesterol
lowering. Azalanstat (Figure 1) has been shown to be selective inhibitor of
mammalian lanosterol 14α-demethylase.

The cis-(2S,4S) enantiomer of azalanstat is approximately two orders of
magnitude more effective than the cis-(2R,4R) enantiomer for inhibition of
cellular cholesterol biosynthesis using human fibroblasts in tissue cultures.[2]

Synthesis of azalanstat (RS-21607-197) involves the trans-ketalization of
1-(imidazol-1-yl)-4-(4-chlorophenyl)-butan-2-one with (S)-solketal tosylate to
produce the cis-(2S,4S) and trans-(2R,4S) ketal tosylate intermediates of
azalanstat (Figure 2). Use of (R)-solketal tosylate yields the corresponding cis-
(2R,4R) and trans-(2S,4R) ketal tosylate intermediates. Coupling of the ketal
tosylate intermediates with 4-aminothiophenol gives (2S, 4S)-4-[(4-
aminophenylthio)-methyl]-2-[2-(4-chlorophenyl)-ethyl]-2-[(1H-imidazol-1-yl)-
methyl]-1,3-dioxolane (azalanstat) and its corresponding stereoisomers. High
performance liquid chromatography (HPLC) using chiral bonded phase columns
was utilized to establish controls for the stereochemical purity of the ketal
tosylate intermediates and of azalanstat during synthesis.

The purpose of this study was to elucidate the enantioselectivity of
azalanstat and its ketal tosylate intermediates in chiral HPLC separations. As a
biologically active azole, azalanstat shares several structural features (ketal
functionality, imidazole heterocycle, substituted phenyl ring) with many azole
antifungal agents which inhibit the biosynthesis of ergosterol from squalene.[3]
The enantioselectivity observed for azalanstat, therefore, may provide insight on
stereoisomer separations of other chiral azoles and of related compounds with
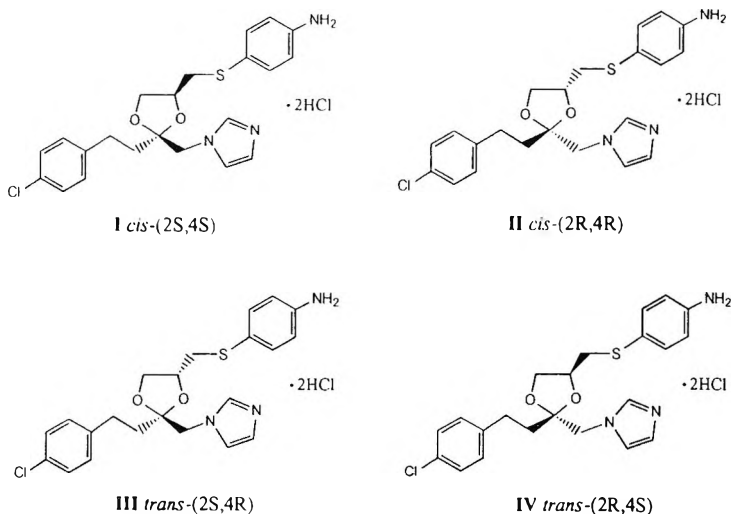similar structural characteristics.

Figure 1. Structure of azalanstat (**I**) and its stereoisomers: **I** *cis*-(2S,4S) stereoisomer; **II** *cis*-(2R,4R) stereoisomer; **III** *trans*-(2S,4R) stereoisomer; **IV** *trans*-(2R,4S) stereoisomer. The *cis* and *trans* designations of the stereoisomers indicate the relative configuration of the aminophenylthio)methyl substituent at C_4 and the (imidazolyl)-methyl substituent at C2 in the 1,3-dioxolane ring.

Resolution of the enantiomers of azalanstat and its ketal tosylate intermediates was accomplished using an Ultron ES-OVM ovomucoid protein bonded-phase column and a Chiralcel OD-R cellulose carbamate phase column in the reversed-phase mode. Normal phase separation of the enantiomers of azalanstat and its ketal tosylate intermediates was achieved by employing a Chiralpak AS and a Chiralpak AD amylose carbamate phase column, respectively. Other chiral columns were also employed in this study in an effort to detail the enantioselectivity exhibited for azalanstat and its ketal tosylate intermediates in chiral HPLC separations.

MATERIALS

A Varian Series 9010 solvent delivery system, a Polychrom 9065 diode-array detector with the LC Star 9021 workstation, Polyview, and 3DView chromatographic and spectral processing software, and a 9095 autosampler were employed for chromatographic separations and data collection.   A Varian
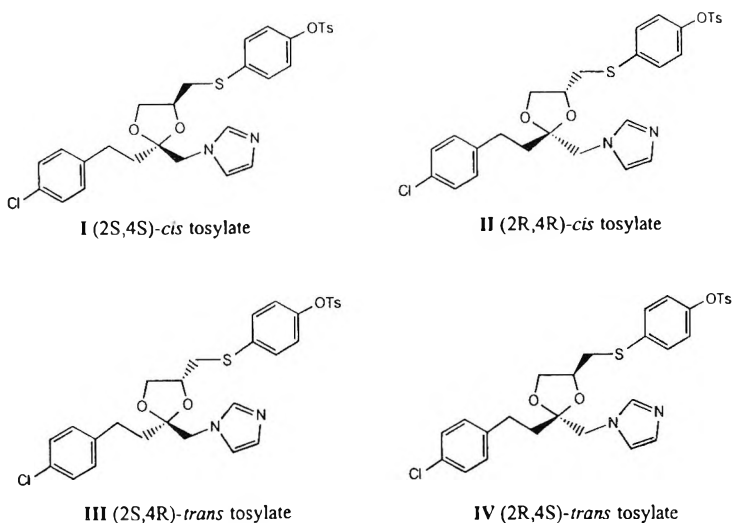
Figure 2. Structures of the ketal tosylates of azalanstat and their stereoisomers: **I** (2S,4S)-*cis* tosylate; **II** (2R.4R)-*cis* tosylate; **III** (2S,4R)-*trans* tosylate; **IV** (2R,4S)-*trans* tosylate.

Model 5000 HPLC system with a Kratos Model 783 UV absorbance detector and a Spectra-Physics Chromjet integrator were also used in this work. A Waters Mod-1 HPLC system was also employed for some separations. A Shimadzu CT-6A HPLC column oven was used for control of column temperature where required. A Rheodyne automated fixed loop injector equipped with a 20µL sample loop was used in these studies.

A Zorbax Rx C8 (Mac-Mod Analytical) 5µm column (250mm x 4.6mm i.d.) was employed for reverse phase separation of the diastereomers of azalanstat and its ketal tosylate intermediate. Normal phase separations of the diastereomers of azalanstat were carried out with a Supelcosil LC-Si (Supelco Inc.) 3µm column (33mm x 4.6mm i.d.).

Reversed-phase chiral HPLC separations were carried out with an Ultron ES-OVM (Mac-Mod Analytical) ovomucoid protein bonded-phase column (5µm, 150mm x 4.6mm i.d.) and with a Chiralcel OD-R (Chiral Technologies Inc.) cellulose tris-(3,5-dimethylphenyl carbamate) phase column (10µm, 250mm x 4.6mm i.d.). Normal phase chiral separations utilized Chiralcel OD cellulose tris-(3,5-dimethylphenyl carbamate) phase and Chiralcel OJ cellulose

tris-(4-methyl benzoate) phase columns as well as Chiralpak AD amylose tris-(3,5-dimethylphenyl carbamate) phase and Chiralpak AS amylose tris-[(S)-1-phenylethyl carbamate] phase columns (Chiral Technologies Inc., 10µm, 250mm x 4.6mm i.d.).

In addition, a Pirkle-type Chirex 3019 phase (Phenomonex, Inc.) 5µm column (250mm x 4.6mm i.d.) with a bonded phase consisting of a (S)-tert-butyl-leucine moiety coupled to (S)-1-(α-naphthyl)ethylamine via a urea linkage was employed for normal phase separation of the ketal tosylate stereoisomers.

B & J Brand (Baxter Healthcare, Burdick and Jackson Division) high-purity acetonitrile, methanol, 1,2-dichloroethane, and 2-propanol as well as HPLC-grade water from a Milli-Q water purification system (Millipore Corp.) and punctillious grade ethanol (Quantum Chemical Co.) were employed for chromatographic studies.   Potassium dihydrogen phosphate and sodium perchlorate, reagent grade, were obtained from J. T. Baker Company. Heptane sulfonic acid was purchased from Eastman-Kodak Chemical Company.

Azalanstat (RS-21607), its stereoisomers, its ketal tosylate intermediates, and related compounds were synthesized by previously reported procedures (see ref. 2).

METHODS

All chromatographic analyses were carried out in a similar manner. Azalanstat and its ketal tosylate intermediates were dissolved in a minimal volume of either isopropanol, methanol or acetonitrile and diluted to volume with mobile phase for HPLC separations.   Solutions of approximately 0.05mg/mL of the analyte were freshly prepared just prior to analysis. Unless otherwise stated, a detection wavelength of 220nm was employed in these studies.

A Zorbax Rx C8 column with a 0.02M phosphate buffer/0.01M heptane sulfonic acid-methanol (41:59) mobile phase at a flow rate of 1.0mL/min was employed for reverse phase HPLC separations of the diastereomers of the ketal tosylate intermediate with a detection wavelength of 220nm. For analysis of azalanstat diastereomers, a Zorbax Rx C8 column was employed with a 0.05M phosphate buffer (pH 3.0)-methanol (45:55) mobile phase at a flow rate of 1.5mL/minute. Normal phase separations of the diastereomers of azalanstat were carried out with a Supelcosil LC-Si column using a hexane/2-propanol (78:32) mobile phase at a flow rate of 1mL/minute.

Chiral HPLC separations of azalanstat and its ketal tosylate intermediate were carried out with several reversed-phase and normal-phase chiral columns. An Ultron ES-OVM ovomucoid protein column with a 0.02M phosphate buffer (pH 5.5)-ethanol (73:27 for *cis* stereoisomers and 67:33 for *trans* stereoisomers) mobile phase at a flow rate of about 0.5 mL/minute and column temperature of 35 °C was used for reverse phase chiral analysis of the ketal tosylate intermediates.

An Ultron ES-OVM ovomucoid protein chiral column with a 0.02M phosphate buffer (pH 4.6)-ethanol (78:22) mobile phase at a flow rate of about 0.8mL/minute and column temperature of 35°C was used for reverse phase chiral analysis of azalanstat.

A Chiralcel OD-R cellulose carbamate phase column with a 0.5M perchlorate buffer-acetonitrile (40:60) mobile phase at a flow rate of 1mL/minute and a column temperature of 35 °C was employed for reverse phase chiral HPLC separations of the ketal tosylate intermediates. The Chiralcel OD-R column was utilized with a 0.5M perchlorate buffer-methanol (5:95) mobile phase at a flow rate of 1 mL/minute for separation of the enantiomers of azalanstat.

Chiralpak AD and AS amylose carbamate phase columns as well as a Chiralcel OD cellulose carbamate phase column and a Chiralcel OJ cellulose ester phase column were utilized for normal phase chiral separations of azalanstat and the ketal tosylate intermediates.

A 2-propanol/hexane mobile phase (20:80) at a flow rate of 1 mL/minute was employed separation of the enantiomers of the ketal tosylate intermediates using the Chiralpak AD column. A 2-propanol-hexane mobile phase (32:68) at a flow rate of 1 mL/minute was employed for separation of the enantiomers of azalanstat using a 3.3cm LC-Si silica gel column coupled on-line to the Chiralpak AS column.

Various mixtures of 2-propanol-hexane and ethanol-hexane were utilized in methods development work with the Chiralcel OD and OJ cellulose based columns and with the Chiralpak AD and AS amylose based columns for separation of the stereoisomers of azalanstat and its ketal tosylate intermediates. In addition, a Chirex 3019 phase column employing a (S)-tert-leucine with a urea linkage to (S)-1-(α-naphthyl)ethylamine as an electron-donor bonded phase with an ethanol-dichloroethane-hexane (10:2:1) mobile phase at a flow rate of 1.0mL/min was utilized for normal phase separation of the ketal tosylate enantiomers.
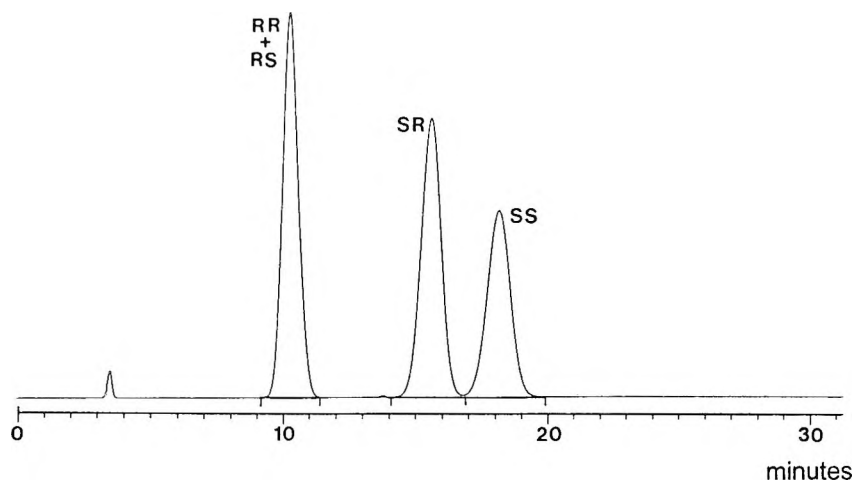
Figure 3. Chiral HPLC separation of the stereoisomers of azalanstat: **SS** *cis*-(2S,4S) stereoisomer (azalanstat); **RR** *cis*-(2R,4R) stereoisomer; **SR** *trans*-(2S,4R) stereoisomer; **RS** *trans*-(2R,4S) stereoisomer.   Conditions: Ultron ES-OVM column, 78% 20mM KH$_2$PO$_4$ (pH 4.6)/22% EtOH, 0.8mL/min, 35°C, 220nm.

RESULTS AND DISCUSSION

Initial studies of the separation of the stereoisomers of azalanstat and its ketal tosylate intermediates employed an Ultron ES-OVM ovomucoid protein bonded-phase column.   Although the *cis*-(2R,4R)/*cis*-(2S,4S) and *trans*-(2S,4R)/*trans*-(2R,4S) enantiomeric pairs could be separately resolved using different ethanol-buffer mobile phases for both compounds, one of the *cis*-stereoisomers and one of the *trans* stereoisomers coeluted on the ovomucoid protein chiral column. Off-line reverse phase HPLC separation of the *cis* and *trans* diastereomers using a C8 column, together with resolution of enantiomers on the ovomucoid bonded-phase column, afforded control of the stereochemical purity of azalanstat during synthesis.

Investigation of chiral separations of azalanstat, its ketal tosylate intermediates, and related compounds was initiated in order to examine the enantioselectivity of several HPLC chiral columns in detail.

Chiral HPLC Separations of the Stereoisomers of Azalanstat

An Ultron ES-OVM ovomucoid protein column with a 0.02M phosphate buffer (pH 4.6)-ethanol mobile phase (78:22 for *cis* stereoisomers and 70:30 for *trans* stereoisomers) at a flow rate of 0.5 mL/minute and column temperature of 35 °C was used for reversed-phase chiral analysis of azalanstat. Figure 3 displays the separation of the stereoisomers of azalanstat using an Ultron ES-OVM chiral column with a 0.02M phosphate buffer (pH 4.6)-ethanol (78:22) mobile phase at a flow rate of 0.8mL/minute and column temperature of 35 °C. As can be seen, under these conditions the *cis*-(2R,4R) stereoisomer and the *trans*-(2R,4S) stereoisomer of azalanstat coelute.

Results of chiral separations of several analogs of azalanstat have shown that N-methylation of the imidazole ring along with attachment of the imidazole side chain at the 5-position increases the stereoselectivity obtained with the Ultron ES-OVM chiral column relative to azalanstat. For example, resolution of all four stereoisomers of the N-methylated imidazole analog of azalanstat was achieved employing a mobile phase identical to that used for the parent compound (Figure 4).

In contrast, the des-amino analog of azalanstat, which differs in structure from the parent compound only by the absence of the amino substituent of the thiophenol ring, yields stereoselectivity on the ovomucoid column very similar to that of the parent compound. Based on these results, it appears that neither hydrogen bonding nor protonation of the amino substituent of the aniline group (pK_a=4.1) is critical to the stereoselectivity observed for azalanstat with the Ultron ES-OVM ovomucoid bonded-phase column. N-methylation of the imidazole ring of azalanstat apparently enhances the stereoselectivity of the column for these isomers.

A Chiralcel OD-R reversed-phase cellulose carbamate based column was also employed for separation of the stereoisomers of azalanstat. A mobile phase of methanol-0.5M sodium perchlorate buffer (95:5) was found to yield separation of the *cis* enantiomers (α=1.5) and of the *trans* enantiomers (α=1.6). However, the *cis*-(2S,4S) stereoisomer coeluted with the *trans*-(2S,4R) stereoisomer under these conditions.

Several normal-phase chiral HPLC columns were investigated for separation of the stereoisomers of azalanstat. Chiralcel OD and OJ functionalized cellulose phase columns, as well as Chiralpak AD and AS functionalized amylose phase columns, were examined. The Chiralcel OD and OJ cellulose phase columns were found to exhibit a higher degree of retention, but lower stereoselectivity, for the isomers of azalanstat compared to the Chiralpak AD
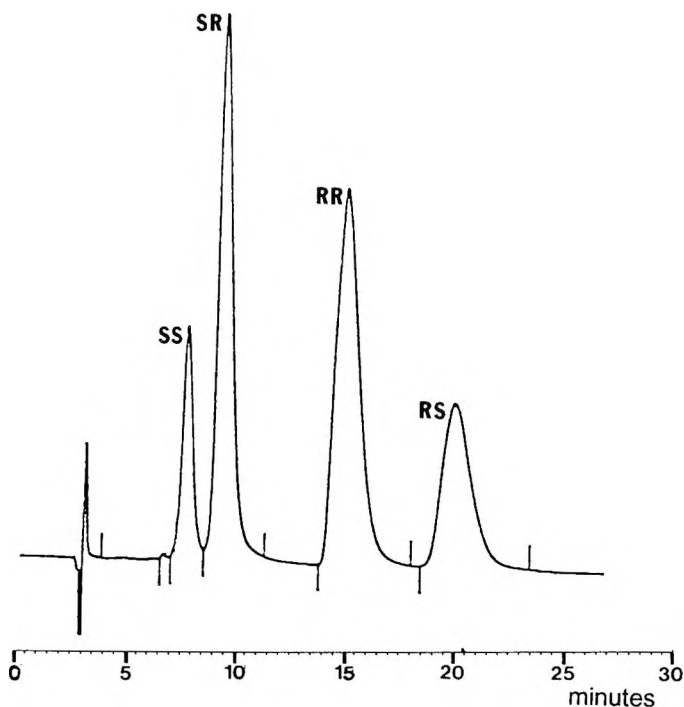
Figure 4. Chiral HPLC separation of the stereoisomers of the N-methylated imidazole analog of azalanstat: **SS** cis-(2S,4S) stereoisomer; **RR** cis-(2R,4R) stereoisomer; **SR** trans-(2S,4R) stereoisomer; **RS** trans-(2R,4S) stereoisomer. Conditions: Ultron ES-OVM column, 78% 20mM KH_2PO_4 (pH 4.6)/22% EtOH, 0.8mL/min, 35°C, 220nm.

and AS amylose phase columns. Konishi, et al.[4] also observed a high degree of retention (k' ≥ 20) for sulconazole, a related imidazole, with the Chiralcel OD and OJ columns.

Although the Chiralpak AD amylose carbamate phase column provided high enantioselectivity (α=3.5) for the *trans* enantiomers of azalanstat, coelution was observed for the *cis* enantiomers. Optimum overall selectivity for the *cis* and *trans* enantiomers of azalanstat was displayed by the Chiralpak AS amylose carbamate phase column using a 2-propanol - hexane mobile phase (32:68) at a flow rate of 1 mL/minute (α=1.7 and 1.2, for the *cis* and the *trans*
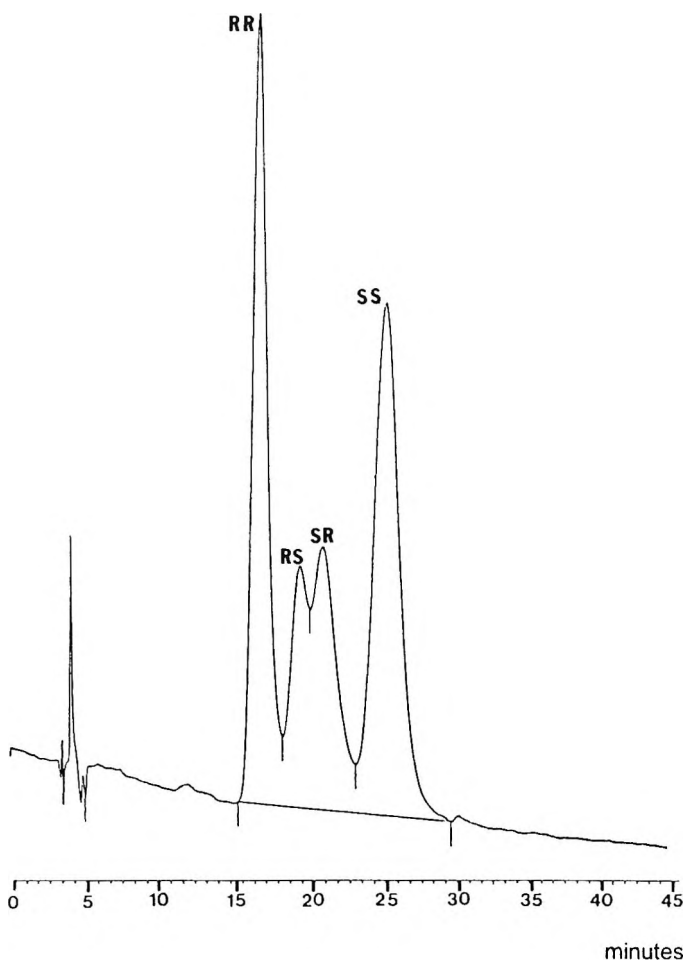
Figure 5. Coupled column HPLC separation of the stereoisomers of azalanstat: **SS** *cis*-(2S,4S) stereoisomer (azalanstat); **RR** *cis*-(2R,4R) stereoisomer; **SR** *trans*-(2S,4R) stereoisomer; **RS** *trans*-(2R,4S) stereoisomer. Conditions: Supelcosil LC-Si column (3.3cm x 4.6mm i.d.) coupled on-line with a Chiralpak AS column (25cm x 4.6mm i.d.), 2-propanol-hexane (32:68), 1mL/min, 220nm.

enantiomers, respectively). However, as was seen for the Chiralcel OD-R reversed-phase chiral column, the *cis*-(2S,4S) stereoisomer coeluted with the *trans*-(2S,4R) stereoisomer under these conditions.
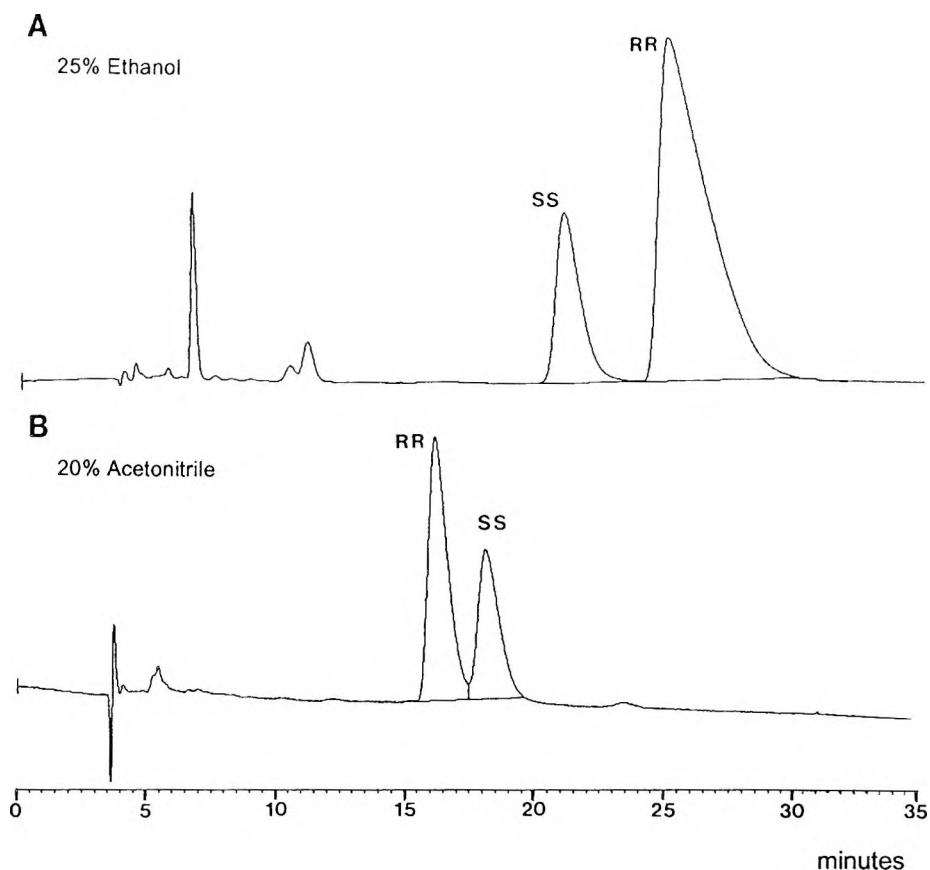
Figure 6. Chiral HPLC separation of the (2S,4S)-*cis* tosylate and (2R,4R)-*cis* tosylate enantiomers of the ketal tosylate intermediate of azalanstat as a function of organic solvent modifier with an ovomucoid bonded-phase column. **RR** (2R,4R)-*cis* tosylate enantiomer; **SS** (2S,4S)-*cis* tosylate enantiomer. Conditions: Ultron ES-OVM column, 35°C, 0.5mL/min, 220nm; (A) 75% 20mM KH_2PO_4 (pH 5.5)/25% ethanol; (B) 80% 20mM KH_2PO_4 (pH 5.5)/20% acetonitrile.

Resolution of all four stereoisomers of azalanstat was achieved by separation of the diastereomers on a 3.3cm silica gel column, coupled on-line with a Chiralpak AS amylose carbamate phase column, for separation of the enantiomers in the normal phase mode (Figure 5). A coupled-column approach using a silica gel column and a Chiralcel OD column with a switching valve was employed by McKean, et al.[5] for normal-phase separation of the stereoisomers

of an anti-emetic quinuclidine dibenzofurancarboxamide with multiple chiral centers. Rizzi[6] also utilized a coupled column approach for reversed-phase separation of the stereoisomers of 5-phenyltetrahydrooxazol-2-one and related compounds with an octylsilica-cellulose triacetate column combination.

Chiral HPLC Separations of the Stereoisomers of the Ketal Tosylate Intermediates of Azalanstat

Reverse phase chiral analysis of the ketal tosylate intermediates was carried out using an Ultron ES-OVM ovomucoid bonded-phase column with a 0.02M phosphate buffer (pH 5.5)-ethanol mobile phase (73:27 for *cis* stereoisomers and 67:33 for *trans* stereoisomers) at a flow rate of 0.5 mL/minute and a column temperature of 35 °C. Analogous to results observed for the stereoisomers of azalanstat with the Ultron ES-OVM column, the *cis*-(2S,4S) stereoisomer and the *trans*-(2S,4R) stereoisomer of the ketal tosylate intermediate coeluted using these ethanol-phosphate buffer mobile phases.

A reversal in elution order of the *cis*-(2S,4S) and *cis*-(2R,4R) enantiomers of the ketal tosylate intermediate of azalanstat was exhibited by the Ultron ES-OVM column with a change in organic modifier from ethanol to acetonitrile (Figure 6). A plot of log k' (the logarithm of the capacity factor) of the *cis*-(2S,4S) and the *cis*-(2R,4R) enantiomers as a function of ethanol/acetonitrile mixtures used as organic modifiers is shown in Figure 7.

The enantiomers coeluted at a mobile phase organic modifier content of about 10% ethanol/12% acetonitrile with 78% phosphate buffer. Higher amounts of acetonitrile caused the *cis*-(2R,4R) enantiomer to elute before the *cis*-(2S,4S) enantiomer. Control of the enantioselectivity of this separation was important in order to allow the undesired enantiomer [in this case the *cis*-(2R,4R) enantiomer] to elute *before* the desired enantiomer thereby providing a more accurate assessment of enantiomeric purity.

This unusual enantioselectivity in the reverse phase separation of the *cis*-ketal tosylates was attributed to a putative change in binding domains or recognition sites in the ovomucoid protein as a function of the organic modifier of the mobile phase. These results suggest that use of acetonitrile in conjunction with alkanol modifiers may be exploited to affect changes in selectivity with this chiral column. A similar reversal in enantiomer elution order as a function of the addition of organic solvents was observed by Haginaka, et al.[7] in studies of the enantioselectivity of propanolol and its ester
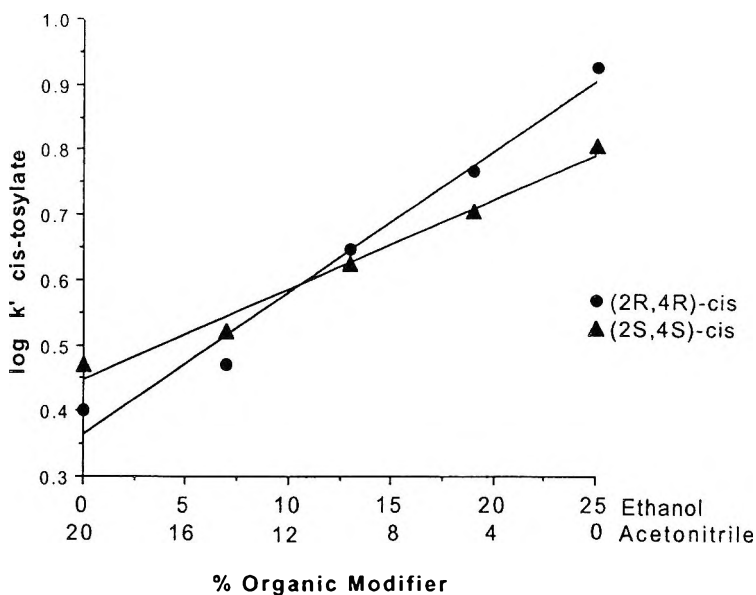
Figure 7. Plot of log k' of the (2R,4R)-cis and (2S,4S)-cis enantiomers of the ketal tosylate intermediate of azalanstat versus ethanol/acetonitrile mixtures as organic modifiers in the mobile phase with an ovomucoid bonded-phase column. Conditions: Ultron ES-OVM column, 20 mM KH_2PO_4 (pH 5.5) buffer with ethanol/acetonitrile mixtures used as organic modifiers in percentages as listed on the plot, 0.5 mL/min, 35°C, 220 nm.

derivatives on an ovomucoid bonded-phase column. Multiple binding sites on the ovomucoid protein phase column and/or at least two chiral recognition mechanisms, along with possible conformational changes in the ovomucoid bonded phase structure, were postulated for the observed effect with propanolol.

A Chiralcel OD-R reverse phase column was also employed for separation of the stereoisomers of the ketal tosylates. A mobile phase of 0.5M perchlorate buffer-acetonitrile (40:60) at a flow rate of 1mL/minute, and a column temperature of 35°C, was utilized for reverse phase chiral HPLC separations of the ketal tosylate intermediates.

Although the cis-(2S,4S) and the cis-(2R,4R) enantiomers can be readily resolved (α=1.5) under these conditions, the trans-(2S,4R) and trans-(2R,4S) enantiomers coelute.
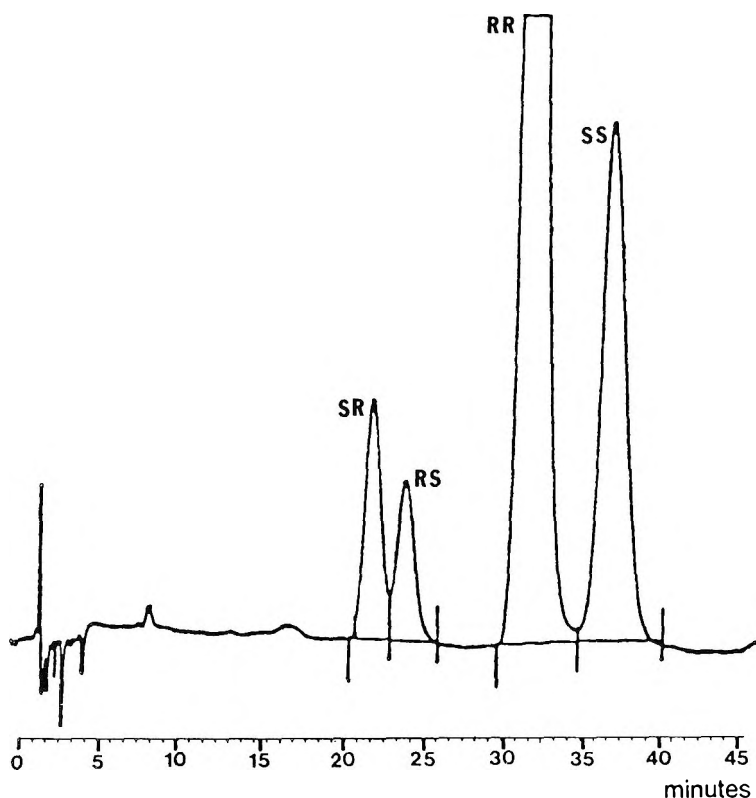
Figure 8. Chiral HPLC separation of the stereoisomers of the ketal tosylate intermediates of azalanstat: **SS** (2S.4S)-*cis* tosylate; **RR** (2R,4R)-*cis* tosylate; **SR** (2S,4R)-*trans*tosylate; **RS** (2R,4S)-*trans* tosylate. Conditions: Chiralpak AD column, 2-propanol-hexane (80:20), 1mL/min, 220nm.

A Chirex 3019 phase Pirkle-type chiral HPLC column, employing a (S)-tert-leucine with a urea linkage to (S)-1-(α-naphthyl)ethylamine as a bonded phase, was investigated for separation of the stereoisomers of the ketal tosylate intermediate. This column has been shown to afford resolution of the stereoisomers of several structurally-related azole compounds.[8] Poor selectivity (α ≤ 1.1) for the enantiomers of the ketal tosylates was exhibited by this column using a mobile phase of 2-propanol-dichloroethane-hexane. Cleveland[9] has recently published a summary of several Pirkle-type chiral stationary phases of this nature for the HPLC separation of pharmaceutical racemates.

A comparison of the Chiralpak AD and AS amylose carbamate phase columns for the separation of the stereoisomers of the ketal tosylate, indicated that the Chiralpak AS column yields higher retention (about a two-fold increase in k') but lower enantioselectivity ($\alpha < 1.1$ for the cis-tosylate enantiomers) than the Chiralpak AD column. Resolution of all four stereoisomers of the ketal toslylate intermediate was achieved with a Chiralpak AD column using a 2-propanol-hexane (20:80) mobile phase (Figure 8). Since the only difference between the Chiralpak AS and AD columns is the functionality of the derivatized amylose phase, the tris-(3,5-dimethylphenyl carbamate) phase of the Chiralpak AD column apparently yields higher selectivity for the stereoisomers of the ketal tosylate than the tris-[(S)-1-phenylethyl carbamate] phase of the Chiralpak AS column.

ACKNOWLEDGEMENTS

REFERENCES

1. J. Trzaskos, S. Kawata, J. L. Gaylor, J. Biol. Chem., **261**, 14651-14657 (1986).

2. K. A. M. Walker, D. J. Kertesz, D. M. Rotstein, D. C. Swinney, P. W. Berry, O. -Y. So, A. S. Webb, D. M. Watson, A. Y. Mak, P. M. Burton, B. Mills-Dunlap, M. Y. Chiou, L. G. Tokes, L. J. Kurz, J. R. Kern, K. W. Chan, A. Salari, G. R. Mendizabal, J. Med. Chem., **36**, 2235-2237 (1993).

3. T. J. Franklin, G. A. Snow, **Biochemistry of Antimicrobial Action**, Chapman and Hall Ltd., New York, 1989, pp.137-160.

4. K. Konishi, K. Oda, K. Nishida, T. Aida, S. Inoue, J. Am. Chem. Soc., **114**, 1313-1318 (1992).

5. R. McKean, N. Kumar, R. Quinty, J. Chrom. Sci., **31**, 465-468 (1993).

6. A.M. Rizzi, J. Chromatogr., **513**,195-207 (1990).

7. J. Haginaka, C. Seyama, H. Yasuda, K. Takahashi, J. Chromatogr., **598**, 67-72 (1992).

8. N. Oi, H. Kitahara, R. Kira, J. Chromatogr., **535**, 213-219 (1990).

9. T. Cleveland, J. Liq. Chrom., **18**, 649-671 (1995).

THE USE OF HPLC TO DETERMINE THE SATURATE CONTENT OF HEAVY PETROLEUM PRODUCTS

Jay M. Chaffin, Moon-Sun Lin, Meng Liu,
R. R. Davison, C. J. Glover,* J. A. Bullin

Department of Chemical Engineering
and
The Texas Transportation Institute
Texas A&M University
College Station, TX 77843-3122

ABSTRACT

The refractive index response factors for several pure saturate fractions isolated from heavy petroleum products were determined using a μ-Bondapak aminopropylmethylsilyl bonded amorphous silica HPLC column. The response factors for saturates obtained from asphalts had an average refractive index response factor of 1.06 ± 0.096 V/g and the saturates obtained from industrial supercritical fractions had an average refractive index response factor of 1.13 ± 0.048 V/g. The difference between these two values can probably be attributed to the fact that different researchers prepared the pure saturates. Based on this assumption, it was possible to obtain an overall response factor for saturates from high boiling petroleum materials. The overall average response factor for the saturates from these heavy petroleum products was determined to be 1.10 ± 0.079 V/g. The data collected in this study indicate that petroleum jelly, with a response factor of 1.05 V/g, may be used as an adequate saturate calibration standard for asphalt and asphalt related materials.

1669

INTRODUCTION

Much effort has been expended in determining the chemical composition of asphalt and other heavy petroleum products. Composition data are required by refiners who wish to upgrade their residues. Residue upgrading by catalytic cracking requires that the metals (especially Ni and V) content of the feed be as low as possible so that the catalyst deactivation is minimized. It is widely known that the metals concentrate in the most highly condensed, most polar molecules (asphaltenes) in petroleum residues.[1,2,3] If the content of this highly polar fraction is too high, catalytic cracking may not be economical. In addition, chemical or group-type composition information is necessary, because many residue processing parameters have been determined empirically based on the aromatic and paraffinic contents of the feedstock, in order to maximize yield of high value products.

The chemical composition of petroleum residues is also important to the scientist, especially the asphalt chemist who is interested in correlating asphalt behavior to chemical composition. At least one method for determining composition based on chemical reactivity[4] is routinely used. Generally, these chemical reactivity classification methods only allow for empirical correlations, since the fractionated components are irreversibly altered in the separation process.[5] Although the fractions from such separations can be analyzed individually, the properties determined from individual analyses are undoubtedly not representative of their properties in the unfractionated asphalt.

To eliminate the irreversible changes that the chemical reactivity separation methods produce, several chromatographic techniques for asphalt group-type fractionation have been proposed over the past several decades. Many of the group-type fractionation methods, including the method of Rostler and Sternberg,[4] entail performing a binary fractionation of the material based on solubility in some arbitrary solvent. The solvents of choice typically have been paraffinic hydrocarbons. The insoluble fraction, if present, is separated by filtration and is referred to as the asphaltene fraction, or simply asphaltenes. The paraffin-soluble fraction is called maltenes or petrolenes. It is widely known that the quantity of asphaltenes increases with decreasing carbon number and increased branching in paraffinic solvents. As discussed previously, the asphaltene fraction contains most of the metal-bearing species. The asphaltenes have been shown to be responsible for the highly viscous nature of asphalts.[6,7]

More complicated separations focus on further separation of the maltene fraction. The most well known of these is the column chromatography method of Corbett.[8] This method has since been adapted by the American Society for Testing and Materials (ASTM D4124) as the standard method for determining asphalt composition. In the standard method, the asphaltenes are separated by

precipitation from a 100:1 (vol% n-C_7:wt% sample) solution and the maltenes are then separated into saturates, naphthene aromatics, and polar aromatics by elution chromatography using an open column containing activated alumina. The maltenes are loaded onto the column and solvents of increasing solvent strength are used to elute the various fractions. N-heptane is added to the column, followed by toluene, a mixture of 50:50 (vol%:vol%) toluene:methanol, and finally trichloroethylene.

The saturate-like molecules, having little affinity for the alumina, are eluted first with n-C_7 up to the elution of the n-C_7/Toluene solvent front. The polar aromatics, which are highly retained on the alumina, concentrate at the TCE/Toluene:MeOH solvent front and elute last. The naphthene aromatics elute between the saturates and the polar aromatics. The difficulty of this separation arises from the fact that the solvent fronts are not distinct. In fact, the solvent fronts rarely, if ever, travel down the column uniformly. This is crucial as the separation cut-points are determined by visual inspection and can be highly subjective.

In the mid 1970s to early 1980s, petroleum chemists began to use the relatively new analytical technique of high performance liquid chromatography (HPLC) for group-type analyses of petroleum and coal derived materials.[9,13] One primary advantage of HPLC is the elimination of cut-point subjectivity. Low solvent volume (80 mL vs. 1500 mL), low solvent toxicity (n-C_6 vs. Toluene and TCE), and much shorter analysis times (10-40 min. vs. several days) are additional benefits of using HPLC.

Suatoni and Swab utilized a μ-Porasil packing to perform group-type analyses on several high boiling compounds in one of their earlier works.[9] They concluded that the saturate fractions from different materials with similar boiling points possessed nearly the same refractive index (RI) response factor (RF_s) regardless of crude source. Furthermore, they analyzed several compounds with a wide range of boiling points and they showed that the RF_s was a function of residue boiling point range. In essence, they were able to construct a calibration factor correlation based on sample boiling point.

This is explained by inspecting Figure 1 which shows the refractive index of n-alkanes as a function of carbon number,[16] which is intimately related to boiling point. It has been noted elsewhere that unlike the data of Suatoni and Swab, the data presented in Figure 1 suggest that the refractive index may approach a limiting value.[17]

In a later experiment, Gayla and Suatoni reported data that indicated that the RF_s values for saturates obtained from coal liquids with widely varying boiling points were *identical* for three out of the four materials studied.[15]
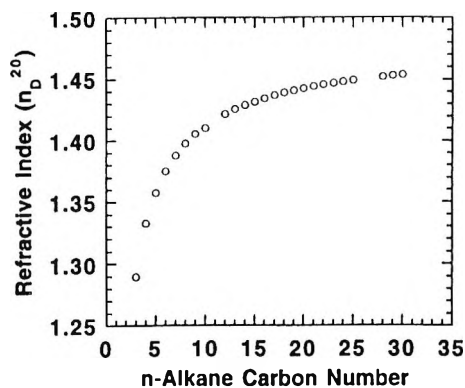
Figure 1. Refractive index of n-alkanes up to C_{30} as a function of n-alkane carbon number. Data taken from Ref. 16.

Dark and McGough performed separation of asphalts using a μ-Bondapak column and multiple solvents to produce 9 separate fractions.[14] They used RF_s values determined from crude oils rather than the RF_s values from the asphalts they investigated to quantify the various fractions. They indicated that the RF_s values were in error, but they concluded that relative comparisons could be made. The reason for this error is evident from Figure 1. Two different crude oils may have widely different average boiling points (average n-alkane carbon numbers), and thus, have widely different RF_s values. Furthermore, the average boiling point of a crude oil is significantly different from the average boiling point of its own residue.

In a later work, Dark concluded that the best agreement between HPLC crude oil saturate content and open column saturate content was obtained when the HPLC saturate content was determined by difference, rather than by direct methods.[18] This work is commonly cited in more recent publications and, as a result, most of the subsequent HPLC studies have focused on determining the content of the aromatic components using various detectors and obtaining the saturate content by difference.[19-22]

In fact, some researchers have abandoned the use of detector calibration altogether, and have instead relied on gravimetric methods.[23] Lundanes and Greibrokk were able to obtain calibration factors for saturates obtained from crude oil residues, but only after GPC fractionation was performed to narrow the molecular weight range (ie. boiling point range) of the sample.[17]

This work is an attempt to determine if accurate quantitation of the saturate content in asphalt and asphalt related materials can be accomplished using refractive index response factors. Because most refiners typically operate their vacuum distillation towers at similar conditions, it is natural to assume that the highest boiling residues (asphalts) should all have similar RF_s values, as demonstrated by Suatoni and Swab. Furthermore, if the RF_s values for high boiling residues are similar, it may be possible to isolate a *suitable* standard saturate calibration material.

MATERIALS

This experiment involved the analysis of industrial supercritical fractions (ISCF) obtained from a number of different refiners, and asphalts obtained from the Strategic Highway Research Program (SHRP) materials reference library (MRL). The other material analyzed in this study is petroleum jelly obtained from a local supermarket.

Supercritical fractions were analyzed because they are typically products of residue upgrading. They are also of interest due to their potential for use as either asphalt additives or asphalt recycling agents. Most currently available recycling agents are by-products of lube oil manufacture.

To minimize the aromatic content in lube oils, the process conditions are typically quite conservative, resulting in recycling agents with high saturate contents. It is recommended, that recycling agents contain no more than 30% saturates in order to produce good quality recycled asphalt mixtures.[24] This is because saturates and asphaltenes are inherently incompatible.

Supercritical fractionation is one potential industrial method for controlling the saturate content in recycling agents. Thus, it is essential to be able to accurately quantify the saturate content in ISCFs. In this work, the ISCFs have been given arbitrary designations to protect the identities of the companies supplying material.

Several "standard" asphalts were obtained from the SHRP MRL. These SHRP asphalts have been studied extensively throughout the world and a large data base of chemical and physical properties exists for these asphalts. The SHRP reference included at the end of this paper is by no means an exhaustive compilation of available data.[25]

METHODS

HPLC Standards Preparation

To perform quantitation of the saturate content in the heavy petroleum products, it was necessary to obtain standard materials. Because it is not possible to purchase "saturates" from chemical suppliers, it was necessary to perform preparative column chromatography to isolate saturate fractions from various petroleum products. Several variations of the Corbett procedure were utilized. Initially, the "pure" saturates were prepared according to the procedure outlined in ASTM D4124. As the experiment continued, this procedure was modified first by substituting n-hexane for n-heptane and then by performing prefractionation according to the "giant Corbett" procedure described by Peterson et al.[26] in order to produce larger quantities of the pure fractions.

The paraffin fraction from the "giant Corbett" procedure was then fractionated following the method in ASTM D4124 to produce a pure saturate fraction and a slightly saturate-contaminated light naphthene fraction. Using these methods, pure saturate fractions were obtained for eight ISCF materials and four core SHRP asphalts.

Instrumentation and Sample Preparation

A WATERS 600E multisolvent delivery system was utilized for gel permeation chromatography (GPC) and HPLC analyses of the petroleum products investigated in this study. Injection was accomplished with a Waters 700 WISP autoinjector. A WATERS 410 differential refractometer (RI) was utilized for sample detection. Data acquisition and processing were performed using Baseline 810 software.

For GPC analyses, helium-sparged HPLC grade tetrahydrofuran (THF) was used as the mobile phase at a flow rate of 1 mL/min. Three columns of decreasing pore size of 1000, 100, and 50 Å were utilized in series to accomplish separation.

The 1000 and 100 Å columns are 7.8 mm ID x 300 mm long and are packed with 7 μm ultrastyragel particles. The 50 Å column is 7.8 mm ID × 600 mm long and is packed with 5 μm PLGel particles. Samples were prepared by dissolving 0.2 ± 0.01 g of sample in 10 mL of THF. The samples were then filtered through 0.45 μm PTFE membrane syringe filters and 100 μL aliquots were injected onto the columns. Molecular weight was determined from calibration with polystyrene standards. The columns and detector were operated isothermally at 313.2 K.

For HPLC analyses, helium-sparged HPLC grade n-hexane was utilized as the mobile phase. The flow rate was controlled at 2 mL/min. A single column 7.8 mm ID × 300 mm long packed with 10 μm μ-Bondapak aminopropylmethylsilyl bonded amorphous silica was used for the analyses. The column was backflushed fifteen minutes after injection to speed the elution of the polar aromatics and shorten the analysis time. Samples were prepared by dissolving 0.20 ± 0.01 g of sample in 10 mL n-hexane. The "pure" saturate samples were prepared by dissolving 0.100 ± 0.005 g in 10 mL n-hexane due to the limited quantity of material. Even so, several of the "pure" saturate fractions were exhausted in this study. After the samples were filtered through preweighed 0.45 μm PTFE membrane syringe filters, 20 μL aliquots of the maltene fraction were injected onto the column. Sample elution was monitored by both the RI detector and a UV detector (WATERS 486 Tunable Absorbance Detector). The UV detector was utilized to monitor the purity of the saturate fractions and was operated at a wavelength of 254 nm. The columns and detectors were operated isothermally at 308.2 K. The saturate content was determined from the pure saturate refractive index RF_s, as described in the results and discussion section.

Response Factor Determination

A representative asphalt RI chromatogram is shown in Figure 2. Three peaks are evident. The first, sharp peak signifies elution of the saturates. The second, broader peak is produced by elution of the (naphthene) aromatics. The final peak, which elutes approximately 30 minutes after injection indicates elution of the polars (aromatics). The resolution between the saturates and aromatics, in general, is not sufficient to allow an accurate determination of the saturate peak area. As a result, the peak height is used rather than the peak area for quantitation purposes. The RF_s is calculated by dividing the peak height by the mass of the pure saturate fraction weighed into the scintillation vial.

RESULTS AND DISCUSSION

Pure Saturates

The RF_s values and molecular weights for pure saturates obtained from the 12 different petroleum materials and the petroleum jelly are listed in Table 1. Average RF_s values for asphalt saturates, ISCF saturates, all of the heavy petroleum product saturates studied in this work, and the petroleum jelly are listed in Table 2. It is immediately obvious from the data in Table 2 that the
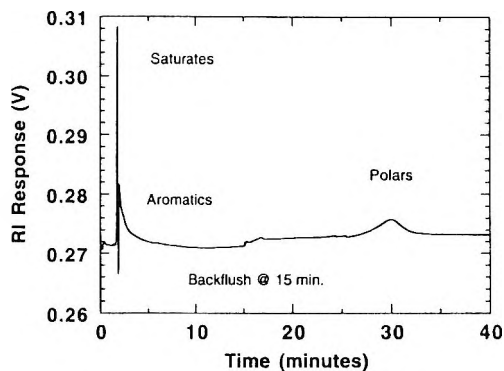
Figure 2. Refractive index chromatogram of SHRP AAC-1 separated on a 7.8 mm by 300 mm μBondapak aminopropylmethylsilylbonded amorphous silica HPLC column using n-hexane as the mobile phase at a flow rate of 2 mL/min.

Table 1

GPC Molecular Weights and HPLC Refractive Index Response Factors for 13 Saturate Fractions

Saturate Source Material	M_n	M_w	RF_s (V/g)
AAA-1	611	842	1.10
AAD-1	515	706	1.02
AAF-1	914	1142	1.24
AAM-1	1576	2285	1.03[a]
ISCF A	970	1328	1.16
ISCF B	934	1322	1.11
ISCF C	1157	1529	1.18
ISCF D	1215	1635	1.19
ISCF E	952	1220	1.09
ISCF F	906	1325	1.11
ISCF G	816	1218	1.13
ISCF H	901	1188	1.05
Petroleum Jelly	800	1164	1.05

[a] Three different "pure" saturate samples analyzed.

Table 2

Average Refractive Index Response Factors for Saturate Groups

Group	RF_s (V/g)
Asphalt saturates[a]	1.06 ± 0.096
ISCF saturates[a]	1.13 ± 0.048
All saturates analyzed	1.10 ± 0.079
Petroleum Jelly	1.05

[a] pure asphalt saturate fractions and pure ISCF saturate fractions isolated by different researchers at different times

saturates from industrial supercritical fractions have a slightly higher overall RF_s than the asphalt saturates. Even though this is expected based on the slightly higher molecular weights of the ISCF saturates, this difference in average RF_s may be attributed to the fact that the ISCF saturates were produced nearly a year after the asphalt saturates and the fact that the two different groups were isolated by different researchers.

Furthermore, the saturate fraction obtained from asphalt AAM-1 has the highest molecular weights of all samples analyzed but has one of the lowest response factors. Therefore, it is natural to conclude, that the variations in RF_s values are due mainly to operator subjectivity (one of the main problems associated with the open column method) and are not indicative of any real difference between the saturates.

This argument may naturally be extended to say that petroleum jelly is similar enough to the asphalt and ISCF saturate fractions that it has the potential for use as a "standard" saturate for the HPLC determination of saturate content in heavy petroleum products such as asphalts. Even if the petroleum jelly does not have *exactly* the same RF_s as the materials examined in this study, it may still be a suitable calibration standard. The petroleum jelly not only has approximately the same RF_s value as the asphalt and ISCF saturate fractions but it is also of similar molecular weight. It should be noted that the molecular weight values reported in Table 1 represent alkanes with carbon numbers between 37 and 112. The molecular weights reported in Table 1 may seem high, but they match values for saturate fractions obtained from both vapor pressure osmometry and field ionization mass spectrometry.[27] The UV chromatograms of all of the saturate fractions analyzed indicated approximately the same amount of UV active species in each fraction, including the petroleum jelly.

Asphalt Saturate Contents

Once it was determined that the saturates from the different asphalts, supercritical fractions, and the petroleum jelly were all similar, it was possible to determine the saturate contents of any unknown sample. This was done by injecting an unknown sample onto the columns and determining the peak height for the saturate fraction. The saturate content in the sample was determined by dividing the sample peak height by the appropriate RF_s and then dividing by the sample mass used and multiplying by 100 to obtain saturate content in terms of weight percent (wt%).

The saturate contents, in wt%, of the eight SHRP core asphalts are listed in Table 3. This table shows the saturate contents of the asphalts determined using the asphalts own saturate RF_s, the average asphalt RF_s, the overall average RF_s, and the RF_s of the petroleum jelly in comparison with values obtained from the literature [Appendix A, Ref. 25]. The values obtained from HPLC calibration using the various response factors are remarkably similar to each other but are, in general, not the same as those obtained from the literature. Upon closer investigation it is evident that the saturate contents determined by HPLC for all of the asphalts except AAD-1 are higher than the literature values. However, this does not mean that the HPLC values are incorrect. In fact, the HPLC saturate contents are probably much more accurate. The differences between the HPLC determined saturate contents and the saturate contents determined by the traditional method can be attributed to the use of different stationary phases for the different analyses. The aminopropylmethylsilyl bonded phase in the HPLC column retains the naphthene aromatics better than the naked alumina in the open column. The increased retention of the naphthene aromatics results in more saturates eluting before the naphthene aromatics elute in the HPLC separation. Data published by Dark support this belief and indicate that even more efficient separation of the saturates and (naphthene) aromatics may be possible using naked silica as the stationary phase.[18] However, using silica as the stationary phase may cause irreversible adsorption of the polar (aromatic) fraction.[9]

The increased retention of the naphthene aromatics and large deviation from the literature saturate value is most evident for asphalt AAM-1. While the use of an average RF_s or the petroleum jelly RF_s might possibly result in a large deviation from the "true" value, it is unlikely that the use of the RF_s for the saturates from AAM-1 would cause the deviations evident in Table 3. That is, using the RF_s for the saturates from a given asphalt should result in accurate saturate contents for that given asphalt. Further support for the inaccuracy of the data obtained from the open column techniques can be seen in the variability of the literature values themselves. The literature saturate contents reported in Table 3 [Appendix A, Ref. 25] differ from other values reported in the same reference [Table 3, Ref. 25].

Table 3

Saturate Content of SHRP Core Asphalts
Using Various Calibration Standards

Asphalt	MRL %S	HPLC %S Asphalt's Own RF$_s$	HPLC %S Asphalt Ave. RF$_s$	HPLC %S Overall Ave. RF$_s$	HPLC %S Petroleum Jelly RF$_s$
AAA-1	10.6	10.8	11.1	10.8	11.2
AAB-1	8.6	--	12.4	12.1	12.5
AAC-1	12.9	--	17.3	16.8	17.5
AAD-1	8.6	7.6	7.3	7.1	7.4
AAF-1	9.6	10.7	12.5	12.1	12.6
AAG-1	8.5	--	9.6	9.3	9.7
AAK-1	5.1	--	6.0	5.8	6.0
AAM-1	1.9	12.0	11.6	11.2	11.7

This only substantiates the statement that the cut-points for the traditional open column technique are subjective, sometimes highly subjective. HPLC techniques eliminate most, if not all, operator subjectivity if a suitable calibration standard is used. The data collected in this study indicate that petroleum jelly may be a suitable standard.

CONCLUSIONS

All of the previous work on HPLC calibration has relied on the tacit assumption that the saturate data from the standard open column separation methods are correct and that the HPLC saturate contents must be determined in such a way as to minimize the difference between the two values even if this requires obtaining the saturate content by difference. This belief that the open column saturate contents represent the true saturate contents has undoubtedly hindered development of HPLC as an analytical tool in characterization of heavy petroleum products even though it has been known for over ten years that bonded phase HPLC provides better separation of the naphthene aromatics from the saturates.

A natural consequence of this is that the saturate contents determined by HPLC should be more representative of the "true" saturate content. Even with improved and/or complete resolution of the saturate and naphthenic fractions, accurate quantitation of the saturate *character* in the asphalt may never

be possible as a molecule containing a benzene ring with an aliphatic side chain with thirty carbon atoms will be grouped as a naphthene aromatic even though it probably exhibits entirely saturate-like behavior in the material.

It has been shown in this study that the refractive index response factors for saturates obtained from heavy petroleum products are similar to each other and to the response factor for petroleum jelly. Therefore, petroleum jelly, with a response factor of 1.05 V/g, may be an *adequate* saturate calibration standard for asphalt and asphalt related materials.

ACKNOWLEDGEMENTS

REFERENCES

1. C. A. Savastano, Fuel Sci. Technol. Int., **9**, 855-871 (1991).

2. J. F. Branthaver, M. Nazir, J. C. Petersen, S. M. Dorrence, Liq. Fuels Technol.
   (now Fuel Sci. Technol. Int.), **1**, 355-369 (1983).

3. J. F. Branthaver, M. Nazir, J. C. Petersen, S. M. Dorrence, M. J. Ryan, Liq. Fuels Technol. (now Fuel Sci. Technol. Int.), **2**, 67-89 (1984).

4. F. S. Rostler, H. W. Sternberg, Ind. Eng. Chem., **41**, 598-608 (1949).

5. R. M. White, W. R. Mitten, J. B. Skog, Proc. Assoc. Asphalt Paving Technol., **39**, 492-531 (1970).

6. M. S. Lin, K. M. Lunsford, C. J. Glover, R. R. Davison, J .A. Bullin, **Asphaltenes: Fundamentals and Applications**, Editors E. Y. Sheu, O. C. Mullins, in press.

7. M. S. Lin, C. J. Glover, R. R. Davison, J. A. Bullin, Transportation Research Record, **1507**, 86-95 (1995).

8. L. W. Corbett, Anal. Chem., **41**, 576-579 (1969).

9. J. C. Suatoni, R. E. Swab, J. Chromatogr. Sci., **13**, 361-366 (1975).

10. J. C. Suatoni, H. R. Garber, B. E. Davis, J. Chromatogr. Sci., **13**, 367-371 (1975).

11. J. C. Suatoni, R. E. Swab, J. Chromatogr. Sci., **14**, 535-537 (1976).

12. J.C. Suatoni and H.R. Garber, J. Chromatogr. Sci., **14**, 546-548 (1976).

13. W. A. Dark, W. H. McFadden, J. Chromatogr. Sci., **16**, 289-293 (1978).

14. W. A. Dark, R. R. McGough, J. Chromatogr. Sci., **16**, 610-615 (1978).

15. L. C. Gayla, J. C. Suatoni, J. Liq. Chromatogr., **3**, 229-242 (1980).

16. **Handbook of Chemistry and Physics**, Editors R. C. Weast, M. J. Astle, W. H. Beyer, **68** (1987).

17. E. Lundanes, T. Greibrokk, J. Liq. Chromatogr., **8**, 1035-1051 (1985).

18. W. A. Dark, J. Liq. Chromatogr., **5**, 1645-1652 (1982).

19. S. W. Bishara, E. Wilkins, Transportation Research Record, **1228**, 183-190 (1989).

20. S. A. Beg, F. Mahmud, D. K. Al-Harbi, Fuel Sci. Technol. Int., **8**, 125-134 (1990).

21. M. A. Ali, W. A. Nofal, Fuel Sci. Technol. Int., **12**, 21-33 (1994).

22. W. A. Dark, J. Liq. Chromatogr., **6**, 325-342 (1983).

23. L. Carbognani, A. Izquierdo, Fuel Sci. Technol. Int., **8**, 1-15 (1990).

24. J. A. Epps, D. N. Little, R. J. Holmgreen, R. L. Terrel, Guidelines for Recycling Pavement Materials, NCHRP-224 (1980).

25. M. Mortazavi, J. S. Moulthrop, The SHRP Materials Reference Library, SHRP-A-646 (1993).

26. G. D. Peterson, R. R. Davison, C. J. Glover, J. A. Bullin, Transportation Research Record, **1436**, 38-46 (1994).

27. M. M. Boduszynski, J. F. McKay, D. R. Latham, Proc. Assoc. Asphalt
    Paving Technol., **49**, 123-143 (1980).

ANNOUNCEMENT

BASIC PRINCIPLES OF HPLC
AND HPLC SYSTEM TROUBLESHOOTING

A Two-Day
In-House Training Course

The course, which is offered for presentation at corporate laboratories, is aimed at chemists, engineers and technicians who use, or plan to use, high performance liquid chromatography in their work. The training covers HPLC fundamentals and method development, as well as systematic diagnosis and solution of HPLC hardware module and system problems.

The following topics are covered in depth:

- Introduction to HPLC Theory
- Modes of HPLC Separation
- Developing and Controlling Resolution
- Mobile Phase Selection and Optimization
- Ion-Pairing Principles
- Gradient Elution Techniques
- Calibration and Quantitation
- Logical HPLC System Troubleshooting

The instructor, Dr. Jack Cazes, is Editor-in-Chief of the Journal of Liquid Chromatography & Related Techniques, of Instrumentation Science & Technology, and of the Chromatographic Science Book Series. He has been intimately involved with liquid chromatography for more than 30 years; he pioneered the development of modern HPLC technology. Dr. Cazes was Professor-in-Charge of the ACS Short Course and the ACS Audio Course on Gel Permeation Chromatography for many years.

Details of this course may be obtained from Dr. Jack Cazes, P. O. Box 2180, Cherry Hill, NJ 08034-0162, USA. Tel: (609) 424-3505; FAX: (609) 751-8724

LIQUID CHROMATOGRAPHY CALENDAR

1996

JUNE 16 - 21: "HPLC '96: Twentieth International Symposium on High Performance Liquid Chromatography," San Francisco Marriott Hotel, San Francisco, California. Contact: Mrs. Janet Cunningham, Barr Enterprises, P. O. Box 279, Walkersville, MD 21793, USA.

JULY 1 - 3: International Symposium on Polymer Analysis and Characterization, Keble College, Oxford University, U.K. Contact: Prof. J. V. Dawkins, Dept. of Chemistry, Loughborough University of Technology, Loughborough, Leicestershire, LE11 3TU, U.K.

JULY 14 - 18: 5th World Congress of Chemical Engineering, Marriott Hotel, San Diego, California. Contact: AIChE, 345 East 47th Street, New York, NY 10017-2395, USA.

JULY 27 - 31: 37th Annual Meeting of the Aqmerican Society of Pharmacognosy, University of California, Santa Cruz, California. Contact: Dr. Roy Okuda, Chem Dept, San Jose State University, One Washington Square, San Jose, CA 95192-0101, USA. Tel: (408) 924-5000; FAX: (408) 924-4945.

AUGUST 7 - 9: 28th Canadian High Polymer Forum, Sarnia, Ontario, Canada. Contact: Kar Lok, BASF Corp, 11501 Steele Creek Rd, Charlotte, NC, 28273, USA. Tel: (704) 587-8240; FAX: (704) 587-8115.

AUGUST 8 - 10: 3rd Annual Symposium on Biomedical, Biopharmaceutical and Clinical Applications of Capillary Electrophoresis, Mayo Clinic, Rochester, Minnesota. Contact: Dr. S. Naylor, Mayo Foundation, Section of Continuing Education, Rochester, MN 55905, USA.

AUGUST 9 - 14: 31st Intersociety Energy Conversion Engineering Conference (co-sponsored with IEEE), Omni Shoreham Hotel, Washington, DC. Contact: AIChE, 345 East 47th Street, New York, NY 10017-2395, USA.

AUGUST 11 - 15: 26th ACS Northeast Regional Meeting, Western Conn State Univ, Danbury, CT. Contact: A. Alder, 11 Long Ridge Rd, Redding, CT 06896, USA; (203) 938-2920; Email: reglmtgs@acs.org.

AUGUST 11 - 16: 3rd International Hydrocolloids Conference, Sydney, Australia. Contact: Gail Hawke, P. O. Box N-399, Grosvenor Place, Sydney, NSW 2000, Australia. Tel: 61 02 241 3388; FAX: 61 02 241 5282.

AUGUST 11 - 16: ICORS '96: 15th International Conference on Raman Spectroscopy, Pittsburg, Pennsylvania. Contact: Sanford Asher, Chem Dept, University of Pittsburgh, PA 15260, USA. Tel: (412) 624-8570; FAX: (412) 624-0588.

AUGUST 12 - 16: 11th Internationa Congress on Thermal Analysis & Calorimetry, Philadelphia. Contact: The Complete Conference, 1540 River Pk Dr, Sacramento, CA 95815, USA. Tel: (916) 922-7032; FAX: (916) 922-7379.

AUGUST 17 - 20: 31st National Heat Transfer Conference, Westin Galleria, Houston, Texas. Contact: AIChE, 345 East 47th Street, New York, NY 10017-2395, USA.

AUGUST 18 - 23: 17th International Conference on Magnetic Resonance in Biological Systems, Keystone, Colorado, USA. Contact: Conference Office, 1201 Don Diego Ave, Santa Fe, NM 87505, USA. Tel: (505) 989-4735; FAX: (505) 989-1073.

AUGUST 21 - 23: 4th International Symposium on Capillary Electrophoresis, York, UK. Contact: Dr. T. Threlfall, Industrial Liaison Executive, Dept of Chem, University of York, Heslington, York, YO1 5DD, UK.

AUGUST 25 - 29: 212th ACS National Meeting, Orlando, Florida. Contact: ACS Meetings, 1155 16th Street, NW, Washington, DC 20036-4899, USA. Tel: (202) 872-4396; Email: natlmtgs@acs,org.

AUGUST 25 - 30: International Symposium on Metal Hydrogen Systems: Fundamentals and Applications, Les Diablerets, Switzerland. Contact: MH-96, Inst of Physics, Univ of Fribourg, Perolles, CH-1700 Fribourg, Switzerland. Tel: 41 37 299 113; FAX: 41 37 299 772.

AUGUST 25 - 30: 12th International Congress on Chemical & Process Engineering, Prague, Czech Republic. Contact: Organizing Committe, CHISA'96, P. O. Box 857, 111 21 Praha, Czech Republic. Tel: 42 2 353287; FAX: 42 2 3116138.

SEPTEMBER 1 - 4: 4th Inetrnational Symposium on Preparative & Industrial Chromatography & Related Techniques, Basel, Switzerland. Contact: Secretariat Prep'96, Messeplatz 25, CH-4021 Basel, Switzerland. Tel: 41 61 686 28 28; FAX: 41 61 686 21 85.

SEPTEMBER 1 - 6: IUPAC Chemrawn IX, Seoul, Korea. Contact: IUPAC Chemrawn IX, Secretariat, Tongwon B/D 6th Floor, 128-27 Tangjudong, Chongro-ku, Seoul 110-071, Korea. FAX: 82 2 739-6187.

SEPTEMBER 1 - 6: 11th International Symposium on Organosilicon Chemistry, Monpellier, France. Contact: R. Corriu, University of Montpellier II, Place Eugene Batallon, cc007, 34095 Montpellier cedex 05, France. Tel: 67 14 38 01.

SEPTEMBER 1 - 6: 11th Symposium on Quantitative Structure-Activity Relationships: Computer-Assisted Lead Finding and Optimization," Lausanne, Switzerland. Contact: Dr. Han van de Waterbeemd, F. Hoffmann-La Roche Ltd., Dept PRPC 65/314, CH-4002 Basle, Switzerland.

SEPTEMBER 4 - 9: International "Thermophiles '96" Symposium: Biology, Ecology & Biotechnology of Thermophilic Organisms, Athens, Georgia. Contact: J. Wiegel, University of Georgia, Microbiology Department, 527 Biol Sci Bldg, Athens, GA 30602-2605, USA. Tel: 706) 542-2674; fax: (706) 542-2651.

SPETEMBER 7: Field-Flow Fractionation Workshop VIII, Ferrara, Italy. Contact: F. Dondi, Dept of Chem, University of Ferrara, via L. Borsari 46, I-44100 Ferrara, Italy. Tel: 39 532 291154; fax: 39 532 240709.

SEPTEMBER 9 - 11: Sixth International Symposium on Field-Flow Fractionation, Ferrara, Italy. Contact: F. Dondi, Dept of Chem, University of Ferrara, via L. Borsari 46, I-44100 Ferrara, Italy. Tel: 39 532 291154; fax: 39 532 240709.

SEPTEMBER 9 - 11: 110th AOAC International Annual Meeting & Expo, Hyatt, Orlando, Florida. Contact: AOAC International, 2200 Wilson Blvd, Suite 400, Arlington, VA 22201-3301, USA. Tel: (703) 522-3032; FAX: (703) 522-5468.

SEPTEMBER 9 - 12: Saftey in Ammonia Plants & Related Facilities, Westin at Copley Place, Boston, Massachusetts. Contact: AIChE, 345 East 47th Street, New York, NY 10017-2395, USA.

SEPTEMBER 10 - 12: International Thermophiles Workshop: Keys to Molecular Evolution & the Origin of Life, Athens, Georgia. Contact: J. Wiegel, University of Georgia, Microbiology Department, 527 Biol Sci Bldg, Athens, GA 30602-2605, USA. Tel: 706) 542-2674; fax: (706) 542-2651.

SEPTEMBER 11 - 13: Corn Refiners Assn Scientific Conference, Bloomindale, Illinois. Contact: Corn Refiners Assn, 1701 Pennsylvania Ave, NW, Washington, DC 20036, USA. Tel: (202) 331-1634; FAX: (202) 331-2054.

SEPTEMBER 11 - 13: 2nd Workshop on Biosensors & Biol Techniques in Environmental Analysis, Lund, Sweden. Contact: M. Frei-Hausler, IAEAC Secretariat, Postfach 46, CH-4123 Allschwill 2, Switzerland.

SEPTEMBER 15 - 20: 21st International Symposium on Chromatography, Stuttgart, Germany. Contact: Dr. L. Kiessling, Geselleschaft Deutscher Chemiker, Postfach 900440, D-60444 Frankfurt/Main, Germany.

SEPTEMBER 16 - 18: 3rd International Conference on Applications of Magnetic Resonance in Food Science, Nantes, France. Contact: Laboratoire de RMN-RC, 2 rue de la Houssiniere, 44072 Nantes cedex 03, France. Tel: 33 40 74 98 06; FAX: 33 40 37 31 69.

SEPTEMBER 16 - 19: International Ion Chromatography Symposium 1996, University of Reading, Reading, UK. Contact: J. R. Strimaitis, Century International, P. O. Box 493, Medfield, MA 02052, USA. Tel: (508) 359-8777; FAX: (508) 359-8778.

SEPTEMBER 17 - 20: 10th International Symposium on Cap[illary Electrophoresis, Prague, Czech Republic. Contact: Dr. B. Gas, Dept of Physical Chem, Charles University, Albertov 2030, CZ-128 40 Prague 2, Czech Republic.

SEPTEMBER 19 - 21: 19th Annual Gulf Coast Chemistry Conference, Pensacola, Florida. Contact: J. Gurst, Chem Dept, University of West Florida, Pensacola, FL 32514, USA. Tel: (904) 474-2744; FAX: 904) 474-2621.

SEPTEMBER 20 - 24: 12th Asilomar Conference on Mass Spectrometry, Pacific Grove, California. Contact: ASMS, 1201 Don Diego Ave, Santa Fe, NM 87505, USA. Tel: (505) 989-4517; FAX: (505) 989-1073.

SEPTEMBER 28 - OCTOBER 5: **Federation of Analytical Chem & Spectroscopy Societies (FACSS), Kansas City.** Contact: J.A. Brown, FACSS, 198 Thomas Johnson Dr., Suite S-2, Frederick, MD 21702, USA. Tel: (301) 846-4797; FAX: (301) 694-6860.

OCTOBER 17 - 19: 52nd Southwest Regional ACS Meeting, Houston, Texas. Contact: J. W. Hightower, Dept. Chem. Eng., Rice University, Houston, TX 77251, USA.

OCTOBER 24 - 26: 52nd Southwestern Regional Meeting, ACS, Houston, Texas. Contact: J. W. Hightower, Chem Eng Dept, Rice Univ, Houston, TX 77251, USA.

OCTOBER 27 - 31: American Assn of Pharmaceutical Scientists Annual Meeting & Expo, Seattle, Washington. Contact: AAPS, 1650 King St, Alexandria, VA 22314-2747, USA. Tel: (703) 548-3000; FAX: (703) 684-7349.

OCTOBER 29 - 30: ASTM Symposium on Pesticide Formulations & Application Systems, New Orleans, Louisiana. Contact: G. R. Goss, Oil-Dri Corp, 777 Forest Edge Dr, Vrenon Hills, IL 60061, USA. Tel: (708) 634-3090; FAX: (708) 634-4595.

OCTOBER 29 - 31: Cphl Pharmaceutical Ingredients Worldwide '96 Conference, Milan, Italy. Contact: Miller Freeman BV, Industrieweg 54, P. O. Box 200, 3600 AE Maarssen, The Netherlands. Tel: 31 3465 73777; FAX: 31 3465 73811.

NOVEMBER 6 - 8: 31st Midwestern Regional Meeting, ACS, Sioux Falls, South Dakota. Contact: J. Rice, Chem Dept, S. Dakota State Univ, Shepard Hall Box 2202, Brookings, SD 57007-2202, USA.

NOVEMBER 6 - 9: 24th Biennial International Conference on Application of Accelerators in Research & Industry, Denton, Texas. Contact: J. L. Duggan or B. Stippec, University of North Texas, Physics Department, Denton, TX 76203, USA. Tel: (817) 565-3252; FAX: (817) 565-2227.

NOVEMBER 9 - 12: 48th Southeast Regional ACS Meeting, Hyatt Regency Hotel, Greenville, South Carolina. Contact: H. C. Ramsey, BASF Corp., P. O. Drawer 3025, Anderson, SC 29624-3025, USA.

NOVEMBER 10 - 13: 4th North American Research Conference on Organic Coatings Science & Technology, Hilton Head, South Carolina. Contact: A. V. Patsis, SUNY, New Paltz, NY 12561, USA.

NOVEMBER 10 - 14: 10th International Forum on Electrolysis in the Chemical Industry, Clearwater Beach, Florida. Contact: P. Kluczynski, Electrosynthesis Co, 72 Ward Road, Lancaster, NY 14086, USA. Tel: (716) 684-0513; FAX: (716) 684-0511.

NOVEMBER 10 - 15: AIChE Annual Meeting, Palmer House, Chicago, Illinois. Contact: AIChE, 345 East 47th Street, New York, NY 10017-2395, USA.

NOVEMBER 11 - 20: 2nd Latin-American Conference on Biomedical, Biopharmaceutical and Industrial Applications of Capillary Electrophoresis, Santiago, Chile. Dr. E. Guerrero, Servicio Medico Legal, Avenida de la Paz 1012, Santiago, Chile.

NOVEMBER 12 - 14: Plastics Fair, Charlotte, North Carolina. Contact: Becky Lerew, Plastics Fair, 7500 Old Oak Blvd, Cleveland, OH 44130, USA. Tel: (216) 826-2844; FAX: (216) 826-2801.

NOVEMBER 13 - 15: 13th Montreux Symposium on Liquid Chromatography-Mass Spectrometry (LC/MS; SFC/MS; CE/MS; MS/MS), Maison des Congres, Montreux, Switzerland. Contact: M. Frei-Hausler, Postfach 46, CH-4123 Allschwill 2, Switzerland. Tel: 41-61-4812789; FAX: 41-61-4820805.

NOVEMBER 18 - 20: 3rd International Conference on Chemistry in Industry, Bahrain, Saudi Arabia. Contact: Chem in Industry Conf, P. O. Box 1723, Dhahran 31311, Saudi Arabia. Tel: 966 3 867 4409; FAX: 966 3 876 2812.

NOVEMBER 17 - 22: Eastern Analytical Symposium, Garden State Convention Center, Somerset, New Jersey. Contact: S., Good, EAS, P. O. Box 633, Montchanin, DE 19710-0635, USA. Tel: (302) 738-6218; FAX: (302) 738-5275.

NOVEMBER 24 - 27: Industrial Research for the 21st Century, 1996 Biennial Meeting, Red Lion Resort, Santa Barbara, California. Contact: R. Ikeda, DuPont Central Research Dept., P. O. Box 80356, Wilmington, DE 19880-0356, USA. Tel: (302) 695-4382; FAX: (302) 695-8207; Email: ikeda@esvax.dnet.dupont.com.

DECEMBER 17 - 20: First International Symposium on Capillary Electrophoresis for Asia-Pacific, Hong Kong. Contact: Dr. S. F. Y. Li, Dept of Chemistry, National University of Singapore, Kent Ridge Crescent, Singapore 119260, Republic of Singapore.

1997

APRIL 13 - 17: 213th ACS National Meeting, San Francisco, California. Contact: ACS Meetings, ACS, 1155 16th Street, NW, Washington, DC 20036-4899, USA. Tel: (202) 872-6059; FAX: (202) 872-6128; Email: natlmtgs@acs.org.

APRIL 14 - 19: Genes and Gene Families in Medical, Agricultural and Biological Research: 9th International Congress on Isozymes, sponsored by the Southwest Foundation for Biomedical Research, Hilton Palacio del Rio, San Antonio, Texas. Contact: Mrs. Janet Cunningham, Barr Enterprises, P. O. Box 279, Walkersville, MD 21793, USA.

MAY 5 - 9: 151st ACS Rubber Div Spring Technical Meeting, Anaheim, California. Contact: L. Blazeff, P. O. Box 499, Akron, OH 44309-0499, USA. Tel: (216) 972-7814; FAX: (216) 972-5269.

MAY 23 - 24: ACS Biological Chemistry Div Meeting, San Francisco, California. Contact: K. S. Johnson, Dept of Biochem & Molec Biol, Penn State Univ, 106 Althouse Lab, University Park, PA 16802, USA. Tel: (814) 865-1200; FAX: (814) 865-3030; Email: kaj@ecl.psu.edu.

MAY 27 - 30: ACS 29th Central Regional Meeting, Midland, Michigan. Contact: S. A. Snow, Dow Corning Corp., CO42A1, Midland, MI 48686-0994, USA. Tel: (517) 496-6491; FAX: (517) 496-6824; Email: usdcc6fc@bmmail.com.

MAY 28 - 30: 31st ACS Middle Atlantic Regional Meeting, Pace Univ, Pleasantville, NY. Contact: D. Rhani, Chem Dept, Pace University, 861 Bedford Rd, Pleasantville, NY 10570-2799, USA. Tel: (914) 773-3655; Email: reglmtgs@acs.org.

MAY 28 - JUNE 1: 30th Great Lakes Regional ACS Meeting, Loyola University, Chicago Illinois. Contact: M. Kouba, 400G Randolph St, #3025, Chicago, IL 60601, USA. Email: reglmtgs@acs.org.

JUNE 22 - 25: 27th ACS Northeast Regional Meeting, Saratoga Springs, New York. Contact: T. Noce, Rust Envir & Infrastructure, 12 Metro Park Rd, Albany, NY 12205, USA. Tel: (518) 458-1313; FAX: (518) 458-2472; Email: reglmtgs@acs.org.

JUNE 22 - 26: 35th National Organic Chemistry Symposium, Trinity Univ., San Antonio, Texas. Contact: J. H. Rigby, Chem Dept, Wayne State Univ., Detroit, MI 48202-3489, USA. FAX: (313) 577-2099

SEPTEMBER 7 - 11: 214th ACS National Meeting, Las Vegas, Nevada.
Contact: ACS Meetings, 1155 16th Street, NW, Washington, DC 20036-4899,
USA. Tel: (202) 872-4396; (202) 872-6128; Email: natlmtgs@acs.org.

**SEPTEMBER 21 - 26: Federation of Analytical Chemistry & Spectroscopy
Societies (FACSS), Cleveland, Ohio.** Contact: J. A. Brown, FACSS, 198
Thomas Johnson Dr, Suite S-2, Frederick, MD 21702, USA. Tel: (301) 846-
4797; FAX: (301) 694-6860.

**OCTOBER 19 - 22: 49th ACS Southeast Regional Meeting, Roanoke,
Virginia.** Contact: J. Graybeal, Chem Dept, Virginia Tech, Blacksburg, VA
24061, USA. Tel: (703) 231-8222; Email: reglmtgs@acs.org.

**OCTOBER 21 - 25: 33rd ACS Western Regional Meeting, Irvine,
California.** Contact: L. Stemler, 8340 Luxor St, Downey, CA 90241, USA.
Tel: (310) 869-9838; Email: reglmtgs@acs.ord.

**OCTOBER 26 - 29: 8th Symposium on Handling of Environmental &
Biological Samples in Chromatography and the 26th Scientific Meeting of
the Group of Chromatography and Related Techniques of the Spanish
Royal Society of Chemistry, Almeria, Spain.** Contact: M. Frei-Hausler,
IAEAC Secretariat, Postfach 46, CH-4123 Allschwill 2, Switzerland. FAX: 41-
61-4820805.

**OCTOBER 29 - NOVEMBER 1: 32nd ACS Midwest Regional Meeting,
Lake of the Ozarks, Osage Beach, Missouri.** Contact: C. Heitsch, Chem Dept,
Univ of Missouri-Rolla, Rolla, MO 65401, USA. Tel: (314) 341-4536; FAX:
(314) 341-6033; Email: reglmtgs@acs.org.

**NOVEMBER 11 - 15: 5th Chemical Congress of North America, Cancun,
Mexico.** Contact: ACS Meetings, 1155 16th St, NW, Washington, DC 20036-
4899, USA. Tel: (202) 872-6286; FAX: (202) 872-6128; Email:
miscmtgs@acs.org.

**NOVEMBER 16 - 21: Eastern Analytical Symposium, Garden State
Convention Center, Somerset, New Jersey.** Contact: S. Good, EAS, P. O.
Box 633, Montchanin, DE 19710-0635, USA. Tel: (302) 738-6218; FAX:
(302) 738-5275.

1998

MARCH 29 - APRIL 2: 215th ACS National Meeting, Dallas, Texas.
Contact: ACS Mtngs, 1155 16th Street, NW, Wash, DC 20036-4899, USA.

JUNE 10 - 12: 53rd ACS Northwest Regional Meeting, Columbia Basin College, Pasco, Washington. Contact: K. Grant, Math/Science Div, Columbia Basin College, 2600 N 20th Ave, Pasco, WA 99301, USA. Email: reglmtgs@acs.org.

JUNE 13 - 19: 26th ACS National Medical Chemistry Symposium, Virginia Commonwealth Univ/Omni Richmond Hotel, Richmond, Virginia. Contact: D. J. Abraham, Virginia Commonwealth Univ, Dept of Med Chem, P. O. Box 581, Richmond, VA 23298, USA. Tel: (804) 828-8483; FAX: (804) 828-7436.

AUGUST 23 - 28: 216th ACS National Meeting, Boston, Massachusetts. Contact: ACS Meetings, 1155 16th Street, NW, Washington, DC 20036-4899, USA. Tel: (202) 872-4396; FAX: (202) 872-6218; Email: natlmtgs@acs.org.

SEPTEMBER 7 - 11: 15th International Symposium on Medicinal Chemistry, Edinburgh, Scotland. Contact: M. Campbell, Bath University School of Chemistry, Claverton Down, Bath, BA2 7AY, UK. Tel: (44) 1225 826565; FAX: (44) 1225 826231; Email: chsmmc@bath.ac.uk.

NOVEMBER 4 - 7: 50th ACS Southwest Regional Meeting, Resw Triangle Pk, North Carolina. Contact: B. Switzer, Chem Dept, N Carolina State University, Box 8204, Raleigh, NC 27695-8204, USA. Tel: (919) 775-0800, ext 944; Email: switzer@chemdept.chem.ncsu.edu.

1999

MARCH 21 - 25: 217th ACS National Meeting, Anaheim, Calif. Contact: ACS Meetings, 1155 16th Street, NW, Washington, DC 20036-4899, USA. Tel: (202) 872-4396; FAX: (202) 872-6128; Email: natlmtgs@acs.org.

AUGUST 22 - 26: 218th ACS National Meeting, New Orleans, Louisiana. Contact: ACS Meetings, 1155 16th Street, NW, Washington, DC 20036-4899, USA. Tel: (202) 872-4396; FAX: (202) 872-6128; Email: natlmtgs@acs.org.

OCTOBER 8 - 13: 51st ACS Southeast Regional Meeting, Knoxville, Tennessee. Contact: C. Feigerle, Chem Dept, University of Tennessee, Knoxville, TN 37996, USA. Tel: (615) 974-2129; Email: reglmtgs@acs.org.

2000

MARCH 26 - 30: 219th ACS National Meeting, Las Vegas, Nevada.

Contact: ACS Meetings, 1155 16th Street, NW, Washington, DC 20036-4899, USA. Tel: (202) 872-4396; FAX: (202) 872-6128; Email: natlmtgs@acs.org.

AUGUST 20 - 24: 220th ACS National Meeting, Washington, DC. Contact: ACS Meetings, 1155 16th Street, NW, Washington, DC 20036-4899, USA. Tel: (202) 872-4396; FAX: (202) 872-6128; Email: natlmtgs@acs.org.

2001

APRIL 1 - 5: 221st ACS National Meeting, San Francisco, Calif. Contact: ACS Meetings, 1155 16th Street, NW, Washington, DC 20036-4899, USA. Tel: (202) 872-4396; FAX: (202) 872-6128; Email: natlmtgs@acs.org.

AUGUST 19 - 23: 222nd ACS National Meeting, Chicago, Illinois. Contact: ACS Meetings, 1155 16th Street, NW, Washington, DC 20036-4899, USA. Tel: (202) 872-4396; FAX: (202) 872-6128; Email: natlmtgs@acs.org.

2002

APRIL 7 - 11: 223rd ACS National Meeting, Orlando, Florida. Contact: ACS Meetings, 1155 16th Street, NW, Washington, DC 20036-4899, USA. Tel: (202) 872-4396; FAX: (202) 872-6128; Email: natlmtgs@acs.org.

SEPTEMBER 8 - 12: 224th ACS National Meeting, Boston, Mass. Contact: ACS Meetings, 1155 16th Street, NW, Washington, DC 20036-4899, USA. Tel: (202) 872-4396; FAX: (202) 872-6128; Email: natlmtgs@acs.org.

2003

MARCH 23 - 27: 225th ACS National Meeting, New Orleans, Louisiana. Contact: ACS Meetings, 1155 16th Street, NW, Washington, DC 20036-4899, USA. Tel: (202) 872-4396; FAX: (202) 872-6128; Email: natlmtgs@acs.org.

SEPTEMBER 7 - 11: 226th ACS National Meeting, New York City. Contact: ACS Meetings, 1155 16th Street, NW, Washington, DC 20036-4899, USA. Tel: (202) 872-4396; FAX: (202) 872-6128; Email: natlmtgs@acs.org.

2004

MARCH 28 - APRIL 1:   227th ACS National Meeting, Anaheim, California. Contact: ACS Meetings, 1155 16th Street, NW, Washington, DC 20036-4899, USA. Tel: (202) 872-4396;   FAX: (202) 872-6128;   Email: natlmtgs@acs.org.

AUGUST 22 - 26:   228th ACS National Meeting, Philadelphia, Pennsylvania. Contact: ACS Meetings, 1155 16th Street, NW, Washington, DC 20036-4899, USA. Tel: (202) 872-4396;   FAX: (202) 872-6128;   Email: natlmtgs@acs.org.

2005

MARCH 13 - 17: 229th ACS National Meeting, San Diego, California. Contact: ACS Meetings, 1155 16th Street, NW, Washington, DC 20036-4899, USA. Tel: (202) 872-4396; FAX: (202) 872-6128; Email: natlmtgs@acs.org.

AUGUST 28 - SEPTEMBER 1: 230th ACS National Meeting, Washington, DC. Contact: ACS Meetings, 1155 16th Street, NW, Washington, DC 20036-4899, USA. Tel: (202) 872-4396;   FAX: (202) 872-6128;   Email: natlmtgs@acs.org.

The **Journal of Liquid Chromatography & Related Technologies** will publish, at no charge, announcements of interest to scientists in every issue of the journal. To be listed in Meetings & Symposia, we will need to know:

a) Name of the meeting or symposium,

b) Sponsoring organization,

c) When and where it will be held, and

d) Whom to contact for additional details.

Incomplete information will not be published. You are invited to send announcements to **Dr. Jack Cazes, Editor, Journal of Liquid Chromatography, P.O. Box 2180, Cherry Hill, NJ 08034-0162, USA.**

INSTRUCTIONS TO AUTHORS

The *Journal of Liquid Chromatography & Related Technologies* is published in the English language for the rapid communication of research results in liquid chromatography and its related sciences and technologies.

Directions for Submission

One complete original manuscript and two (2) clear copies, with figures, must be submitted for peer review. After all required revisions have been completed, and the final manuscript has been accepted, the author will be asked to provide, if possible, a 3½" or 5¼" PC-Compatible computer diskette containing the complete manuscript. Microsoft Word, Word for Windows, WordPerfect, WordPerfect for Windows and ASCII are preferred formats. Text, including tables, and figures, if in electronic format, should be saved in separate files on the diskette. Label the diskette with the corresponding author's last name, the title of the manuscript and the file number assigned to the manuscript.

> Submission of a manuscript on diskette, in a suitable format, will significantly expedite its publication.

Manuscripts and computer diskettes should be mailed to the Editor:

Dr. Jack Cazes
Journal of Liquid Chromatography & Related Technologies
P. O. Box 2180
Cherry Hill, NJ 08034-0162

Reprints

Due to the short production time for papers in this journal, it is essential to order reprints immediately upon receiving notification of acceptance of the manuscript. A reprint order form will be sent to the author with the letter of acceptance for the manuscript. Reprints are available in quantities of 100 and multiples thereof. Twenty (20) free reprints will be included with orders of 100 or more reprints.

Format of the Manuscript

NOTE: Failure to adhere to the following guidelines will delay publication of a manuscript.

1. The preferred dimensions of the printed area of a page are
   6" (15.2 cm) width by 8.5" (21.6 cm) height.
   Use Times Roman 12 point font, if possible.

The general organization of the manuscript should be:

    Title
    Author(s)' names and full addresses
    Abstract
    Text Discussion
    References

2. **Title & Authors**: The entire title should be in bold-face capital letters and centered within the width of the printed area, located 2 inches (5.1 cm) from the top of the page. This should be followed by 2 lines of space, then by the names and addresses of the authors, also centered, in the following manner:

<div align="center">

**A SEMI-AUTOMATIC TECHNIQUE FOR THE
SEPARATION AND DETERMINATION OF
BARIUM AND STRONTIUM IN WATER
BY ION EXCHANGE CHROMATOGRAPHY AND
ATOMIC EMISSION SPECTROMETRY**

F. D. Pierce, H. R. Brown
Utah Biomedical Test Laboratory
520 Wakara Way
Salt Lake City, Utah 84108

</div>

3. **Abstract**: The heading **ABSTRACT** should be typed boldface, capitalized and centered, 2 lines below the addresses. This should be followed by a single-spaced, concise abstract. Allow 2 lines of space below the abstract before beginning the text of the manuscript.

4. **Text Discussion**: Whenever possible, the text discussion should be divided into major sections such as

    INTRODUCTION
    MATERIALS
    METHODS
    RESULTS
    DISCUSSION
    ACKNOWLEDGMENTS

These **major headings** should be separated from the text by two lines of space above and one line of space below. Each major heading should be typed boldface, in capital letters, centered.

Secondary headings, if any, should be placed flush with the left margin, and have the first letter of main words capitalized. Leave two lines of space above and one line of space below secondary headings.

5. The **first line of each paragraph** within the body of the text should be indented a half inch.

6. **Acknowledgments**, sources of research funds and address changes for authors should be listed in a separate section at the end of the manuscript, immediately preceding the references.

7. **References** should be numbered consecutively and placed in a separate section at the end of the manuscript. They should be typed single-spaced, with one line space between each reference. Each reference should contain names of all authors (with initials of their first and middle names); do not use *et al.* for a list of authors. Abbreviations of journal titles will follow the American Chemical Society's Chemical Abstracts List of Periodicals. The word **REFERENCES**, in boldface type, should be capitalized and centered above the reference list.

Following are acceptable reference formats:

Journal:

1. D. K. Morgan, N. D. Danielson, J. E. Katon, Anal. Lett., 18, 1979-1998 (1985).

Book:

1. L. R. Snyder, J. J. Kirkland, **Introduction to Modern Liquid Chromato-graphy**, John Wiley & Sons, Inc., New York, 1979.

Chapter in a Book:

1. C. T. Mant, R. S. Hodges, "HPLC of Peptides," in **HPLC of Biological Macromolecules**, K. M. Gooding, F. E. Regnier, eds., Marcel Dekker, Inc., New York, 1990, pp. 301-332.

8. Each page of manuscript should be numbered lightly, with a light blue pencil, at the bottom of the page.

9. Only standard symbols and nomenclature, approved by the International Union of Pure and Applied Chemistry (IUPAC) should be used. **Hand-drawn characters are not acceptable.**

10. Material that cannot be typed, such as Greek symbols, script letters and structural formulae, should be drawn carefully with dark black India ink. Do not use any other color ink.

Additional Typing Instructions

1. The manuscript must be prepared on **good quality white bond paper,** measuring approximately 8½ x 11 inches (21.6 cm x 27.9 cm). International paper, size A4 is also acceptable. The typing area of the first page, including the title and authors, should be 6" (15.2 cm) wide by 8.5" (21.6 cm) height.

2. All text should be **typed single-spaced**.

3. It is essential to use **dark black** typewriter or printer ribbon so **that clean, clear, solid characters** are produced. Characters produced with a dot/matrix printer are not acceptable, even if they are "near letter quality" or "letter quality." Erasure marks, smudges, hand-drawn corrections and creases are not acceptable.

4. **Tables** should be typed as part of the text, but in such a way as to separate them from the text by a 2-line space above and below the table. Tables should be inserted in the text as close to the point of reference as possible. **A table may not be longer than one page.** If a table is larger than one page, it should be divided into more than one table. The word **Table** (followed by an Arabic number) should precede the table and should be centered above the table. The title of the table should have the first letters of all main words in capitals. Table titles should be typed single line spaced, across the full width of the table.

5. **Figures** (drawings, graphs, etc.) should be professionally drawn in black India ink on separate sheets of white paper, and should be placed at the end of the text. They should not be inserted into the body of the text. They should not be reduced to a small size. Preferred size for figures is from 5 inches x 7 inches (12.7 cm x 17.8 cm) to 8½ inches by 11 inches (21.6 cm x 27.9 cm). Photographs should be professionally prepared, black and white, *glossy* prints. A typewriter or lettering set should be used for all labels on the figures or photographs; they may not be hand drawn.

Captions for figures should be typed single-spaced on a separate sheet of white paper, along the full width of the type page, and should be preceded with the

word **Figure** and an Arabic numeral. All figures and lettering must be of a size that will remain legible after a 20% reduction from the original size. Figure numbers, name of senior author and an arrow indicating "top" should be written in light blue pencil on the back of the figure. Indicate the approximate placement for each figure in the text with a note written with a light blue pencil in the margin of the manuscript page.

6. The reference list should be typed single-spaced. A single line space should be inserted after each reference. The format for references should be as given above.

Manuscripts which require correction of English usage will be returned to the author for major revision.

Keep state-of-the-art theoretical and applied research developments at your fingertips with...

Advances in Chromatography

Volume 36

edited by

PHYLLIS R. BROWN
University of Rhode Island, Kingston

ELI GRUSHKA
Hebrew University of Jerusalem, Israel

October, 1995 / 464 pages, illustrated / $175.00

The rapidly expanding growth of the literature on chromatography, capillary electrophoresis, field flow fractionation, and other separation techniques makes it difficult for any individual to maintain a coherent view of progress in the field. Rather than attempt to read the avalanche of original research papers, investigators trying to preserve even a modest awareness of advances must rely upon **authoritative surveys.**

Featuring reliable, **up-to-the-minute reviews** of major developments in separations, this critically praised series separates the most important advances from an overabundance of supplementary materials.

Internationally acclaimed experts analyze the most current innovations in their areas of specialization!

Providing more than 850 bibliographic citations, allowing for further, in-depth study of recent trends in research, **Volume 36** examines timely subjects such as

- multilinear regression, canonical correlation, and factor and principal component methods of analysis in the evaluation of retention data matrices
- molecular recognition mechanisms in the liquid chromatographic separation of fullerenes
- the latest techniques in the use of capillary electrophoresis and mass spectrometry for sequencing antisense oligonucleotides
- analytical tools and separation methods for the analysis of drugs of abuse in biological fluids
- the applications of high-performance liquid chromatography coupled with nuclear magnetic resonance spectroscopy
- and much more!

Advances in Chromatography is an indispensable resource for all researchers who need to use separation methods effectively—especially analytical, organic, inorganic, clinical, and physical chemists; chromatographers; biochemists and biological chemists; agrochemists; chemical, materials, pollution, and quality control engineers; biotechnologists; toxicologists; pharmacologists; pharmacists; physiologists; zoologists; botanists; food, cosmetic, polymer, and environmental scientists; microbiologists; virologists; oceanographers; research and quality control scientists in academia, government, hospitals, and industry; and upper-level undergraduate and graduate students in these disciplines.

CONTENTS

ISBN: 0—8247—9551—2

This book is printed on acid-free paper.

Contents Continued

JOURNAL OF LIQUID CHROMATOGRAPHY & RELATED TECHNOLOGIES

CONTENTS